Replies to both referees RC1 (T. Albrecht) and RC2 on “Precipitation Ansatz dependent Future Sea Level Contribution by Antarctica based on CMIP5 Model Forcing” by Christian B. Rodehacke et al.

We thank the Referees for reviewing our manuscript and their encouraging comments. We have compiled our replies to all raised issues and points in this document. The Referee's texts containing all aspects are in black print, while our responses to each item are in blue. This pdf file contains both in consecutively order both replies

(This page is left empty intentionally.)

Interactive comment on “Precipitation Ansatz dependent Future Sea Level Contribution by Antarctica based on CMIP5 Model Forcing” by Christian B. Rodehacke et al.

Torsten Albrecht (Referee)
Received and published: 8 February 2020

General comments:

Rodehacke and colleagues investigate the effects of multiple climate model forcings (from CMIP5) in Antarctica. They assess the spatial heterogeneity in temperature and precipitation estimates over the period 1850-2100 for different emission scenarios and the spread among the 9 selected climate models. The ratio of precipitation anomalies and temperature anomalies is compared to paleo estimates at 6 ice core locations and regional variations from the spatial mean are discussed. Applied to the ice sheet model PISM they run an ensemble of simulations up to the year 5000 with both the anomaly forcing fields from the climate models and the simplified (spatial mean) parameterization (as often used in previous studies) and find quite some differences in the projected ice mass changes (converted in units of sea-level equivalents).

While in this study the temperature-scaled precipitation results in long-term ice losses, the directly applied precipitation anomalies generate net mass gains. Given the numerous previous projection studies, this is a surprising result. However, for given model settings this discrepancy can to some extent be explained in the manuscript. Overall, the study is well structured and the manuscript clearly-arranged. The main manuscript is separated into introduction, material and methods, results and discussions, conclusions and an appendix part. Due to its length of 42 pages including figures and references and 20 pages in the Appendix, it is sometimes difficult for the reader to follow the line of thought. The conclusions with almost 3 pages should be condensed, many discussed aspects could be merged into the introduction and discussion part. In general, the manuscript needs some additional work to improve the readability and to clarify the main key messages for the reader and avoid redundant informations. Also typos and the german-style syntax sometimes hampers the reader to fully grasp the content of the manuscript.

Figures have good quality and are informative, some are overloaded with up to 27 curves. Literature is sufficiently covered with 97 references. The investigation of the impact of climate boundary conditions on the future evolution of the Antarctic ice sheet supports the publication in ESD. However, as the main focus seems to be on the evaluation of climate model result and the systematic and comprehensive sensitivity analysis of the ice sheet model to the two different types of precipitation forcing, this study would also very well fit into a model-specific journal like GMD.

This study by Rodehacke et al. has the potential to be a valuable contribution to the scientific community of ice sheet modelers, as it considers relevant aspects of commonly used boundary conditions with potentially serious consequences for estimates of future sea-level change.

I encourage the authors to consider the following detailed suggestions and to improve the manuscript accordingly.

Thank you very much for reviewing our manuscript, your engagement, and your encouraging comments.

Specific comments:

1. The title should be refomulated. It is not easy to understand the content before having read the abstract. Also I wonder, if the more word “Ansatz” is commonly known in the wider scientific community apart from mathematicians. I would suggest: “Future sea-level contribution from the Antarctic Ice Sheet for different precipitation forcings based on CMIP5 models”

We are aware that the word Ansatz of German-origin is not widely used. But we prefer concise wording. Ansatz describes precisely the problem. The way how the precipitation is described/implemented in a mathematically and physical sense. In contrast, the suggested title is misleading because we do not use a different set of forcings, actually. However, we implement the available climate states differently to drive our ensemble of ice-sheet simulations.

2. As a surprising result the simulated Antarctic Ice Sheet gains mass under future global warming for directly applied climate model anomalies (temperature and precipitation). As this part has some delicate political implications it needs a clear discussion of the responsible model settings.

We are aware of the political implications of our results. Therefore, we have already discussed various influencing factors in the conclusion section, which you suggest to shorten. Hence, we do not see the need to expand this conclusion and the extensive discussion further because those parts would not be read by those who would like to misuse our results for their agenda. However, we extend both the "abstract" and "Plain Language Summary" sections to indicate the limitations of our study. In addition, we introduce the limitation of our forcing choices and its physical foundation.

In the abstract, we add “In contrast to various former studies, only the historical (1850--2005) and scenario (2006--2100) forcing drive our ensemble of simulations, which neglects unavoidable continuous warming consistent with the higher climate scenarios beyond the year 2100.”

We append to the "Plain Language Summary" section: “Since we use only the available climate scenarios until the year 2100, any additional warming after 2100 may turn the ice gain into an ice loss under a strongly changing climate.”

In addition, we add to the “Material and Methods” section, a paragraph discussing the above-indicated limitation: “The repetition of the last 30 years of climate forcing beyond the year 2100 is a simplification, which is not entirely consistent with the applied climate scenarios. An ongoing growing atmospheric greenhouse concentration triggers changes in the climate system. While the atmospheric radiation reacts immediately, the redistribution of the accompanied heating within the global ocean is much slower (Hansen et al., 2011). This delay is critical because the majority of the additional heat ends in the worldwide ocean (Church et al., 2011, 2013b). Consequently, further warming is inevitable after the cessation of greenhouse emissions (Hansen et al., 2005). Our simulations do not reflect this ongoing warming. Also, a disintegrating Greenland ice sheet will raise the global sea level, and, as a consequence of Greenland’s reduced gravitational pull (Whitehouse, 2018), the sea level rise is in particular pronounced around Antarctica (Mitrovica et al., 2001). A rising sea level potentially migrates the grounding lines inshore, which ultimately destabilizes ice shelves and causes a more vulnerable Antarctic ice sheet. Despite, the same gravitational effect may buttress Antarctica, whether Antarctica’s ice loss is slow enough (Gomez et al., 2010) and Greenland stabilizes. However, the ongoing thermal expansion of the ocean, which is currently the driver of the rising sea level (Rietbroek et al., 2016), will probably destabilize Antarctica. Therefore, our ensemble of ice sheet simulations is not a projection.”

2a. Although the equilibrium state fits well observations of ice thickness and grounding line, the involved mass fluxes may not. Total ice loss rates by melting and in particular by calving are overestimated by a factor of 2-3 depending on the used eigencalving rate constant. Hence also the

surface mass balance seems to be overestimated accordingly. The authors imply that the uncertainties in the regional climate model results (RACMO), which are used as a present day reference field, are large enough to overestimate in particular the large slow-flowing and very dry inner-continental regions of the EAIS, where small absolute changes in precipitation can have large consequences for the total mass balance of the equilibrium state. Also, it is not clear from the description in the manuscript how the yearly cycle in the PDD scheme is estimated from the climate models (annual mean and summer temperatures) in order to obtain estimates of the surface mass balance components for given air temperature and precipitation forcing. A potential misfit in boundary conditions may be compensated for by a well-chosen set of model parameters, such that the equilibrium state bounds observational constraints. However, this potential overfitting of the initial equilibrium state may then have consequences for the projected ice mass changes, as the authors already speculate. In general, the equilibrium state method favors rather stable ice sheet configurations, which may not be realistic.

PDD: We have utilized the in PISM implemented PDD. During our analysis, we've compared the original surface mass balance (SMB) coming from the named RACMO data set with the SMB calculated by the PDD approach with and without considering a lapse rate of -7K km^{-1}. All these SMB are identical. Only if the surface elevation between the RACMO data set and the simulated elevation differ, the lapse rate shifts the air temperature, which introduces a difference in the SMB. The contemporary near-surface air temperature (we use the 2m-air temperature), except for the Antarctic Peninsula, is well below the freezing point temperature of meteoric freshwater (Figure A1a). Even the maximal warming of 8 Kelvin (Figure A1d), which occurs offshore, does not drive widespread surface melting generating ice mass loss. Therefore, the here used parametrized SMB calculated by the PDD approach is not critical. Please see, also, specific technical comment l.143 below, where we address the issue with the used PDD approach in more detail. In addition, we added a new appendix figure highlighting the surface mass balance; please see figure A16.

2b. The authors state one main difference to previous studies related to the forcing after the year 2100, which is commonly extrapolated into the future, while in this study it remains quasi constant (within 30 years variability). There seems to be another important difference in the methodology of this study in comparison to other studies. All climate model anomalies are inferred with respect to a preindustrial control simulation. However, the reference climate of the 19th century does not really match the modern climate, which the used mean background fields (from RACMO as mean over period 1979–2011 and from World Ocean Atlas as climatological mean) are related to. This precedure minimized the shock at the beginning of each simulation at 1850, but it adds some anomaly to the present-day background field when arriving at present-day in the simulations and it overestimates the future temperatures and precipitation rates applied to the Antarctic Ice Sheet. I encourage the authors to run some test simulations with shifted anomaly (negative anomaly in the preindustrial era and vanishing anomaly in present-day period).

It is right that we have not corrected the difference between the pre-industrial and the recent historical period (RACMO: 1979—2011, WOA: 1955—2006), since this difference is neglectable, e.g., 2m-air temperature (Figure 3b).

We would have liked to use instead of the RACMO atmospheric fields verified and validated distributions representing the pre-industrial state. However, these are not available (to our knowledge), except you consider spatially regridded shallow ice cores, which are subject to a distinct uncertainty, or fields coming from global climate models or could be deduced from these climate models. Since global climate models are not free of biases, we would have introduced an error, which is probably much larger than the mentioned offset. We have done experiments where CMIP5 model output has driven our ice-sheet model directly. We see that the simulations, which are driven by anomalies, are much less impacted by climate model biases.

Nevertheless, let us do a gedankenexperiment (Popper, 1935), where we would have considered this effect. A most probably slightly reduced surface mass balance would have been balanced by a slightly lower lateral ice loss via iceberg calving and basal melting to obtain a quasi-equilibrium state. This state would have been our initial state. Now we would run our ensemble from 1850 to the year 2100 and continue as we have done. The precipitation increase would be slightly less, the basal melting loss would also be slightly less, and the balance between these would be similar. We are confident about this conclusion because of our already existing ensemble with members showing a small increase. These members support this conclusion. With the current setup, which considers a slightly too strong forcing, we may promote enhanced basal melting (quadratic equation). However, the diagnostically deduced sea-level impact of the two ways to describe the sea-level dependence of the precipitation boundary condition (Figure 6b and 6d) is independent of the used reference state.

To conclude, the here used setup could be improved, but the conclusion is robust about the mentioned reference period of the background data set.

Popper, Karl. 1935. Logik Der Forschung. Edited by Philipp Frank and Moritz Schlick. Schriften zur Wissenschaftlichen Weltauffassung. Vienna: Springer Vienna. ISBN: 978-3-7091-2021-7.

2c. Regarding the basal melt parameterization, no details on sensitivity can be found in this study nor in the cited study by Sutter et al., 2019. What technique is used to extrapolate ocean temperatures into the ice shelf cavities? Are basin-wise overflow depths considered? Are extrapolated ocean temperatures vertically interpolated at the ice shelf base? Can refreezing occur? A simimar melt parameterization with quadratic dependency on thermal forcing has been calibrated in Jourdain et al., 2019 (https://doi.org/10.5194/tc-2019-277). They show that the choice of the particular parameterization and the associate parameters can have a huge impact on the ice sheet response. The authors discuss that the used melt parameterization may underestimate the melting and therefore apply bias-corrected melt rates as a sensitivity check, which does not cause considerable changes in the ice sheet response. The effect of basal melt could be also strongly intensified by using the melt interpolation across the grounding line (optional in PISM).

We have extended the description regarding the extrapolation (please see specific issue l.144), which also answers the question regarding the overflow depths. As part of the ocean forcing, we use the full 3D ocean temperature distribution so that the actual temperature at the ice shelf base drives the ocean melting, whereas our approach does not consider refreezing. In our understanding, ocean-driven basal melting does not occur beyond (inshore) the grounding line, because grounded ice stifles the flow of ocean water.

Since we use a sub-grid scale grounding line parameterization, we could have allowed partial basal melting proportional to the floating fraction. In pilot studies, the impact of the fractional basal melting has shown a minor effect on our simulations. Studies suggest that tides amplify frontal melting and locally also basal melting (Padman et al., 2018). In contrast, a tidal-driven front, which develops near the groundling line, hinders the flow of water which ultimately lowers the basal melting near the grounding line (Holland, 2008). First ocean observations in the groundline zone of the Ross Ice Shelf show low basal melting rates (Begemann et al., 2018). We decided to compute melting only for fully floating grid cells.

Begeman, Carolyn Branecky, Slawek M. Tulaczyk, Oliver J. Marsh, Jill A. Mikucki, Timothy P. Stanton, Timothy O. Hodson, Matthew R. Siegfried, Ross D. Powell, Knut Christianson, and Matt A. King. 2018. “Ocean Stratification and Low Melt Rates at the Ross Ice Shelf Grounding Zone.” Journal of Geophysical Research: Oceans 123 (10): 7438–52. https://doi.org/10.1029/2018JC013987.

Holland, Paul R. 2008. “A Model of Tidally Dominated Ocean Processes near Ice Shelf Grounding Lines.” Journal of Geophysical Research 113 (C11): C11002.

https://doi.org/10.1029/2007JC004576.

Padman, Laurie, Matthew R. Siegfried, and Helen A. Fricker. 2018. “Ocean Tide Influences on the Antarctic and Greenland Ice Sheets.” Reviews of Geophysics 56 (1): 142–84. https://doi.org/10.1002/2016RG000546.

If we drive a newer PISM version (V1.1.4), where the ocean-driven basal melting is parameterized with the PICO submodel as part of PISM (Reese et al., 2018), with climate forcing from our climate model (AWI-CM, which is not part of the here use CMIP5 models), we also detect a growing Antarctic ice sheet. Therefore, we are confident that our parameter choices are not decisive and that our results are robust.

Reese, Ronja, Torsten Albrecht, Matthias Mengel, Xylar Asay-Davis, and Ricarda Winkelmann. 2018. “Antarctic Sub-Shelf Melt Rates via PICO.” The Cryosphere 12 (6): 1969–85. https://doi.org/10.5194/tc-12-1969-2018.

3. The authors define different ways of expressing (integrated) mass changes in terms of sea-level equivalent changes and I would wish that it should be made clear when just a theoretical unit conversion is applied (potential sea level change) or when it is an actual sea-level contribution in terms of projected ice mass change. And if the latter it should be clearly defined whether only ice masses above flotation are considered. What diagnostic has been in fact used here?

Clarified by adding the following paragraph and applying related changes through the manuscript: ”In this manuscript, we distinguish between potential sea level and simulated sea level. The potential sea level is the transformation of an ice mass or freshwater volume into a global sea level by applying a global ocean area of $3.61 \cdot 10^{14}\,m^2$ (Gill, 1982). In contrast, the simulated sea level is a diagnostic of the ice sheet model, which takes into account the total mass above flotation and the global ocean area. ”

4. The manuscript states that the used coarse resolution of 16km may have consequences for the adequate representation of ice stream dynamics. I assume that this model choice is a consequence of the initial equilibriumn state, which requires hundred thousands model years to evolve. The authors state that basal resistance is described by a Mohr-Coulomb law with plastic till, but they do not discuss relevant parameters involved, such as the till friction angle or the till water decay rate. What is the vertical resolution of the enthalpy module? These parameters can strongly affect the ice stream dynamics also for coarse resolutions.

The till water decay rate amounts to 3.1687646154128e-11 meter $seconds^{-1}$. We have not activated the hydrological model. The till fraction angle ranges from 10° for our bedrock at and below 700 m below the contemporary sea level at the start in the year 1950. With rising bedrock altitude, the friction angle increases linearly until 200 m above sea level and stabilizes at 30° (Figure I). Our mean vertical resolution is 67.9 m. Albrecht et al. (2020) show that a lower vertical resolution leads to a bigger ice sheet under transient forcing and, also, it promotes a more stable ice sheet.

Albrecht, Torsten, Ricarda Winkelmann, and Anders Levermann. 2020. “Glacial-Cycle Simulations of the Antarctic Ice Sheet with the Parallel Ice Sheet Model (PISM) -- Part 1: Boundary Conditions and Climatic Forcing.” The Cryosphere 14 (2): 599–632. https://doi.org/10.5194/tc-14-599-2020.

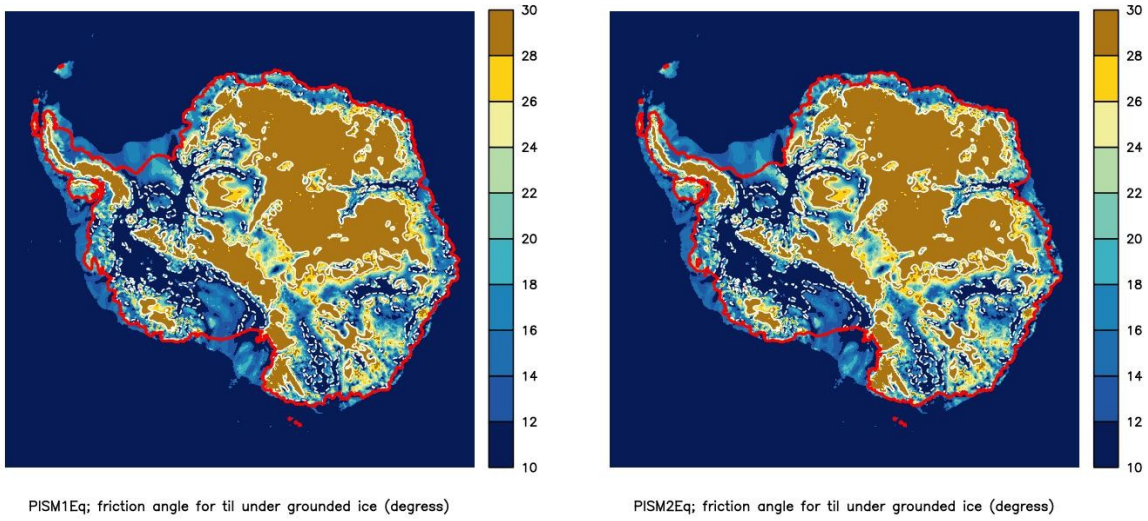

Figure I: Till fraction angle for till under grounded ice. The left (right) side shows the fraction angle for the initial states PISM1Eq (PISM2Eq). The red contour outlines the ice sheet or ice shelf outer edge. Under ice, the dash, and white contour line follow the -700m and the 200m, respectively, bedrock altitude in the year 1850.

5. The authors use a rather old PISM version (v0.7), most likely for consistency reasons (initMIP and other model intercomparisons). However, PISM has evolved over the last years and some relevant aspects have been improved, which may affect the results of this study. For instance, the authors mention a bug in the elastic part of the LC solid Earth model, but also the viscous part was flawed and considered changes in ice shelf thickness as loads. Accordingly strong melt would cause uplift of the cavity bed and hence result in a stabilized grounding line. Also the till water distribution along the grounding line has been fixed meanwhile causing a much higher grounding line sensitivity. I guess also the sea-level potential diagnostic has been fixed meanwhile (now substracting the part below flotation). These are many good arguments in favor of a more recent PISM version and they suggest that Antarctic Ice Sheet simulations could respond with much higher sensitivity to the same forcing applied.

In our code basis, we fixed some code issues, such as the reproducibility and restart issues, which are also related to the bedrock code. In our simulations, we consider the viscous-part of the glacial isostatic adjustment (GIA) and do not use the elastic part. As explained below, an improved GIA model would maintain a more stable configuration of the grounding line, so that the discussed sea-level decline under a warming climate would be even more pronounced. Please see the special technical comment l.151. Please see also our reply to the technical issue of the appendix figure A15, where we state that we have a relatively stable grounding line in our simulations while the calving front retreat is more pronounced.

Technical corrections:

l.2: “heavier precipitation fallen on Antarctica will counteract any stronger iceberg discharge...”=>“precipitation will likely increase even more and may counteract stronger iceberg discharge...”

A warming climate accompanies increased precipitation due to the Clausius-Clapeyron relation. Hence we prefer: “Simulated future projections reveal that heavier precipitation, fallen on Antarctica, may counteract amplified iceberg discharge and increased basal melting of floating ice shelves driven by a warming ocean.”

l.3: “from nine CMIP5 models future projections”=>“future projections from nine CMIP5 models”

We follow your request.

l.5: “The spatial and temporal varying climate forcings drive ice-sheet simulations. Hence, our ensemble inherits all spatial and temporal climate patterns, which is in contrast to a spatial mean forcing.:” => “The spatially and temporally varying climatic forcing drive the ice-sheet simulations, such that all climate patterns are represented in our ensemble, which is fundamentally different from using spatial means as forcing.”

We follow your suggestion and use: “The spatially and temporally varying climatic forcing drives ice-sheet simulations, such that our ensemble represents all climate patterns, which is fundamentally different from using spatial means as forcing.”

l.7: Regardless of the applied boundary condition and forcing, some areas will lose ice in the future, such as the glaciers from the West Antarctic Ice Sheet draining into the Amundsen Sea.” => ..., our ensemble study suggests that some areas will lose ice in the future, …

Done.

l.10: “This strip also shows...” instead of using “... too.”

Rewritten as requested.

l.25: “How strong the precipitation grows in a warming atmosphere, may be explained by the dissimilarity between the applied methods to describe the precipitation.” => The discrepancy of the simulation results between the applied methods to describe the precipitation illustrates the uncertainty of the possible range of future precipitation growth in a warming atmosphere.

We follow your suggestion and use: “The discrepancy of the simulation results between both methods describing the precipitation illustrates the uncertainty of the possible range of future precipitation growth in a warming atmosphere.”

l.30: “...impacts globally numerous economic activities...” => “...impacts numerous economic activities globally...”

Done.

l.31: “... or dedicated model simulations of, for instance, ice-sheet models.” => “... or process-based model simulation, e.g. ice-sheet models.”

Changed.

l.34: “... are simplified descriptions by analytical equations” => “... are either simplified descriptions based on linear multiple-regression analysis ... or”

Rephrased as requested.

l.36: “The simplified forcing, which usually does not show a dedicated spatial structure” => As surface elevation is a key variable in those parameterizations, the geometry of the ice sheet in fact leave some characteristic spatial structure.

We might have been misunderstood, hence we clarify: “The simplified temporal forcing, which usually does not show a dedicated spatial structure ...”

l.58: “temperature scaling” => “temperature scaling factor for precipitation” or “precipitation-temperature scaling ”

Thanks, we use: “temperature scaling factor for precipitation”

l.71: Add comma before “probably”

Done.

l.124: Maybe omit “full” here.

It's like the term “Full Stokes”, which is not entirely correct but everybody uses this term. We would like to keep it for clarity.

l.126: As in the title, I would recommend to use: “The type of precipitation forcing” or “the used method for applying precipitation forcing” instead of “the Ansatz of the precipitation”.

Since a noun has to start with a lower case at the beginning, we correct it. As stated above, the word ansatz describes what we mean precisely.

l.130: “The latter is common, while some keep the surface mass balance constant.” => “The latter approach is commonly used, in particular in paleo applications, while some sensitivity studies keep the surface mass balance constant.”

We follow your request.

l.138: It could help the reader to have some definition of the piControl simulation here, e.g. “pre-industrial coupled atmosphere/ocean are performed at constant pre-industrial CO2 levels for x model years”.

We cite literature and clarify the sentence introducing this paragraph: “Nine CMIP5 models deliver the following climate scenarios (see Table 1, Taylor et al. (2012)): control run under pre-industrial conditions (piControl), the historical period (1850-2005), as well as RCP2.6, RCP4.5, and RCP8.5 (2006-2100, Vuuren et al. (2011)).”

l.140: “... differ commonly marginally.” => “...show in general marginal differences.”

Rephrased as suggested.

l.144: How does this extrapolation works? Is there a diffusion scheme applied for each vertical ocean temperature level? What are the source regions, the continental shelf or also the deeper ocean regions (this is not so clear from Fig. 3e), which are separated from the deeper cavity regions by the continental shelf? There is also no detailed description in Sutter et al., 2019, even though sub-shelf melting is a key process here.

We clarify: “... extrapolated horizontally into the ice shelves to mimic isopycnical flow: The operator 'fillmiss2' of the Climate Data Operators' (\href{https://code.mpimet.mpg.de/projects/cdo}{cdo}) tool kit acts on the original CMIP5 ocean grid.”

l.146: “... following the positive degree day (PDD) approach, where the annual 2mair temperature standard deviation comes from daily CMIP5 model values.” Does this mean that every year one different PDD standard deviation is applied to the whole computational setup or is it grid-cell wise?

In l.143 it is mentioned that “annual mean forcing” is ued, but what about the summer temperature anomaly to estimate the yearly cycle?

We use the PDD implementation of the PISM and perform the computation for each grid-cell; we clarify: “To allow for surface melting under a warming climate, the surface mass balance (SMB) is calculated following the positive degree day (PDD) approach (Braithwaite, 1995; Hock, 2005; Ohmura, 2001) as implemented in the PISM model (ThePISM Authors, 2015a, b). The turn of the hydrological year occurs on day 91 and the PDD factor for snow and ice are 0.3296 cm(IE) Kelvin^{-1} day^{-1} and 0.8792 cm(IE) Kelvin^{-1} day^{-1}, respectively. Here, the evolving annual 2m-air temperature standard deviation is derived from daily CMIP5 model values for each ice sheet model grid-cell.” Besides, at the end-of-the-21-century, summer temperatures are in general still too cold to drive widespread surface ablation.

l.148: “16 km” => What is the reason for this relatively coarse resolution, the availability of an equilibrium state?

We have run a much larger ensemble of several thousand members. Here we analyze only a subset of this full ensemble.

l.149: “utilizes” => “applies”

Changed to “employs”

l.151: Also the viscous part in v0.7 was somewhat unrealistic, as also ice shelf thickness change has been considered as loads in the LC bed deformation model, which has strong effects on grounding line sensitivity.

We are aware that the viscous part of the GIA model could better represent the impact of a changing ice shelf thickness. In our understanding, the updated implementation would maintain a more stable configuration of the grounding line, which would support firmer ice shelves and a more durable ice sheet. Ultimately, the here discussed sea-level decline under a warming climate would be even more pronounced.

l.154: “... pressure-dependent melting temperature” => Add “...of the ice”

Done.

l.157: “...while the grounding line position is determined on a sub-grid space (Feldmann et al., 2014).” => Add “... to interpolate basal friction.”

Rephrased.

l.161: “...stress field divergence... ” => “... divergence of the strain/velocity field” or “trace of the strain-rate field”

We accept the second suggestion, joyfully.

l.161: You should add units “m s” here as the Levermann et al. 2012 paper uses “m a”.

Good point, we add as requested the units.

l.162: “(PISM1Eq and PISM2Eq)“=>This can be confusing, either you switch the order here or the order of the eigencalving constants in the sentence before.

We changed as suggested.

l.163: “Ocean temperatures from the World Ocean Atlas 2009 (Locarnini et al., 2010) and the multi-year mean surface mass balance (SMB) from the RACMO 2.3/ANT model (Van Wessem et al., 2014) drive PISM during spin-up (Table 2).” => Hence, this is a present-day forcing equilibrium.

This is correct. Please, also see our related reply to your specific comments 2b.

l.169: “... releasing less carbon dioxide.” => Maybe add “(e.g. RCP2.6).”

We followed your suggestion.

l.171: “the RCP8.5 scenario path” => “the high emission RCP8.5 scenario path”

Done.

l.175: maybe add a “\,” in the unit “\unit{cmyear−1}”

Good catch; done as suggested.

l.176: “...warms by nearly 1 ± 0.18 #C (Figure 3c).” => Add “in the same period”

Done.

l.177: ”... these increases become stronger.” => “this warming trend/rate becomes stronger.”

We use: “this warming trend becomes stronger.”

l.179: “current trends” => “currently observed trends”

Done.

l.189: “Areas of heavy precipitation under the reference climate (Figure 2b) also receive the highest increments.”

Sorry, but it is unclear.

l.195: “Also, the Amundsen Sea in front of Pine Island Glacier and Thwaites Glacier is cold. Here, the temperature might be too cold, which justifies the applied melting correction.” => Which melt correction did you use? And “too cold” with respect to World Ocean Atlas?

“Here, the climatological temperature distribution might be too cold because it does not replicate the confined flow of warm water masses through glacier-scoured troughs towards ice shelves. To overcome this limitation, we apply a spatially restricted melting correction. It increases the melting by 50% for the Ronne Ice Shelf region, and it quadruples melting for coastal parts of the West Antarctic Ice Sheet between the Antarctic Peninsula and the Getz Ice Shelf (east of the Ross Ice Shelf).”

l.205: “...do not necessarily grow in parallel.” => Do you mean they are “not necessarily correlated”?

We use: “not necessarily correlate.”

l.209: “ice-sheet” => “Ice-sheet”

Changed.

l.214: The unit of Eq. 1 should read % K−1, hence #T should be in the denominator.

Indeed! We corrected.

l.215: So P0 equals Pt=0 in Eq. 1?

We correct: “$P_{t=0}=0=P(t_{ref})$”

l.217: Eq. 2 should have a number. And should #P be replaced by P0?

We follow your advice and label this equation. In addition, we expanded the equation, so that it

becomes clear that it should be ΔP.

l.221: “...these locations. The difference is distinct for Vostok...” =>“...ice core locations. The difference is most prominent for Vostok ice core...”

We revise as requested.

l.226: “Thus, we can safely restrict the analysis on the first 50 years.” => of which simulation?

To avoid ambiguity, we expand the sentence: “Thus, we can safely restrict the analysis and use as a reference for the computation of the anomalies the first 50 years of the piControl climate.”

l.230: “Map 1” => “Map in Figure 1”

We rephrase as suggested.

l.233: “... c-like area” => “...half-moon-shaped area” or just “... c-shaped area”

We prefer to use the second suggestion: “c-shaped area”

l.242: ”We detect a slight trend to higher values if we restrict the analysis to ground ice.” Maybe mention at this point that the difference results from excluded ice shelf regions, which are associated with x% of the total glacierized area and which are characterized by relatively shallow surface elevation along the ocean margin

We extend to: “We detect a slight trend to higher values if we restrict the analysis to ground ice (87.5 % of the glaciated area, see Table 4); it excludes floating ice shelves with low elevation along the coasts.”

l.243: “the difference between scenarios is more decisive” => “the impact of the choice of the scenarios is larger...”

Rephrased with “However, the scenario selection is decisive, while the choice between … ”

l.245: “... Within their variability, many ensemble members are invariant against the applied scenario...” => “The sensitivity of many ensemble members to the range of applied scenario is within their variability...”

Taken.

l.250: “... Antarctica’s large-scale drainage basins.” => Please provide a reference here, e.g. Zwally et al., 2015

As suggested we added citations for different oceanographic zones and drainage basins.

l.251: “This division...” => “This chosen division...”

Done.

l.253: “...with a tendency of higher values...” => “...with a tendency towards higher values...”

Done.

l.261: “The region “Siple Coast” as a part of the “WAIS” region is different in many aspects. It has the smallest area..” =>so it has a low weight in the spatial mean?!

Each area has its own spatial mean regardless of its actual area size. We clarify: “The region 'Siple Coast' (area $0.69 \cdot 10^6 km^2$, see Table 4) as a part of the 'WAIS' region (area $4.26 \cdot 10^6 km^2$) is different in many aspects. It has the smallest area compared to the other regions (Table 4)”

l.263: “...while the spread of trends among individual ensemble members is substantial.” => Why

not provide a number range at some points in the text?

We link to the requested information provided in one of our figures: “ the spread of trends among individual ensemble members is substantial (Figure 5).”

l.267: “... trend in snow accumulation ...” =>“... trend in observed snow accumulation...” to make sure that you switched from model results to observations in this paragraph

Yes, we adjust as requested.

l.273: “... a unrealistic declining February sea ice trend” => “... an unrealistically declining February sea ice trend”

We follow your suggestion.

l.280: “which is also reflected by the maxima in these regions.” => maxima in scaling factors?

Clarified by “the scaling factor maxima in these regions”

l.281: “Also, the Ross Ice Shelf and the adjacent Siple Coast feature on average the lowest scaling factors across the entire ice sheet. Some individual ensemble members project even negative scaling: precipitation deficit for rising temperatures.” Is this related to the Frieler et al., 2015 study or does this repeat the previous paragraph?

Clarified: “As before, the Ross Ice Shelf and the adjacent Siple Coast feature, on average, the lowest scaling factors across the entire ice sheet (Figures 4 and 5). Some individual ensemble members project even negative scaling: precipitation deficit for rising temperatures (Figures 4 and 5).”

l.296: “The integrated precipitation shows a more pronounced temporal change, because the integral and not the mean precipitation is calculated, where the vast light precipitation regions lessen the average precipitation signal.” Isn’t the difference just a scaling factor, i.e. the considered area? I guess you are talking about a power-law distribution with a large weight of the continental areas with very low precipitation?

Clarified: “The integrated precipitation shows a more pronounced temporal change because the vast interior, characterized by light precipitation, governs the integral.”

l.301: “... under the precipitation anomalies,” =>“... for applied precipitation anomalies,”

Rephrased as requested.

l.306: “if we would apply this low scaling of 2 % K−1.” Isn’t this mentioned in the beginning of the sentence?

Indeed, hence it is discarded.

l.316: “Over the entire Antarctic continent, precipitation and temperature grow simultaneously in climate model simulations of the future.” => To summarize, precipitation and temperature, as average over the entire Antarctic continent, grow simultaneously in climate model simulations of the future.”

Done.

l.320: “the on Antarctica accumulated snowfall” => “the snowfall accumulated on Antarctica”

Done.

l.325: “... the implemented precipitation boundary condition...” => “... the applied precipitation boundary condition...” or “... the choice of the precipitation boundary condition...”

We follow your second suggestion.

l.327: “These together constitute the ensemble of ice-sheet simulations.” =>It would be nice to provide the size of the ensemble (3 sceanarios x 9 climate models x 2 reference periods x 2 precipitation forcing = 108 simulations?)

We write “ … ensemble of 208 ice-sheet simulations (Table 1)” and add additional information to the corresponding table caption “Since we do not use the RCP2.6 scenario of the CCSM4 model, the ensemble comprises 26 anomaly forcing scenarios. The climate anomalies are computed relative to the first or last 50 years of the corresponding piCtrl. Each scenario starts from the initial condition PISM1Eq (Figure A10) or PISM2Eq (Figure A11) and is driven by two precipitation conditions (see main text for details, e.g. section 3.2). Hence, the ensemble of anomaly ice sheet simulations has 208 members.”

l.332: “...detected trend of about 2 mm decade−1 (sea-level equivalent) fades within the first 400 years...” => How can this trend be justified? Is the present-day reference forcing different from the one used in the spin-up? Or is this due to bed deformation? What figure shows this trend? It should be shown somewhere (Fig. 6?) as it amount to about 2cm after 100 model year and is substracted from the prejection results, right?

We take the explanation from the discussion to here and address in addition the remark l548.

l.337: “ than the simulations” => than in the simulations

Done.

l.338: Insert comma

Done.

l.340: “A ring of a pronounced negative thickness difference follows the coast, where the precipitation anomaly (Figure 2e, h, k) is enhanced.” => “However, we find a negative thickness difference within a narrow band along the coast, where the precipitation anomalies (Figure 2e, h, k) suggest less accumulation that the scaling.”

We do not come to this conclusion about the scaling because the ocean also influences the ice thickness along the coast. So we keep the descriptive character.

l.344 “... are negative” Please be more precise in this paragraph, what quantity is negative.

Rephrased: “Furthermore, as part of the WAIS these values are present in the coastal strip from the Antarctic Peninsula to the Ross Ice Shelf and along the eastern flank of the Transantarctic Mountain Range (Figure 4).”

l.347: K-1 superscript

Good catch; done.

l.349: “... the ice thicknesses of the ensemble means..” => “... the mean ice thickness of each of the respective sub ensembles...”

Rephrased as requested.

l.354: “This reduction marks those outlet glaciers and ice shelves that are extremely vulnerable.” Doesn’t it say that ice losses under global warming are larger than gains?

Regardless of the applied RCP8.5 climate forcing coming from our pool of climate models (Table 1), these outlet glaciers and ice shelves lose mass, where the corresponding ice thickness is negative. Consequently, the loss outweighs the gain.

l.359: “... ice-shelf weakening, ice thinning ...” => “... ice-shelf weakening, as well as ice thinning ...”

Rephrased as suggest and reordered: “ice-shelf thinning, as well as ice-shelf weakening, ”

l.365: “...and restrict ourselves first to the model year 2100, where the precipitation anomalies of the period 1850-2100 shape the ice-sheet thickness distribution of the year 2100.” => “the history of precipitation anomalies”

Rephrased: “and restrict ourselves first to the model year 2100, when the transient forcing of period 1850--2100 excites changing ice thicknesses.”

l.367: “Directly at margins apart from the vast ice shelves, the attributed model that drives either the maximum or minimum ice thickness shows a noisy small scale pattern, which is driven by the variety of the involved models (Figure 8d, e).” => I guess you want to say, that the maximum or minimum ice thickness in marginal regions cannot be associated with a particular climate model, while in contrast, for ice shelf regions...

Thanks, we modified as requested.

l.372: “... while it also drives its thinning of the Ross Ice Shelf (Figure 8e) predominantly.” => “... while it causes predominantly thinning within the main Ross Ice Shelf (Figure 8e).”

Done.

l.373: “Since the spatial pattern of the atmospheric and ocean forcing that promotes or undermines the ice thickness is not necessarily aligned, this may explain the small scale noisy pattern along the coast.” => Maybe this explanation is not sufficient. The coastal regions is where most of the (nonlinear) dynamical changes on the considered time scales occur in response to both ocean and atmospheric forcing.

Various studies show commonly a linear behavior, but we add this though, joyfully.

l.388: “NorESM1-M influences the WAIS, which is in accordance with the detected lowest scaling in the Siple Coast (Figure 5), CSIRO-Mk3-6-0 has an impact around the South Pole, MRI-CGCM3 has coastal zone in the EAIS, while the control of MPI-ESM-LR and, to a lesser extent, HadGEM2-ES spreads across the entire continent.” => The reader may get lost here by the wording. Make sure that you are talking about the attribution of the minimum ice thickness to different climate models. You could also add percentages of the Antarctic area in the text to quantify the dominance. Similar issue for the maximum in l.398 ff.

Adding more information, such as the suggested percentages, would inflate the text and its complexity. Also, these values are most probably specific to the here used selection of climate models and do not represent a particular physical process. Therefore, we would like to drop this idea. Nevertheless, we simplify the sentence structure and break the sentences into pieces to help the reader: “NorESM1-M influences the WAIS, which is supported by its lowest scaling in the Siple Coast region (Figure 5). CSIRO-Mk3-6-0 has an impact around the South Pole, MRI-CGCM3 affects the coastal zone in the EAIS. The control of MPI-ESM-LR and, to a lesser extent, HadGEM2-ES spreads across the entire continent.”

l.393: “If we now turn towards the temperature scaled model simulations, the mean, maximum, and minimum ice thickness distribution...” => “If we now turn towards those model simulations, in which the temperature-scaled precipitation forcing has been applied, both the mean, maximum, and minimum ice thickness distribution...”

Changed as requested.

l.396: “The latter shows that the ocean controls ice-shelf thickness changes in our simulations

primarily.” => “The latter shows that primarily the ocean controls ice-shelf thickness changes in our simulations.” or “The latter shows that the ocean primarily controls ice-shelf thickness changes in our simulations.”

Changed as suggested.

l.402: “precipitation driven” => “precipitation-driven”

Done.

l.409: Are you referring to all three scenarios here or just RCP8.5?

Clarified: “For all climate scenarios, ...”

l.413: “...is quasi-constant until 2000 and declines afterward (Figure A15). For RCP8.5, the basal melting increases at the end of the 21st century quadratic.” => “...remains quasi-constant until 2000 and declines afterwards (Figure A15). For RCP8.5, the basal melting increases at the end of the 21st century quadratically.”

Done.

l.415: “... while the basal melting increases by approximately 33 % since the year 2000.” => until 2100?

Rephrased: “between the years 2000 and 2100.”

l.417: “The basal melting rates for PISM1Eq and PISM2Eq are similar, however, the loss rates for PISM1Eq are slightly larger than PISM2Eq (Figure A13).” => This means more basal melting for smaller ice shelf area? What is the portion of refreezing?

It is correct that smaller ice shelves are subject to more basal melting, while refreezing does not occur.

l.420: “Since floating ice shelves nourish both ice losses, these ice losses do not impact the sea-level directly.” => “Although floating ice shelves are subject to both types of ice loss, these ice losses do not directly impact the sea-level.

We follow your suggestion partly and write: “Since floating ice shelves nourish both ice losses, these ice losses do not directly impact the sea-level.”

l.423: “ generates ” => “ would consequently generate ”

Done.

l.425: “is not a 1:1 relation.” => “is obviously not a 1:1 relation.”

Done.

l.426: Shouldn’t there be a time period involved, e.g. by 2100?

To avoid any ambiguity, we added as requested, even if we haven't changed the discussed period (1850-2100).

l.427: “It is less than integrated precipitation anomalies...” => “This is less than the integrated precipitation anomalies..., which explains the total mass gains.”

Added.

l.429: “Anyhow, the integrated basal melting rates are too low and the calving rates are too high compared to observational estimates in our ensemble of ice-sheet model simulations.” => What does too low and too high mean here, beyond observational uncertainty? Maybe quantify in terms

of percent?

We link to the corresponding figures, because in all figures depicting the total mass loss (Figure 11), calving rates (Figure A12), and basal melting rates (Figure A13), independent estimates are provided by symbols. In addition, the reported uncertainties of these estimates are provided, if they are larger than the corresponding symbol sizes, as stated in each corresponding figure caption.

l.436: “ loses mass ” => “ lost mass ”

Rephrased to “have lost mass”

l.449: “the basal melting rated of grounded ice” => “the basal melt rate at he base of the grounded ice”

I'm sorry, but to my knowledge, basal melting occurs at the base. Since we would like to avoid this pleonasm, we keep the original sentence.

l.449: “Please note that this is not driven by any trend in the continued ice-sheet simulations under the reference climate (Table 2) since we have substracted this trend.” => “Please note that there is no drift involved, as we subtracted the trend from the continued ice-sheet simulations under the reference climate (Table 2).”

Thanks, changed.

l.451: “We also detect an amplified signal for the simulations driven by the precipitation anomalies than scaled precipitation, which corresponds to the above diagnosed sea level impact of the precipitation (Figure 6).” => Please reformulate!

Reformulated: “We also detect an amplified signal for the simulations driven by the precipitation anomalies compared to those forced by temperature-scaled precipitation anomalies, which corresponds to the above diagnosed sea-level impact of the precipitation (Figure 6)”

l.453: Maybe add “net mass gain”, which is associated with a negative sea-level contribution, but whether the global sea level falls is not only determined by Antarctica.

Rephrased: “... , gain mass causing a falling sea level”

l.455: Please reformulate, such that the reader understands that you talk about a constant rate on the one hand and a linearly increasing integrated melt rate on the other hand.

Rewritten: “The basal melting of grounded ice does not impact the sea-level evolution, because this basal melting rate is nearly constant so that the corresponding integrated sea-level equivalent grows linearly for all scenarios from 1850 until 2100, and only after the year 2500 these curves diverge.”

l.456: “Ultimately, the more vibrant growth of the accumulation in comparison to the negligible increasing combined loss of iceberg calving and basal melting of ice shelves drive the falling sea level in our simulations after the year 2000 (Figure 12).” => “Also the combined loss of iceberg calving and basal melting of ice shelves does not vary much over the considered period. Consequently, the growth of the accumulation in our simulations explains the net mass gains and hence the negative sea-level contributions from Antarctica after the year 2000 (Figure 12).”

We follow your advice and use “Also, the combined loss of iceberg calving and basal melting of floating ice shelves does not vary considerably over the considered period. Consequently, the growth of simulated accumulation explains the net mass gains and, hence, the negative sea-level contributions from Antarctica after the year 2000 (Figure 12).”

l.461: “ temperature scaled precipitation ” Add hyphen!

Thanks for indicating. We followed your suggestion and adjusted the manuscript accordingly.

l.462: “As a consequence, these will contribute after the year 3200 (RCP8.5) and 3900 (RCP2.6) to a globally rising sea level on average in our simulations, which outruns the formerly fallen sea level since 1850.” =>“As a consequence, these simulations produce on average a positive contribution to the global sea level after the year 3200 (RCP8.5) and 3900 (RCP2.6), which compensates for the negative contributions since 1850.”

Done.

l.470: “the deduced Antarctica’s sea level contribution” => Please reformulate

Reformulated: “simulated sea-level contribution of Antarctica”

l.471: “representing the observational-based ocean-driven basal melting.” So you directly apply basal melt fluxes and no ocean-temperature based melt parameterization any more?

We still use the growth of the simulated basal melting rates covering the period from 1850 to 5000, but the time series are adjusted to reproduce current estimates of basal melting rates. Unfortunately, these observational estimates present only the contemporary period. Please see the appendix for further information. We replace “representing” by “emulating” so that we obtain: “a corrected time series emulating the observational-based ocean-driven basal melting.”

l.475: “Under the assumption that only a fraction of the adjusted basal mass contributes to the global sea level, we apply the simulated ratio of the sea level change to the total ice mass change.” => The authors should better motivate that this conversion serves to express mass changes in terms of sea-level equivalents.

The introduction of this section has been modified and offers a clear motivation: “This analysis shall reveal if a more vibrant basal melting rate in concert with the simulated ice sheet mass evolution leads to a less pronounced ice sheet growth or drives even ice loss. Ultimately, does a more vigorous melting of ice shelves raise the simulated sea level of all ensemble members?”

l.478: “ sea level correction” Or do you mean “adjusted basal melt flux”?

We clarify: “By adjusting the basal melting flux, the determined temporal evolution of the sea level correction”

l.480: Maybe omit “as its evolution, which considers the correction, highlights”

Good point, we follow your suggestion.

l.481: “..., we obtain too extensive corrections...” => “... we would obtain large corrections...”

Done.

l.482: “This sea-level rise is larger” => “This corresponding sea-level rise would be larger”

Changed.

l.485: “raises ” => “could raise”

We rephrase: “would raise”

l.486: “ do not impact the sea level.” => “ do not impact the sea level directly.”

Done.

l.487: “ration” => “ratio”

Fixed.

l.490: “ how the precipitation is implemented in ice-sheet simulations” => Better say: “how

precipitation forcing is applied/estimated in ice-sheet simulations”

Rephrased: “specified”

l.493: “ In this case, numerical projections” => “ In this case, our numerical projections”

Extended as suggested.

l.498: “such as the ocean-ice-shelf-ice-sheet interactions.” => “such as the interaction between ocean, ice shelves, and ice sheet.”

Done.

l.497: “ thence”

Rarely use adverb with the meaning of 'therefrom.'

l.506: “ overwhelm ” or better overcompensate

Exchanged “overwhelm” by “overcome.”

l.508: “, the total amount would be identical,” => “, the average amount of precipitation change would be identical to the average precipitation anomaly,”

We prefer: “the integrated precipitation would be identical”

l.509: “proper” => “adequate” or “realistic”

Rephrased as suggested: “realistic”

l.510: “shall” => “should”

We use US English, where, to our knowledge, the auxiliary (modal) verb 'shall' is used in formal writing and expresses determination. It's different in British English. Hence, we would like to keep it.

l.514: “... which have been identified across sixteen models” => You should add “within a recent model intercomparison exercise”

Done.

l.523: “This observed retreat and the related ice loss will continue in our simulations under RCP8.5.” => “This observed retreat and the related ice loss will continue, most likely represented in our simulations by the scenario RCP8.5.”

Reordered: “In our simulations under the RCP8.5 scenario, this observed retreat and the related ice loss will continue.”

l.527: “ further to the west” => relative to where?

Further to the west of the discussed area (Wilkens Basin in the hinterland of George V Land) as part of the EAIS.

l.531: Maybe put references after “lose ice”, if they say so.

Indeed, references should be at the end.

l.532: “according to our simulations.” => “which is consistent in our simulations.”
l.532: “ will thin in the future.” => reference or does the ensemble suggest so?

Rephrased and clarified: “According to the ensemble projecting the future, for them, continuous ice loss is inevitable. It also shows that the Ferringo Ice Stream flowing into the Bellingshausen Sea

will thin in the future."

l.537: " reproduces appropriate " => " adequately reproduces "

Changed by "reasonably reproduces"

l.548: "Even if we apply anomalies on top of the reference background fields, we can not exclude a shock-like behavior of the simulations entirely directly following the decades after the year 1850." => This is strange, could you quantify the variability around the 50-years mean?

It is not strange because, at the start of the simulations, the climatic anomaly fields of the first years are not necessarily identical to the 50-years averages. The first few years may be warmer or colder than the mean. Please inspect the early decades of the ensemble mean's forcing (Figure 3) to obtain an impression of the climate variability.
We combine this point with the issue l332 above, where most of the paragraph is located now.

l.853: "because the water masses of this range flow into the ice-sheet cavities and are in contact with large parts of ice shelve bases. " => "because the water masses at this depth potentially can flow into the ice-sheet cavities and reach large parts of ice shelves' bases. "

I disagree with "potentially" because it is actually in contact with the ice shelf base either after direct inflow (for example in the Amundsen Sea) or after modification (for example in the Filchner-Ronne Ice Shelf); see for example Thompson et al. (2018). To avoid any ambiguity, we write: "because these water masses flow into the ice-sheet cavities and are in contact with the ice shelve bases."

l.854: "Highest temperature increases occur in the Bellingshausen and Amundsen Seas..." => Is this an observation or does the climate models suggest so?

Clarified: "Highest temperature increases occur in the Bellingshausen and Amundsen Seas as part of the West Antarctic Ice Sheet (WAIS) and some spots along the East Antarctic Ice Sheet (EAIS) according to observations (Schmidtko et al., 2014; Jacobs, 2006)."

l.856: " flow already " => "already flow" as observations suggest?

We write: "In the Bellingshausen and the Amundsen Sea, warm water masses flow into ice-shelf cavities as indicated by observations (Arneborg et al., 2012; Thompson et al., 2018) and model simulations (Nakayama et al., 2018)."

l.857: "massive" => "largest"

Exchanged "tremendous" for "massive."

l.865: " Temperature Scaling" => " Estimate of temperature scaling of precipitation from climate models"

We use instead: "Temperature Scaling of Precipitation derived from Climate Models"

l.868: " depend on if we determine " => " depend on the time period we chose as a reference "

Replace: "depend on if we determine the anomalies" by "depend on the time period we chose as a reference".

l.871: "However, all these differences do not changes the spatial structure significantly, and they have a neglectable impact compared to the choice of the driving model." => "However, these differences do not significantly change the spatial structure. Their impact is negligible compared to the choice of the driving model."

Done as suggested.

l.877: “The detected precipitation deficit...” => Could you provide a definition here, is this negative scaling or just scaling below average?

Clarified: “the detected precipitation deficit (shrinking precipitation rates), captured by reanalysis data … .”

l.880: “is small” => you could mention the relative size of the ice shelves, or you could account for ice shelves separately?

Yes, we could, but the manuscript is already pretty long. Therefore we will not further investigate this point.

l.907: “while in both cases the thickness calving is active”=>It would be very interesting if PISM could differentiate between the three calving styles in the reporting.

I agree it would be nice, but I have not kept the data that allows differentiating the individual contributions due to storage space limitations.

l.909: Make sure you the reader notices that you switched to observations.

Clarified: “According to observational estimates control iceberg calving and basal ice-shelf melting the overall mass loss of Antarctica, while the relative contribution is the subject of current research.”

l.919: “just termed basal melting rates” => why not “basal melt rates”
l.919: “the second ice mass loss process” => second largest process or does this just relate to the previous paragraph?

We rephrase: “The basal melting rate of floating ice shelves (hereinafter basal melting rates) is the second ocean-driven ice mass loss process beside iceberg calving.”

l.920: “The basal melting rate anomaly is computed relative to the 50 years between 1951 and 2000.” Please indicate how this period compares to the observations of the World ocean atlas used as reference field?

The WOA2009 says: “For the present atlas we attempted to reduce the effects of irregular space-time sampling by the averaging of five 'climatologies' computed for the following time periods: 1955-1964, 1965-1974, 1975-1984, 1985- 1994, and 1995-2006. The first-guess field for each of these climatologies is the 'all- data' monthly mean objectively analyzed temperature data.” (Locarnini, et al., 2010; page 6).

Locarnini, R. A., A. V. Mishonov, T. P. Antonov, T.P. Boyer, and H.E. Garcia. 2010. “World Ocean Atlas 2009, Volume 1: Temperature.” Edited by S Levitus. Vol. 1. U.S. Government Printing Office, Washington, D.C. https://www.nodc.noaa.gov/OC5/WOA09/pr_woa09.html.

l.921: “ We could identify immediately that the basal melting rates have risen between 10 % and 100 % since the 1850s (Figure A13)” => “The inferred an increase in basal melt rates by 10-100% over the period 1850-x?”

Rephrased to: “In general, the basal melt rate increases by 10 %--100 % over the period 1850-2100 (Figure A13).”

l.922: “independent of the initial state selection” => “independent of the selection of the initial state” or simply “independent of the initial state”

Done.

l.922: “ and reference to compute the” => “ as well as to the reference period selected for the computation of the”

Done.

l.925: “ subject to not negligible trend ” => Please be more precises!

We quantified the trend: “For instance, the average of the global absolute 2m-air temperature difference between the first and last 50 years of piControl amounts 0.17 K (median 0.12 K) for all CMIP5 models considered in our study. In contrast, MIROC-ESM's value is 0.67 K.”

l.926: “In the future, the basal melting rate will further increase between 10 % and more than 100 %.” => In future projections, the modeled basal melt rate further increases … until the year x”

To avoid a pleonasm, we write: “In future projections, the basal melting rate increases between 10% and more than 100% until the year 2100”

l.927: “ specialized ocean simulations” => “high-resolution ocean simulations”

Rephrased to “dedicated ocean simulations.”

l.931: “ is apparent.” => “ is clear/distinct.”

Changed to “is self-evident.”

l.937: “ or reach a maximum of around 2100 and scenarios” => “and reach a maximum around the year 2100. Scenarios...” The maximum in basal melting in Fig. A13 and A14 seems to occur for all climate forcings a few decades before 2100, is there an explanation for this phenomenon?

The applied running mean of 5 years and the constructed forcing after the year 2100 causes the visual shift of the maximum. We use the forcing until the year 2100 and repeat afterward recurrently the last 30 years of the forcing (2071-2100). For instance, the depicted forcing in the year 2100 corresponds to the weighted sum of the forcing of the years 2098, 2099, 2100, 2101(=2071), and 2102(=2072). We have clarified it by reordering the sentences in the figure captions of Figure A12/A13 and adding, in addition, these two sentences: “After the year 2100, the forcing of the last thirty years until 2100 drives the model recurrently.” and “The applied running means shift the apparent maximum backward in time so that it occurs visually before the year 2100.”. The last sentence is added to figure caption A14 too.

l.939: “our approach works where the last 30 years of the forcing until 2100 is recurrently applied afterward.” Please reformulate

We reformulate: “Since the temporal variability remains high also after 2100, our approach works to construct the forcing beyond the year 2100 (see section 2: "Material and Methods").”

l.942: “ show a minimum of around 3500 ” => “ show a minimum around the year 3500”

We rephrase as suggested.

l.945: “ ocean temperature anomalies are warmer” => “ ocean temperature anomalies are larger” or “more pronounced”

We write now: “This result reflects the dependence of the basal melting on the ocean temperature because a warmer climate scenario induces higher ocean temperature anomalies.”

l.948: “ and an average decrement for RCP4.5 ” => What does this mean?

Rephrased: “and an intermediate decrement of RCP4.5”

l.954: “while the highest calving occurs under scenarios with a lower forcing.” => This is surprising, do you have ideas for an explanation? Might this be related to the much smaller ice shelf area and hence shorter ice shelf front? The sentence in l.964 is not so clear on this assessment.

Why is this surprising? However, we sharpen the last sentence of this paragraph: “The total area of ice shelves is, in general, smaller when a warmer climate scenario impacts these ice shelves (Figure A15) and the degraded total ice shelf area downgrades the calving probability. Ultimately, the integrated calving rate is lower under a warmer climate.”

l.967: “Starting from original simulated ablation flux...” => Please start even earlier and explain briefly what the intention of this correction is. You take the modeled fluxes, modify them and apply them in additional sensitivity simulations? Is the reference flux usually obtained from observations? Maybe provide a figure to visualize the magnitudes.

We write “Since the simulated ocean-driven basal melting rates are lower than observational-based estimates (Figure A13), the impact of flux corrected basal melting rates on the model results are discussed in the main text (Section 3.7.1 "Sea level contribution of corrected basal melting" on page 15). This section describes the method.”

l.980: Please provide some motivation here: “In order to provide an estimate of how ice shelf mass changes result in equivalent sea-level changes...”?

We write now: “To relate the sea-level change to the ice mass evolution, we define the ratio p(t) of the sea level temporal deviation to the ice mass temporal deviation as p(t) = … .”

l.998: “the sea level rise of 30 cm is larger than the actual sea level rise “ => “the corresponding sea level rise of 30 cm would be larger than the observed sea level rise“ Please make sure in the wording that this is just a unit conversion and no dynamical estimate.

Changed as requested.

l.1000: “rise the” => “contributes to the”

Done.

l.1001: omit “(Equation A5)”

Done.

l.1002: “If” => “Whether”

Done.

l.1006: “ losses” => “lose”

Corrected.

l.1009 and l.1010 and l.1012: “temperature scaled” => “temperature-scaled”

Thanks for indicating; we've adjusted the entire text accordingly.

Figures:

Fig. 1: As this is the overview figure, the reader may expect the sector definitions of Table 4 visualized here, as done in Fig. 4.

As requested, we added the boundaries of the defined regions and adjusted the figure caption accordingly.

Fig. 2: The color scale in panel a is somewhat counterintuitive with the coldest areas in red. Why not using a temperature colorscheme similar to panel c)?

We prefer different properties of different color schemes to avoid confusion. In addition, we use color schemes that are aware of different types of color blindnesses.

Fig. 3: “is an extension into the sea” => maybe provide some estimate of the width. Also, the anomaly seems to be relative to the start period (at 1850), while for the ocean forcing, in l.920 in the Appendix a reference period 1950-2000 is indicated?

We extend the caption:”… is an extension into the sea (typical width of about 500 km).”
It is indeed correct that we talk about a different reference period (1951-2000) in line 920 as part of the appendix section “A2 Marginal ice loss by ocean-driven basal melting and iceberg calving.” There, we compare our growth rates of the basal melting rates with independent studies cited a few lines below (line 926-929). These studies determine the growth rates until the end of the century relative to 1951-2000.

Fig. 4: Which are the dotted regions here? Sector outline seem to overlay each other.

Solved. Indeed, in the submitted version, the dotted regions are absent while it is available in our version. Apparently, the size reduction of the submitted file has striped the dotted pattern. We apologize for being sloppy.

Fig. 6: This figure is simply overloaded, I recommend to split somehow.

We have worked with different versions of this plot because we initially shared your impression. However, a printed article allows taking the time needed to see the differences in this information-rich plot. In addition, splitting the figure may hinder the direct comparison of different model forcing scenarios. Therefore, we would like to keep the current figure.

Fig. 11: You should mention that ice loss is the combination of calving and melt.

The extended figure caption begins with: “Temporal evolution of the ocean-driven ice loss rates of the fringing ice shelves around Antarctica for the period from 1850 to 2100. The ice loss comprises iceberg discharge and basal melting of ice shelves. ... ”

Fig. A1: You should mention in the caption that the 50 cm year−1 contour is larger than in previous figures.

I assume you refer to Figure 2 when you talk about the previous figure. The extended figure caption ends with “Figure 2 shows the corresponding ensemble mean fields, where the white contour line in the precipitation field corresponds to 30 cm year-1.”

Fig. A2: Where are the “white-grey lines” mentioned in the caption?

We replaced “white-grey” with “light-grey”

Fig. A3: Please increase the size of the climate model labels.

The entire figure has a new label layout.

Fig. A4: It would help if the individual panels would use the same y-axis. Why is it important to distinguish between grounded ands glacierized here? Why not between grounded and floating?

This appendix figure has deliberately individual y-axis for each panel. Otherwise, the bunch of lines could not be separated in each panel. We are aware that this is a busy plot, but we are confident that the interested reader welcomes the provided rich set of information.

In simplified terms, the melting of grounded ice contributes to the global sea level, while the mere disintegration of floating ice does not. Hence the diagnosed sea-level contribution of grounded ice is vital.

To get an idea of how much snow accumulates on all glacierized ice, regardless if it is floating or grounded, we present these. Since we analyze precipitation anomalies, the change of precipitation rates may be of interest to the following communities. Those who have an interest in the evolution of the surface mass balance, use remote satellite products to analyze precipitation or water vapor transport changes in the Southern Ocean, and those running automated weather stations in coastal areas or floating ice shelves, for instance.

Fig. A5: “where all additional mass loss rises immediately the sea level” => “assuming that all additional mass loss is converted into a sea-level equivalent”

We change this part to “assuming that all additional mass loss rises the global sea level”

Fig. A6: unit for y-axis is also m?

Yes, we have indicated that this Figure is like Figure A5 and the y-axis says “Sea level contribution (m).” However, since your question expresses a misunderstanding, we adjust the figure caption and add explicitly the unit “(in meter)”: ”... The sea level (in meter) is computed relative to the year 2000. ...”

Fig. A7: Omit the in “of the each” in the caption.

We assume you suggest to erase “of the each ensemble member.” We follow your suggestion.

Figs. A10+11: It would be nice to indicate that the difference is simply the eigencalving parameter and describe whether and where differences (in calving front location) occur.

We have added for each state the total ice volume and ice area (grounded ice and floating ice) in an additional table as part of the appendix. We link from the figure captions of both Figures (A10 and A12) to this table. This table should allow the reader to distinguish both states. A copy of this table is listed below:

Field	PISM1Eq	PISM2Eq	Ratio: PISM1Eq/PIMS2Eq
Area: grounded ice (km2)	1.255e7	1.257e7	0.9985
Area: floating ice (km2)	2.005e6	1.569e6	1.278
Volume: grounded ice (km3)	2.588e7	2.605e7	0.9936
Volume: grounded ice above z=0 (km3)	2.313e7	2.325e7	0.9947
Ratio: all grounded ice / grounded ice above z=0 (%)	89.35	89.25	1.001
Volume: floating ice (km3)	6.681e5	5.421e5	1.232

Fig. A15: Could you state to what extent the trends can be attribute to grounding line retreat vs. calving front retreat?

If the grounding line retreated while the calving front stayed fixed, the ice shelf area would increase. Since the grounding does not advance on a large scale, a calving front that retreats faster

than the grounding line is required to obtain a shrinking ice shelf area. Therefore the shrinking ice shelf area is dominated by a retreating calving front. We hope this answers your question.

References:

Frieler, Katja, Peter U. Clark, Feng He, Christo Buizert, Ronja Reese, Stefan RM Ligtenberg, Michiel R. Van Den Broeke, Ricarda Winkelmann, and Anders Levermann. "Consistent evidence of increasing Antarctic accumulation with warming." Nature Climate Change 5, no. 4 (2015): 348-352.

Jourdain, N. C., Asay-Davis, X., Hattermann, T., Straneo, F., Seroussi, H., Little, C. M., and Nowicki, S.: A protocol for calculating basal melt rates in the ISMIP6 Antarctic ice sheet projections, The Cryosphere Discuss., https://doi.org/10.5194/tc-2019-277, in review, 2019.

Levermann, A., Albrecht, T., Winkelmann, R., Martin, M. A., Haseloff, M., & Joughin, I. (2012). Kinematic first-order calving law implies potential for abrupt ice-shelf retreat. The Cryosphere, 6, 273-286.

Sutter, J., Fischer, H., Grosfeld, K., Karlsson, N. B., Kleiner, T., Van Liefferinge, B., & Eisen, O. (2019). Modelling the Antarctic Ice Sheet across the mid-Pleistocene transition–implications for Oldest Ice. The Cryosphere, 13(7), 2023-2041.

Zwally, H. Jay, Jun Li, John W. Robbins, Jack L. Saba, Donghui Yi, and Anita C. Brenner. "Mass gains of the Antarctic ice sheet exceed losses." Journal of Glaciology 61, C22 no. 230 (2015): 1019-1036.

(This page is left empty intentionally.)

Anonymous Referee #2
Received and published: 23 February 2020

The authors used CMIP5 RCPs outputs for driving icesheet simulations to test how the precipitation boundary condition determines Antarctica's sea-level contribution. They found that the simulated ice-sheet thickness generally grows in a broad marginal strip where incoming storms deliver topographically governed precipitation. They further conducted scaling analysis showing that the scaling is higher across the East Antarctic Ice Sheet but lower across the West Antarctic Ice Sheet and lowest around the Siple Coast.

This study focuses on an interesting topic and potentially contributes to our understanding of further Antarctic icesheet change and sea level rise. Thereby, I would like to support this manuscript be published in Earth System Dynamics after minor revisions.

Thank you very much for reviewing our manuscript and your encouraging comments.

First, the authors may want to notice the effect of evaporation and atmospheric moisture budget on Antarctic icesheet. Evaporation (E) is large and comparable with precipitation (P) over most of Antarctic during SON and DJF. In the atmospheric moisture budget over Antarctic, P-E is generally balanced by horizontal convergence of vertically integrated moisture transport. Given the projected different responses of atmosphere circulation in various RCPs, it is would be nice to discuss the potential roles of atmospheric winds, moisture transports and in turn, P-E in Antarctic icesheet change.

Thanks for indicating these very intriguing points.

We would have liked to compute the surface mass balance with a more physical based surface mass balance scheme that takes into account the balance between radiative and turbulent fluxes as well as the conductivity of heat within the snowpack besides phase changes between liquid water and solid ice. Our model at hand would have been able to determine also the impact of sublimation, which balances, for example in the Dry Valley accumulation (Bliss et al., 2011). However, the data required are not available for all here used CMIP5 models. Hence, we have used a parameterization to compute the surface mass balance. Here, we decided to utilize the widely accepted and used positive degree day (PDD) approach (Hock, 2003), which is justified by the high correlation between the main drivers of ablation (radiation) and the near-surface air temperature (Ohmura, 2001).

Bliss, Andrew K., Kurt M. Cuffey, and Jeffrey L. Kavanaugh. 2011. "Sublimation and Surface Energy Budget of Taylor Glacier, Antarctica." Journal of Glaciology 57 (204): 684–96. https://doi.org/10.3189/002214311797409767.

Hock, Regine. 2003. "Temperature Index Melt Modelling in Mountain Areas." Journal of Hydrology 282 (1–4): 104–15. https://doi.org/10.1016/S0022-1694(03)00257-9.

Ohmura, Atsumu. 2001. "Physical Basis for the Temperature-Based Melt-Index Method." Journal of Applied Meteorology 40 (4): 753–61. https://doi.org/10.1175/1520-0450(2001)040<0753:PBFTTB>2.0.CO;2.

Regionally, the surface mass balance is influenced by sublimation/evaporation in Antarctica. The strength of this process differs by a factor of two between model studies (Agosta et al., 2019; Wessem et al., 2018). The sublimation is strongly correlated with the surface temperature and only significant during summer (Lenaerts et al., 2012). This effect is already included in our background fields to which we add the anomalies of the 2m-air temperature and precipitation. We add the figure A16 to highlight the quality of the here used approach computing the surface mass balance.

In the RACMO model, the snow sublimation includes a wind-driven process, which dominates the sublimation (Wessem et al., 2018). Over the Antarctic continent, surface sublimation and blowing

snow sublimation lose mass on the order of 29 mm yr^{-1} and dispose 17–20% of the total annual precipitation over this region (Déry and Yau, 2002). However, the large-scale effect of surface blowing snow redistribution is negligible (Déry and Yau, 2002). We are confident that the differences between the used CMIP5 models are larger than the described effects and dominate the results. Further analysis of the changes in moisture transport is beyond the scope of this study and would extend this already lengthy manuscript.

Agosta, Cécile, Charles Amory, Christoph Kittel, Anais Orsi, Vincent Favier, Hubert Gallée, Michiel R. van den Broeke, et al. 2019. “Estimation of the Antarctic Surface Mass Balance Using the Regional Climate Model MAR (1979–2015) and Identification of Dominant Processes.” The Cryosphere 13 (1): 281–96. https://doi.org/10.5194/tc-13-281-2019.

Déry, Stephen J., and M.K. Yau. 2002. “Large-Scale Mass Balance Effects of Blowing Snow and Surface Sublimation.” Journal of Geophysical Research 107 (D23, 4679): 17pp. https://doi.org/10.1029/2001JD001251.

Lenaerts, J.T.M., M.R. van den Broeke, W.J. van de Berg, E. van Meijgaard, and P. Kuipers Munneke. 2012. “A New, High-Resolution Surface Mass Balance Map of Antarctica (1979–2010) Based on Regional Atmospheric Climate Modeling.” Geophysical Research Letters 39 (L04501): 5pp. https://doi.org/10.1029/2011GL050713.

Wessem, Jan Melchior van, Willem Jan Van De Berg, Brice P.Y. Noël, Erik Van Meijgaard, Charles Amory, Gerit Birnbaum, Constantijn L. Jakobs, et al. 2018. “Modelling the Climate and Surface Mass Balance of Polar Ice Sheets Using RACMO2 - Part 2: Antarctica (1979-2016).” The Cryosphere 12 (4): 1479–98. https://doi.org/10.5194/tc-12-1479-2018.

Also, I am wondering how the results of authors’ ice sheeting simulations will affect Antarctic sea ice and deepwater formation. How will they modulate the Antarctic sea ice projection in various RCPs? How will they modulate deep convection in the marginal seas of the Antarctica, the formation of Antarctic Bottom Water and the strength of abyssal circulation?

Here we could only speculate since we do not simulate the actual processes in the ocean. Since our manuscript is already long, we prefer to keep this short and do not discuss these important points. In particular, the other referee suggested shortening instead of expanding our manuscript.

Precipitation Ansatz dependent Future Sea Level Contribution by Antarctica based on CMIP5 Model Forcing.

Christian B. Rodehacke[1,2], Madlene Pfeiffer[1], Tido Semmler[1], Özgür Gurses[1], and Thomas Kleiner[1]

[1]Alfred Wegener Institute Helmholtz Centre for Polar and Marine Research, D-27570 Bremerhaven, Germany
[2]Danish Meteorological Institute, DK-2100 Copenhagen Ø, Denmark

Correspondence: Christian Rodehacke (christian.rodehacke@awi.de)

Abstract. Various observational estimates indicate growing mass loss at Antarctica's margins but also heavier precipitation across the continent. Simulated future projections reveal that heavier precipitation, fallen on Antarctica, may counteract amplified iceberg discharge and increased basal melting of floating ice shelves driven by a warming ocean. Here, we use models future projections from nine CMIP5, ranging from strong mitigation efforts to business-as-usual, to run an ensemble of ice-sheet simulations. In contrast to various former studies, only the historical (1850–2005) and scenario (2006–2100) forcing drive our ensemble of simulations, which neglects unavoidable continuous warming consistent with the higher climate scenarios beyond the year 2100. We test how the precipitation boundary condition determines Antarctica's sea-level contribution. The spatially and temporally varying climatic forcing drives ice-sheet simulations, such that our ensemble represents all climate patterns, which is fundamentally different from using spatial means as forcing. Regardless of the applied boundary and forcing conditions, our ensemble study suggests that some areas will lose ice in the future, such as the glaciers from the West Antarctic Ice Sheet draining into the Amundsen Sea. In general, the simulated ice-sheet thickness grows in a broad marginal strip, where incoming storms deliver topographically controlled precipitation. This strip also shows the largest ice thickness differences between the applied precipitation boundary conditions. On average Antarctica's ice mass shrinks for all future scenarios if the precipitation is scaled by the spatial temperature anomalies coming from the CMIP5 models. In this approach, we use the relative precipitation increment per degree warming as invariant scaling constant. In contrast, Antarctica gains mass in our simulations if we apply the simulated precipitation anomalies of the CMIP5 models directly. Here, the scaling factors show a distinct spatial pattern across Antarctica. Furthermore, the diagnosed mean scaling across all considered climate forcings is larger than the values deduced from ice cores. In general, the scaling is higher across the East Antarctic Ice Sheet, lower across the West Antarctic Ice Sheet, and lowest around the Siple Coast. The latter is located on the east side of the Ross Ice Shelf.

Plain Language Summary In the warmer future, the ice sheet of Antarctica will lose more ice at the margin, because more icebergs may calve and the warming ocean melts more floating ice shelves from below. However, the hydrological cycle is also stronger in a warmer world. As a consequence, more snowfall precipitates on Antarctica, which may balance the amplified marginal ice loss. In this study, we have used future climate scenarios from various global climate models to perform numerous ice-sheet simulations. These simulations represent the Antarctic Ice Sheet. We analyze whether Antarctica will grow or shrink. In all our simulations, we find that certain areas will lose ice under all circumstances. However, depending on the method used to describe the precipitation reaching Antarctica in our simulations, parts of the Antarctic Ice Sheet may either grow or

shrink in the future. The discrepancy of the simulation results between both methods describing the precipitation illustrates the uncertainty of the possible range of future precipitation growth in a warming atmosphere. Furthermore, the dissimilarity is pronounced differently between the West Antarctic and East Antarctic Ice Sheet. Since we use only the available climate scenarios until the year 2100, any additional warming after 2100 may turn the ice gain into an ice loss under a strongly changing climate.

1 Introduction

Sea level rise as a symptom of the progressing climate warming is of foremost importance for coastal societies because it impacts numerous economic activities globally and threatens the population along coasts. Antarctica's contribution to the future sea level is projected by either statistical approaches that take advantage of the deduced past behavior or process-based model simulations, e.g. ice-sheet models (Church et al., 2013a). To run ice-sheet models, commonly simplified temporal forcing anomalies for the entire continent are applied on top of spatial background fields (e.g. Golledge et al., 2015; Winkelmann et al., 2012; Pollard and DeConto, 2009). Those background or reference fields are either descriptions based on linear multiple-regression analysis (e.g., surface elevation and latitude dependence (Fortuin and Oerlemans, 1990)) or come from regional climate models or climatological data sets. The simplified temporal forcing, which usually does not show a dedicated spatial structure, follows some ad hoc assumed temporal evolution or is constructed from a set of CMIP5 model simulations, for instance. Here, we use various climate scenarios of an ensemble of CMIP5 models to drive the Parallel Ice Sheet Model (PISM, e.g. Bueler and Brown, 2009; Winkelmann et al., 2011), where we exploit the full temporal and spatial pattern in the atmospheric and oceanographic forcing. This approach is an enhancement to previous studies utilizing CMIP5 ensembles to infer only the temporal evolution of the future forcing (Golledge et al., 2015; Winkelmann et al., 2012).

The coupling between atmospheric warming and the enhanced hydrological cycle is often described as a Clausius-Clapeyron process, where the saturation pressure of water vapor scales exponentially by about $7\,\%$ per Kelvin warming (Held and Soden, 2006) — it is implicitly assumed that the relative humidity does not change. Climate modeling studies representing the Last Glacial Maximum (LGM), the pre-industrial (piControl) and historical period as well as climate warming scenarios (1pctCO2, abrupt4xCO2) show that the global precipitation increases in warmer climates and decreases in colder climates with a rate of $1\,\%\mathrm{K}^{-1}$ to $4\,\%\mathrm{K}^{-1}$ (Held and Soden, 2006; Li et al., 2013). Globally, this rate, which is the mean precipitation scaling, is less than the suggested thermodynamically justified Clausius-Clapeyron process for various reasons. Decreasing precipitation rates in the dry subtropics (Sun et al., 2007), covering a substantial part of the globe, limits the scaling. Dynamical and thermodynamical processes contribute both to the actual precipitation change, even if dynamical changes, such as an altering circulation, play a secondary role globally (Emori and Brown, 2005). The balance of radiative fluxes in/out of the troposphere and the latent energy flux at the surface limits evaporation, which restricts water vapor supply and ultimately the scaling (Allen and Ingram, 2002).

A global analysis of observed precipitation and temperature changes reveals a low or even negative scaling in tropical land regions driven by decreasing soil moisture, a near Clausius-Clapeyron scaling $\approx 7\%\mathrm{K}^{-1}$ over the open ocean, and a super

Clausius-Clapeyron scaling (>7 $\%\mathrm{K}^{-1}$) along extratropical coasts (Yin et al., 2018). In the latter case, the moisture supply by the ocean in concert with the atmospheric circulation generates extreme precipitation events inland. These events cause high temperature scaling factor for precipitation onshore. Ultimately, the local availability and recycling of moisture and the atmospheric dynamics determine the size of the precipitation-temperature scaling (Yin et al., 2018).

In Antarctica, global model simulations until the end of the century show an average scaling of about $7.4\,\%\mathrm{K}^{-1}$ (range: $5.5\,\%\mathrm{K}^{-1}$ – $24.5\,\%\mathrm{K}^{-1}$ Palerme et al., 2017), which is in agreement with CloudSat estimates (years 2007 – 2010, $7.1\,\%\mathrm{K}^{-1}$, Palerme et al., 2017). For the last deglaciation, global climate models suggest a value of about $6\,\%\mathrm{K}^{-1}$ in Antarctica, while future projections of a high-resolution regional climate model show a lower value of $4.9\,\%\mathrm{K}^{-1}$ in contrast to a higher value of $6.1 \pm 2.6\,\%\mathrm{K}^{-1}$ coming from an ensemble of global climate system models (Frieler et al., 2015). Ice core data covering 10,000 years of marked temperature changes reveal a value of $5 \pm 1\,\%\mathrm{K}^{-1}$ (Frieler et al., 2015). In standalone ice-sheet modeling studies, the commonly used temperature scaling factor for precipitation amounts to approximately $5\,\%\mathrm{K}^{-1}$ (e.g. Gregory and Huybrechts, 2006) in Antarctica, as the latitudinal relation obtained from a CMIP5 model ensemble suggests (Golledge et al., 2015). We consider $5\,\%\mathrm{K}^{-1}$ as the reference value further on.

While in most regions both the local availability and recycling of moisture and the atmospheric dynamics determine the size of the precipitation-temperature scaling (Yin et al., 2018), atmospheric dynamics dominate over the deep-frozen interior Antarctic continent, probably due to negligible water buffering capacity of the frozen ground. The ocean surface conditions around Antarctica sets the lower boundary condition for the atmosphere, which accounts for the spread of the precipitation scaling among climate models. Atmosphere simulations over Antarctica, which are driven by boundary conditions from a small ensemble of historical and future climate scenarios, show a weak impact of changed atmospheric conditions or enhanced radiative forcing on the scaling factor (Krinner et al., 2014). In contrast, the ocean conditions are crucial for the precipitation scaling in Antarctica (Krinner et al., 2014). Sea ice cover has a decisive impact, where the mean historical sea ice concentration is more important than the sea ice retreat rate (Bracegirdle et al., 2015).

Across Antarctica, the patterns of increasing as well as decreasing precipitation are consistent with the variability of the large-scale moisture transport resembling the known Southern Hemispheric modes of variability, such as Amundsen Sea Low (ASL) or Southern Annular Mode (SAM) (Fyke et al., 2017). Also, the baroclinic annular mode (BAM) and the two Pacific-South American teleconnections (PSA1 and PSA2) indices influence precipitation over Antarctica (Marshall et al., 2017). An enhanced baroclinic annular mode, which corresponds to high storm amplitudes, increases the precipitation over the coastal East Antarctic Ice Sheet, while an enhanced SAM causes stronger precipitation across the West Antarctic Ice Sheet (WAIS) and the neighboring Antarctic Peninsula. The two Pacific-South American teleconnections impact mainly precipitation over the West Antarctic Ice Sheet beside other regions across the Antarctic continent.

In reanalysis products, no robust or statistically significant precipitation trend exists over Antarctica (Bromwich et al., 2011). This result is in agreement with precipitation observations over the Southern Ocean (Bromwich et al., 2011). However, shallow ice cores across Antarctica reveal a tendency for a positive precipitation trend over the last 50 years and 100 years. Since 1800, the increase of the surface mass balance (SMB) is $7 \pm 1.3\,\mathrm{Gt\,decade}^{-1}$ (Thomas et al., 2017).

In contrast, over the western region of the West Antarctic Ice Sheet (WAIS), next to the Ross Ice Shelf, a negative snow accumulation trend has been detected in monthly reanalysis products (ERA-Interim: 1979–2010 and ERA-20C: 1900–2010), which is confirmed by a composite of 17 firn cores (Wang et al., 2017). The flow of available atmospheric moisture, which feeds the precipitation across the WAIS, is dominated by the Amundsen Sea Low (Thomas et al., 2017). A location shift of the Amundsen Sea Low (ASL), expressed by its longitudinal position, exposes different regions to the inland-directed circulation branch of moisture-rich air masses — on the eastern side of the Low's center — or isolates them from moisture supply due to the offshore directed circulation branch — on the western side. Furthermore, the deepening of the ASL enhances the cyclonic circulation, which strengthens precipitation — southeast of the Low's center — over the Antarctic Peninsula and eastern WAIS. However, less moisture-rich air masses reach the western WAIS, which ultimately leads to an accumulation deficit. Enlarged sea ice extent in the Ross Sea (Haumann et al., 2016; Liu, 2004) damps evaporation to the atmosphere. In contrast, a decreasing sea ice trend in the Amundsen Sea and Bellingshausen Sea (Haumann et al., 2016; Jacobs, 2006) enhances the moisture supply. To conclude, the observed accumulation reduction is driven by the deepening of the ASL and reinforced by a more extensive sea ice extent in the Ross Sea (Wang et al., 2017).

Processes governing the balance between mass gain and mass loss determine if Antarctica contributes to a rising sea level. Antarctica's surface mass balance controls mass gain, while mass loss occurs predominantly by ocean-driven basal melting of ice shelves and iceberg calving (Wingham et al., 2018). For individual ice shelves, the fraction between basal melting and iceberg calving ranges from $10\,\%$ to $90\,\%$ (Depoorter et al., 2013). Estimates about the total mass loss agree within the uncertainties, even if they range from $2200\,\mathrm{Gt\,year^{-1}}$ to $2800\,\mathrm{Gt\,year^{-1}}$ (Depoorter et al., 2013; Liu et al., 2015; Rignot et al., 2013). However, they differ in the relative contribution between basal melting and calving. The overall mass loss is either driven by a nearly equal share between calving ($1321 \pm 144\,\mathrm{Gt\,year^{-1}}$) and basal melting ($1454 \pm 174\,\mathrm{Gt\,year^{-1}}$) (Depoorter et al., 2013), or the basal melting ($1516 \pm 106\,\mathrm{Gt\,year^{-1}}$) contribution is twice as much as the calving ($755 \pm 24\,\mathrm{Gt\,year^{-1}}$) contribution (Liu et al., 2015). The surface mass balance is the difference between mass gain by precipitation — and here predominantly snowfall — and surface meltwater that runs off, because it is not refrozen nor retained in the snowpack. Surface melt ponds (Kingslake et al., 2017) and runoff exist on Antarctic ice shelves (Bell et al., 2017), but their contribution to the total mass balance is considered to be negligible (Van Wessem et al., 2014), except for the (northern) Antarctic Peninsula (Adusumilli et al., 2018).

The focus of this paper is to identify common features of an ensemble of ice-sheet simulations forced by a multimodel forcing ensemble. After the discussion on the temporal and spatial evolution of the climatic boundary conditions from nine CMIP5 models, we diagnose the temperature scaling of the precipitation of these climate models. Afterwards, we investigate how the deduced scaling impacts the global sea level in contrast to spatially homogeneous scaling, e.g inferred from ice core data. The impact of these precipitation conditions on simulated ice-sheet thickness is analyzed before we attribute the climate models, which cause extreme changes. Before we conclude, we estimate differences in Antarctica's sea-level contribution for the variety of applied forcing and precipitation boundary conditions.

2 Material and Methods

The full temporally and spatially varying forcings are obtained from an ensemble of CMIP5 models representing a suite of climate scenarios. These climate forcings drive the Parallel Ice Sheet Model (PISM) in order to estimate Antarctica's future sea-level contribution. In particular, the ansatz of the precipitation determines whether the global sea level rises or falls. We consider two precipitation boundary conditions. (1) On top of the reference background distributions (see Table 2), which drive the ice-sheet model during the spin-up, we utilize both the temperature and the precipitation anomalies from CMIP5 models. (2) We take only the temperature anomalies from CMIP5 models and compute the precipitation anomalies scaled by the temperature anomalies. The latter approach is commonly used, in particular in paleo applications (Applegate et al., 2012; Bakker et al., 2016; de Boer et al., 2013, e.g), while some sensitivity studies keep the surface mass balance constant (Feldmann and Levermann, 2015; Hughes et al., 2017). In some cases, negative temperature scaling is considered unrealistic (Frieler et al., 2012).

Nine CMIP5 models deliver the following climate scenarios (see Table 1, Taylor et al. (2012)): control run under pre-industrial conditions (piControl), the historical period (1850-2005), as well as RCP2.6, RCP4.5, and RCP8.5 (2006-2100, Vuuren et al. (2011)). These models stem from different model families (Knutti et al., 2013) and cover the range of current atmospheric (Agosta et al., 2015) and oceanographic (Sallée et al., 2013a) model uncertainties although model deficiencies such as insufficient resolution can exist across all models. The transient forcing from 1850 until 2100 comprises the historical and scenario periods. Afterward, the last 30 years (2071-2100) are repeated until the year 5000 to keep the natural variability. From the control run of the climate model (piControl), we use either the first or the last 50 years. By this procedure, we could quickly identify a drift in CMIP5 models and assess its impact. Additionally, the number of scenarios is twice as large, since the mean states of the first and last 50 years show in general marginal differences. Anomaly forcing is computed relative to either the first or last 50 years of the control run. In the following, the first 50 years act generally as reference.

The repetition of the last 30 years of climate forcing beyond the year 2100 is a simplification, which is not entirely consistent with the applied climate scenarios. An ongoing growing atmospheric greenhouse concentration triggers changes in the climate system. While the atmospheric radiation reacts immediately, the redistribution of the accompanied heating within the global ocean is much slower (Hansen et al., 2011). This delay is critical because most of the additional heat ends in the worldwide ocean (Church et al., 2011, 2013b). Consequently, further warming is inevitable after the cessation of greenhouse emissions (Hansen et al., 2005). Our simulations do not reflect this ongoing warming. Also, a disintegrating Greenland ice sheet will raise the global sea level, and, as a consequence of Greenland's reduced gravitational pull (Whitehouse, 2018), the sea level rise is in particular pronounced around Antarctica (Mitrovica et al., 2001). A rising sea level potentially migrates the grounding lines inshore, which ultimately destabilizes ice shelves and causes a more vulnerable Antarctic ice sheet. Despite, the same gravitational effect may buttress Antarctica, whether Antarctica's ice loss is slow enough (Gomez et al., 2010) and Greenland stabilizes. However, the ongoing thermal expansion of the ocean, which is currently the driver of the rising sea level (Rietbroek et al., 2016), will probably destabilize Antarctica. Therefore, our ensemble of ice sheet simulations is not a projection.

Atmospheric and oceanic forcing is applied as annual mean forcing on top of the forcing used to spin-up the ice-sheet model (Table 2). Since CMIP5 models do not resolve ice shelves, ocean temperatures are extrapolated horizontally into the ice shelves to mimic isopycnical flow: The operator "fillmiss2" of the Climate Data Operators' (cdo) tool kit acts on the original CMIP5 ocean grid. To allow for surface melting under a warming climate, the surface mass balance (SMB) is calculated following the positive degree day (PDD) approach (Braithwaite, 1995; Hock, 2005; Ohmura, 2001) as implemented in the PISM model (The PISM Authors, 2015a, b). The turn of the hydrological year occurs on day 91 and the PDD factor for snow and ice are $0.3296\,\mathrm{cm(IE)\,Kelvin^{-1}\,day^{-1}}$ and $0.8792\,\mathrm{cm(IE)\,Kelvin^{-1}\,day^{-1}}$, respectively. Across Antarctica, the surface mass balance computed via the PDD approach (Figure A16b) is identical to the one used during the spin-up (Figure A16a). Here, the evolving annual 2m-air temperature standard deviation is derived from daily CMIP5 model values for each ice sheet model grid-cell.

The ice-sheet model PISM — based on version 0.7 — runs on a 16 km equidistant polar stereographic grid and it utilizes a hybrid system combining the Shallow Ice Approximation (SIA) and Shallow Shelf Approximation (SSA). The model employs a generalized version of the viscoelastic Lingle-Clark bedrock deformation model (Bueler et al., 2007; Lingle and Clark, 1985). In our simulations, only the viscous part has been used because of known implementation flaws in the elastic part in our and later PISM versions. The basal resistance is described as plastic till by a Mohr-Coulomb formula to perform the yield stress computation (Bueler and Brown, 2009; Schoof, 2006). The basal melting of ice shelves is proportional to the squared thermal temperature forcing ($\Delta T^2_{\mathrm{force}}$), which is the difference between the pressure-dependent melting temperature of the ice and the actual ocean temperature above melting. Here, the parameterization considers the full depth-dependence of the ocean temperature field, as described in Sutter et al. (2019). Basal ice-shelf melting occurs only in fully floating grid points, while the grounding line position is determined on a sub-grid space (Feldmann et al., 2014) to interpolate basal friction.

The calving occurs at the ice-shelf margin, and three sub-schemes determine it. (1) At the ocean-ice-shelf margin, ice-shelf grid points with a thickness of less than $150\,\mathrm{m}$ calve. (2) Ice shelves calve that extend across the continental shelf edge and progress into the depth ocean (defined by the $1500\,\mathrm{m}$ depth contour). (3) The Eigen-calving parameterization exploits the divergence of the strain/velocity field (Levermann et al., 2012), with the proportionality constant of either $1 \cdot 10^{18}\mathrm{m\,s}$ or $1 \cdot 10^{17}\mathrm{m\,s}$. Two independent spin-up runs delivering our initial conditions (PISM1Eq and PISM2Eq) utilize these constants. Ocean temperatures from the World Ocean Atlas 2009 (Locarnini et al., 2010) and the multi-year mean surface mass balance (SMB) from the RACMO 2.3/ANT model (Van Wessem et al., 2014) drive PISM during spin-up (Table 2). A similar model setup has taken part in the initMIP-Antarctica exercise under the name AWI_PISM1Eq with an adjusted Eigen-calving proportionality constant of $2 \cdot 10^{18}$ and no bed deformation (Seroussi et al., 2019a).

3 Results and Discussions

Depending on the applied CMIP5 forcing scenario, the ensemble mean climate signal is weaker for those scenarios following an aggressive mitigation path and, hence, releasing less carbon dioxide (e.g. RCP2.6). Around Antarctica, the here analyzed

ensemble follows the same pattern (Figure 2 and Figure 3). Since in the past decade greenhouse gas concentrations have followed most closely the high-emission RCP8.5 scenario path, we will focus on RCP8.5 if not otherwise stated.

3.1 Ensemble Forcing

From 1850 until the end of the 21st century, the ensemble mean 2m-air temperature in Antarctica (see the map of Figure 3d) rises steadily by $6\,\mathrm{K}$ with a spread of $1\,\mathrm{K}$ (one standard deviation) (Figure 3a) while the mean precipitation accumulates $9 \pm 3\,\mathrm{cm\,year^{-1}}$ (water equivalent) in addition (Figure 3b). The average potential ocean temperature in the depth range of $150\mathrm{m}$ to $500\mathrm{m}$ depth along Antarctica's coast (see the map of Figure 3e) warms by nearly $1 \pm 0.18°\mathrm{C}$ in the same period (Figure 3c). In particular, since the beginning of 21st century, these warming trend becomes stronger.

These changes are not homogeneous across the Antarctic continent (Figure 2d-l). The atmosphere warms strongest along the Antarctic Peninsula (Mulvaney et al., 2012; Thomas et al., 2009, in agreement with current observed trends), the high plateau of the East Antarctic Ice Sheet (EAIS) and to a lesser degree around the Filchner-Ronne-Ice Shelf region (Figure 2d, g, j). The warming is lowest in the coastal areas of East and West Antarctica that extend (clockwise) from the Greenwich Meridian via Wilkens Land and the Ross Ice Shelf to the Marie Byrd Land, respectively, where the Amery Ice Shelf interrupts this coastal band of moderate temperature rises. Please note that the inland coastal areas of the West Antarctic Ice Sheet (WAIS), the Wilkens Land, and the region between the Greenwich Meridian and the Antarctic Peninsula (western Weddell Sea) warms less than the adjacent ocean and ice-sheet interior.

The precipitation increases marginally across the high plateau of the EAIS and east of the Ross Ice Shelf as part of the WAIS (Figure 2e, h, k). In contrast, the coastal areas, where air masses with much precipitable water make landfall, receive more precipitation. Since these air masses on their way into the interior are uplifted by the steep topography, the precipitation along the coasts is topographically controlled. Areas of heavy precipitation under the reference climate (Figure 2b) also receive the highest increments. The precipitation increases strongest along the western Antarctic Peninsula, where the lifting of eastward flowing air masses by mountain ranges leads to topographic precipitation, which is firmly enhanced; this resembles the observed positive precipitation trend of the Antarctic Peninsula since 1900 (Wang et al., 2017).

Under the control climate, the coldest potential ocean temperatures in the depth range from $150\,\mathrm{m}$ to $500\,\mathrm{m}$ exist offshore the coasts of Antarctica (Figure 2c). We detect the lowest temperatures in front of the Filchner-Ronne, Amery, and Ross Ice Shelves. Also, the Amundsen Sea in front of Pine Island Glacier and Thwaites Glacier is cold. Here, the climatological temperature distribution might be too cold because it does not replicate the confined flow of warm water masses through glacier-scoured troughs towards ice shelves. To overcome this limitation, we apply a spatially restricted melting correction. It increases the melting by $50\,\%$ for the Ronne Ice Shelf region, and it quadruples melting for coastal parts of the West Antarctic Ice Sheet between the Antarctic Peninsula and the Getz Ice Shelf (east of the Ross Ice Shelf).

The subsurface ocean-temperature warms vigorously along sections of the Antarctic Circumpolar Current (ACC) and in the western Weddell Sea at the center of the ocean gyre. For instance, the warm spot in the western Weddell Sea emerges in all ensemble members (Figure 2f, i, l). In the coastal strip surrounding Antarctica, the warming is of medium strength and heterogeneous. There, most robust warming appears in the Amundsen Sea and along the coast of the EAIS (between Wilkens

Land and Terre Adélie) opposite of Australia. Least warming occurs in front of both the western Ross Ice and Filchner-Ronne Ice Shelves and the neighboring Antarctic Peninsula, where the ocean temperatures are lowest in the control climate (Figure 2c).

The spatial structure of the anomalies discussed above is in general independent of the applied forcing scenario, while the scenarios determine, however, the strength of the anomalies. Regardless of the applied scenario, the discussion of the atmospheric climate anomalies indicates already that both precipitation and temperature not necessarily correlate. Instead, regional differences are evident, and a simple scaling of the precipitation with temperature appears to be inadequate.

3.2 Precipitation scaling

Inspired by the Clausius-Clapeyron process, it is often assumed that with a warming atmosphere, the precipitation also raises. Ice-sheet simulations bridging several millennia often rely on climate anomalies deduced from ice cores, for instance. Based on isotopic signatures in ice cores, temperature anomalies are deduced. Inferred accumulation anomalies from these cores are converted into precipitation anomalies. Together with the contemporary climate fields as a reference, the temperature scaling of precipitation is

$$S(t,\boldsymbol{x}) = \frac{1}{\Delta T(t,\boldsymbol{x})}\frac{P_{t=0}(\boldsymbol{x})}{\Delta P(t,\boldsymbol{x})}\cdot[100\%], \tag{1}$$

where ΔT is the temperature anomaly, ΔP the precipitation anomaly, and $P_{t=0} = P(t_{\mathrm{ref}})$ the precipitation reference field. The scaled precipitation is

$$P(t,\boldsymbol{x}) = \Delta P(t,\boldsymbol{x}) + P_{t=0}(\boldsymbol{x}) = \Delta P(t,\boldsymbol{x})\ [1 + \Delta T(t,\boldsymbol{x})\cdot S(t,\boldsymbol{x})]\,. \tag{2}$$

The scaling deduced from ice cores varies in Antarctica between $5\,\%\mathrm{K}^{-1}$ and $7\,\%\mathrm{K}^{-1}$, with a 2-sigma uncertainty of about $1\,\%\mathrm{K}^{-1}$ – $3\,\%\mathrm{K}^{-1}$ (Figure 4, Table 3).

The corresponding scaling of the ensemble mean is generally larger at these ice core locations. The difference most prominent for the Vostok ice core and, to a less degree, also for EDML and EDC, while, within the uncertainties, the scaling of the Law Dome, Talos Dome, and WAIS ice cores are indistinguishable from the corresponding ensemble means. Here, we have computed the scaling by averaging the precipitation of the piControl run (first 50 years) to obtain the reference data and the last 50 years of the RCP8.5 scenario from 2051 until 2100 to get the anomalies. If we replace the reference period by the first 50 years of the historical period (1850-1899), the results are similar, and the values change only slightly. Thus, we can safely restrict the analysis and use as a reference for the computation of the anomalies the first 50 years of the piControl climate.

The spatial distribution of the scaling derived from our ensemble data is spatially heterogeneous and varies stronger than the ice core data suggest. Values in the range between $4\,\%\mathrm{K}^{-1}$ and $6\,\%\mathrm{K}^{-1}$ occur at the Filchner-Ronne Ice Shelf and in the coastal Terre Adélie region (see Map in Figure 1 for place names). Furthermore, as part of the WAIS these values are present in the coastal strip from the Antarctic Peninsula to the Ross Ice Shelf and along the eastern flank of the Transantarctic Mountain Range (Figure 4).

The highest scaling factor emerges on the EAIS, where a c-shaped area as part of the high plateau has factors exceeding $12\,\%\mathrm{K}^{-1}$. This area reaches out to the Dronning Maud Land with very high scaling factors too. The West Antarctic Ice Sheet has scaling factors generally lower than $8\,\%\mathrm{K}^{-1}$ and only on the elevated interior values up to $10\,\%\mathrm{K}^{-1}$ are detected. Over the Ross Ice Shelf and the eastward adjacent Siple Coast, scaling factors are the lowest (Figure 4). Since we detect raised scaling factors at a higher elevation, we aimed at determining whether we could find a relationship between elevation and scaling. However, neither for the entire Antarctic continent nor for defined subregions (see below), we could identify any robust relationship (not shown).

Our analysis focuses now on the scaling factors of all grounded ice, which, if lost, contributes to a rising potential sea level by Antarctica. Additionally, we analyze the scaling factors for the entire continent (label "glaciered"), and four glaciated regions labeled "EAIS Atl", "EAIS Ind", "WAIS", and "Siple Coast" (Figure 5 and Table 4). We detect a slight trend to higher values if we restrict the analysis to ground ice ($87.5\,\%$ of the glaciated area, see Table 4); it excludes floating ice shelves with low elevation along the coasts. However, the scenario selection is decisive, while the choice between "glaciered" and "grounded" is unessential for the ensemble mean as well as for numerous individual ensemble members (e.g., CCSM4, CanESM2, HadGEM2-ES, NorESM1-M). The sensitivity of many ensemble members to the range of applied scenario is within their variability (e.g., CSIRO-Mk3-6-0, CNRM-CM5, MIROC-ESM, MRI-CGCM3) or may hint at an enlarged scaling for weaker scenarios (e.g., MPI-ESM-LR). Frieler et al. (2015) found a low dependence of the scaling factors to four RCP scenarios for the whole Antarctic continent. Anomalies are not as distinctly pronounced in RCP2.6 as in the other scenarios due to the weaker forcing scenario. Please note, that CCSM4 is missing in the RCP2.6 (hence we have hatched the corresponding bar).

The boundaries of the three regions "EAIS Atl", "EAIS Ind", and "WAIS" resemble different oceanographic zones (Whitworth III et al., 2013; Orsi et al., 1999; Foldvik and Gammelsrød, 1988) under the consideration of Antarctica's large-scale drainage basins (Zwally et al., 2015). This chosen division of Antarctica does not produce surface area of equal size. As already indicated by the spatial distribution (Figure 4), the ordering from high to low scaling factors would be "EAIS Atl", "EAIS Ind", and "WAIS". The difference between both "EAIS" regions is minor, with a tendency towards higher values in "EAIS Atl" in the ensemble mean and some individual ensemble members. Some ensemble members do not show a clear trend between the scenario strength and scaling factor. For example, for MRI-CGCM3 the scaling decreases in "EAIS Atl" from RCP4.5 over RCP8.5 to RCP2.6, while in "EAIS Ind" the order is different from RCP8.5, RCP2.6, to RCP4.5 (Figure 5). It indicates again, that regional differences matter.

The region "WAIS" has significantly lower scaling factors than both "EAIS" regions. This difference exists for all ensemble means regardless of the applied scenarios and for almost all individual ensemble members (Figure A3), except some individual ensemble members under the RCP2.6 scenario (MIROC-ESM, MPI-ESM-LR) and the HadGEM2-ES.

The region "Siple Coast" (area $0.69 \cdot 10^6\,\mathrm{km}^2$, see Table 4) as a part of the "WAIS" region (area $4.26 \cdot 10^6\,\mathrm{km}^2$) is different in many aspects. It has the smallest area compared to the other regions (Table 4), and it shows the lowest ensemble mean scaling factors for all scenarios. Also, as before, no clear trend exists between different scenarios across the entire ensemble, while the spread of trends among individual ensemble members is substantial (Figure 5). Furthermore, some members exhibit a negative

scaling, where precipitation decreases for rising temperatures: MPI-ESM-LR under the RCP8.5 scenario and NorESM1-M under all scenarios (RCP8.5, RCP4.5, and RCP2.6). The inverted sign of the scaling is in stark contrast to the ensemble mean.

In the last decades, the detected downward trend in snow accumulation in this area (Wang et al., 2017) occurs while the wider West Antarctic Ice Sheet region belongs to the most rapidly warming regions globally (Bromwich et al., 2012). It underpins that less accumulation can befall under a warming climate. Furthermore, sea ice has expanded in the Ross Sea (Haumann et al., 2016; Liu, 2004). Hence, some ensemble members seem to imitate that expanding sea ice modifies the evaporation from the ocean and impacts the atmospheric circulation, which controls the flow of humid air masses, delivering precipitation to the Siple Coast. Even if NorESM1-M reproduces the overall seasonal sea ice extent cycle better than most CMIP5 models (Turner et al., 2013), it shows an unrealistically declining February sea ice trend in the Ross Sea over 1979-2005 (Turner et al., 2013). MPI-ESM-LR has large negative errors in sea ice extent over the year (Turner et al., 2013). Hence the mimicry of observed features in models may occur for the wrong reason.

In all four large regions ("glaciered", "grounded", "EAIS Atl", "EAIS Ind", and "WAIS"), we see a trend towards lower scalings for weaker forcing scenarios in the ensemble mean, with the exception of "EAIS Ind", where the factors for RCP8.5 and RPC4.5 are indistinguishable. Also, Frieler et al. (2015) found a low dependence of the scaling factors to the RCP scenario in comparison with the dependence on the specific climate model. Here, the region "WAIS" has on average a smaller precipitation scaling than both regions of the East Antarctic Ice Sheet ("EAIS Atl" and "EAIS Ind"), which is also reflected by the scaling factor maxima in these regions (Figure 4). As before, the Ross Ice Shelf and the adjacent Siple Coast feature, on average, the lowest scaling factors across the entire ice sheet (Figures 4 and 5). Some individual ensemble members project even negative scaling: precipitation deficit for rising temperatures (Figures 4 and 5).

The Siple Coast highlights definitely that, at the continental scale, it is not adequate to describe the spatial evolution of the precipitation by a fixed temperature scaling. Since the scaling exceeds mostly the commonly utilized value of $5\,\%\mathrm{K}^{-1}$, for instance, we diagnose the potential sea-level impact of applying the actual scaling distribution (e.g., Figure 4) versus a spatially and temporally constant scaling of $2\,\%\mathrm{K}^{-1}$, $5\,\%\mathrm{K}^{-1}$, or $8\,\%\mathrm{K}^{-1}$ across Antarctica.

3.3 Sea Level Impact of Precipitation Scaling by Temperature

To understand how the precipitation boundary condition impacts Antarctica's contribution to the global sea level, we inspect the precipitation fallen on Antarctica (Figure 6). Therefore, we integrate it over the dark-blue masked region of grounded ice (map on Figure 6), perform a cumulative summation since 1850, and restrict our analysis to all ensemble members driven by RCP8.5 (and anomalies relative to the first 50 years of the control run). Since accumulated precipitation over Antarctica lowers the global sea level under the assumption that ice loss (basal melting or calving) does not occur, the temporally accumulated potential sea-level impact curves have a negative slope (Figure 6a, b). Further on, this quantity is labeled "integrated precipitation."

In this manuscript, we distinguish between potential/diagnosed sea level and simulated sea level. The potential sea level is the transformation of an ice mass or freshwater volume into a global sea level by applying a global ocean area of $3.61 \cdot 10^{14}\mathrm{m}^2$

(Gill, 1982). In contrast, the simulated sea level is a diagnostic of the ice sheet model, which takes into account the total mass above flotation and the global ocean area.

The integrated precipitation declines more forcefully since the beginning of the 21st century, which is driven by the concurrent increase of precipitation over Antarctica (Figure 3a). The integrated precipitation shows a more pronounced temporal change because the vast interior, characterized by light precipitation, governs the integral. After the year 2100, the integrated precipitation declines linearly (Figure 6b), as we adopt the forcing of the years 2071-2100 recurrently. By applying the actual precipitation anomalies (solid lines, Figure 6a, b), the potential sea-level drop is stronger than using a scaling of $5\,\%\mathrm{K}^{-1}$ (dashed lines, Figure 6b) because the models' internal scaling exceeds $5\,\%\mathrm{K}^{-1}$ (Figure 5). Thus, in the year 5000, the maximal sea-level drop of $11\,\mathrm{m}$ (CCSM4) is nearly twice as large for applied precipitation anomalies, compared to less than $6\,\mathrm{m}$ (MIROC-ESM) for the $5\,\%$ scaling.

The difference of the integrated precipitation between $5\,\%\mathrm{K}^{-1}$ scaled and directly-applied precipitation anomalies is always positive (solid lines in Figure 6 c, d). This difference ranges approximately from $1\,\mathrm{cm}$ (CISRO-Mk3-6-0) to $15\,\mathrm{cm}$ (CCSM4) in the year 2100 and from $60\,\mathrm{cm}$ (MPI-ESM-LR) to $550\,\mathrm{cm}$ (CCSM4) in the year 5000. A lower scaling of $2\,\%\mathrm{K}^{-1}$ causes a magnified difference (dotted line in Figure 6 c, d), which corresponds to a reduced potential sea-level impact. It leads to differences ranging from $5\,\mathrm{cm}$ (MPI-ESM-LR) to $21\,\mathrm{cm}$ (CNRM-CM5) in 2100 and from $150\,\mathrm{cm}$ (MPI-ESM-LR) to $850\,\mathrm{cm}$ (CCSM4) in 5000.

A higher scaling of $8\,\%\mathrm{K}^{-1}$ (dashed line in Figure 6c, d) exceeds ice core-based estimates (Table 3, Figure 4), while it corresponds approximately to the ensemble mean (RCP8.5 $\approx 8.2\,\%\mathrm{K}^{-1}$, RCP4.5 $\approx 7.8\,\%\mathrm{K}^{-1}$, Figure 5). Now, only the CCSM4 model exhibits a positive difference because its scaling reaches $11\,\%\mathrm{K}^{-1}$ (Figure 5). Four models are nearly balanced (CNRM-CM5, MRI-CGCM3, HadGEM2-ES, NorESM1-M), while the remaining four feature negative differences (CISRO-Mk3-6-0, CanESM2, MIROC-ESM, MPI-ESM-LR). Hence, the difference range is subject to a change of sign, and the individual differences range from $-5\,\mathrm{cm}$ (CISRO-Mk3-6-0) to $7\,\mathrm{cm}$ (CCSM4) in 2100 and from -170 cm (CISRO-Mk3-6-0) to 280 cm (CCSM4) in 5000.

To summarize, precipitation and temperature, as average over the entire Antarctic continent, grow simultaneously in climate model simulations of the future. In concert with estimates of accumulation changes and temperature anomalies obtained from ice cores, it may (mis)lead us to scale the precipitation by the temporally evolving temperature. Therefore, fixed scaling factors are common. However, a tendency towards higher scaling exists under more vigorous climate trends (Figure 5), and the scaling has a clear spatial dependence (Figure 4 and 5). As a consequence, the accumulated snowfall on Antarctica for future climate projections differs between the methods, which ultimately leads to biased estimates of Antarctica's contribution to the global potential sea level. To assess the introduced bias, we analyze simulations of the Parallel Ice Sheet Model driven with numerous variants of the above-discussed climate conditions and a diverse set of implemented boundary conditions.

3.4 Relation between Precipitation Boundary Condition and Ice Thickness

Starting in the year 1850, we performed numerous ice-sheet simulations to analyze how the applied precipitation boundary condition impacts the ice-sheet thickness distribution. Each climate scenario from an individual climate model (as part of the

ensemble) drives an independent ice-sheet simulation. These together constitute the ensemble of 208 ice-sheet simulations (Table 1). Hence, the average across ice-sheet simulations forms the ensemble mean. For the diagnostic, we also inspect the maximum and minimum thickness at each grid point across all ensemble members. Therefore, the field of joined extreme values could come from a diverse set of ice-sheet ensemble members and, hence, does not necessarily lead to dynamically consistent distribution.

Complementary ice-sheet (control) simulations are performed under the sole utilization of the reference forcing fields (Figure 2a-c). In these simulations, the detected trend of about $2\,\mathrm{mm\,decade^{-1}}$ (sea-level equivalent) fades within the first 400 years and differs slightly between the two initial states (PISM1Eq and PISM2Eq). Even if we apply anomalies on top of the reference background fields, we can not exclude a shock-like behavior of the simulations entirely directly following the decades after the year 1850. Since we compute the anomalies relative to the average over the first or the last 50 years, respectively, of the control run for each climate model, these anomalies are not necessarily zero at the beginning of the year 1850. Hence, the ice-sheet model may experience a small jump, which cause an artificial trend initially. Hence, in the following, the subtracted trend for each single ensemble member depends on its initial state.

In the year 2100, the ice thickness for both precipitation boundary conditions (precipitation anomaly deduced from the applied climate models versus scaled precipitation) increase over large parts of the Antarctic continent (Figure 7b-e). The thickness for the simulations driven by scaled precipitation grows less over substantial parts of the interior than in the simulations forced by the precipitation anomalies (Figure 7a), as the difference between scaled precipitation and applied precipitation anomaly is mostly negative. Thus, simulations driven by the precipitation anomalies accumulate more snow and grow thicker ice, which leads to a stronger sea-level drop. This result supports the analysis above (Figure 6). A ring of a pronounced negative thickness difference follows the coast, where the precipitation anomaly (Figure 2e, h, k) is enhanced. This ring emerges for a significant part of the coastal East Antarctic Ice Sheet (EAIS) and West Antarctic Ice Sheet (WAIS). For the latter ice sheet, the negative area is shifted away from the coast towards the interior (Figure 7a). Also, a negative strip of the thickness difference appears at the south side of the Transantarctic Mountain Range, and some grounded ice streams flowing into the Filchner-Ronne Ice Shelf.

Regions of positive differences coincide with thicker ice for simulations driven by scaled precipitation. These are located south of the Transantarctic Mountain Range at the northern edge of the Ross Ice Shelf, along the coastline of the WAIS, and in the coastal Terre Adélie region. There, the scaling is generally lower or falls behind the constant scaling of $5\,\%\mathrm{K^{-1}}$. However, this does not explain exclusively positive areas.

For both precipitation boundary conditions, the mean ice thickness of each of the respective sub ensembles reveals a widespread weakening of the floating ice shelves, such as Filchner-Ronne, Ross, and Amery Ice Shelves (Figure 7b, d). In the WAIS, both Pine Island Glacier and Ferrigno Ice Stream (an ice stream that flows into the Filchner Ice Shelf) thin drastically. Along the Antarctic Peninsula, general shrinking occurs along the coasts. Also along the marginal EAIS, ice thins.

For some places, the ice thickness thins for both precipitation boundary conditions across all ensemble members as the reduction of the maximal ice thickness highlights (Figure 8c, e). This reduction marks those outlet glaciers and ice shelves that are extremely vulnerable. These are around the Rutford Ice Stream, Foundation Ice Stream, Ronne Ice Shelf, Amery Ice Shelf,

three outlet glaciers (in "EAIS Ind" as part of Wilkens Land, Terre Adélie, and George V Land), northwestern Ross Ice Shelf (Ross Island), and Pine Island together with Thwaites Glacier in the Amundsen Sea (Figure 8c, e).

To conclude, the ice thickness is indeed thicker for simulations driven by the precipitation anomalies (Figure 8). Regardless of the applied precipitation boundary condition, there is widespread ice-shelf thinning, as well as ice-shelf weakening, at the margins in the ensemble mean. Ice thinning for the ensemble member of the maximal thickness highlights the most vulnerable regions, such as Pine Island and Thwaites Glaciers, Amery Ice Shelf and some outlet glaciers of the EAIS.

3.5 Attribution of the driving model

All ensemble members contribute to the ensemble mean, while at a given grid location the maximum and minimum are determined by climate forcing from one particular climate model. We inspect which climate model may lead to ice thickness growth or shrinking and restrict ourselves first to the model year 2100, when the transient forcing of period 1850–2100 excites changing ice thicknesses.

Directly at margins apart from the vast ice shelves, the attributed model that drives either the maximum or minimum ice thickness shows a noisy small-scale pattern (Figure 8d, e). Hence, the marginal regions cannot be associated with a particular climate model. In contrast, the mean and minimum thicknesses of the Filchner-Ronne and Ross Ice Shelves, and also to some extent the Amery Ice Shelf, are highlighted by a nearly unique color patch indicating a reduced thickness. These patches are separated from the surroundings showing either a reduced thinning or even thickening. Intriguingly, the MIROC-ESM model forcing, for instance, thickens grounded ice east and west of the Ross Ice Shelf (Figure 8d), while it also predominantly thins the Ross Ice Shelf (Figure 8e). Hence, the ocean forcing drives the ice-shelf thinning here. Since the spatial pattern of the atmospheric and ocean forcing that promotes or undermines the ice thickness is not necessarily aligned, this may explain the small scale noisy pattern along the coast. Also (nonlinear) dynamical changes on the considered time scales may occur in response to both ocean and atmospheric forcing.

Beyond the direct coast strip, larger areas appear where the forcing from one climate model determines the maximum or minimum thickness, respectively. However, these extended continuous regions are often interrupted by spots controlled by the climate from other models. Also, the pattern is changing during the transient simulation starting in 1850 because the temporal evolution of the 2m-air temperature and precipitation anomalies are different for each climate model as the integrated precipitation highlights (Figure 6a, b). Furthermore, after the year 2100, where the same 30 years forcing period (2071–2100) drives the ice-sheet model recurrently, the pattern evolves further (Figure 9). Because the ice sheet has not reached the quasi-equilibrium to the last 30 years forcing, the pattern alteration is ongoing.

For grounded ice, three models (CCSM4, CNRM-CM5, MIROC-ESM) determine predominantly the growing ice until the year 2100 (Figure 8d), which is in-line with the diagnosed sea-level contribution (solid line, Figure 6a, b). CCSM4 dominates the "EAIS Atl" sector, while CNRM-CM5 dominates a band from the "EAIS Ind" sector clockwise to the Antarctica Peninsula, which is interrupted by regional-scale patches of the MIROC-ESM. A spatial dominance is not apparent for the minimum ice thickness, because the patchwork of five models (CSIRO-Mk3-6-0, HadGEM2-ES, MPI-ESM-LR, MRI-CGCM3, NorESM1-M) dominates the year 2100. NorESM1-M influences the WAIS, which is supported by its lowest scaling in the Siple Coast

region (Figure 5). CSIRO-Mk3-6-0 has an impact around the South Pole, MRI-CGCM3 affects the coastal zone in the EAIS. The control of MPI-ESM-LR and, to a lesser extent, HadGEM2-ES spreads across the entire continent. If we progress into the year 2200, where we have applied the 30 years forcing more than three times, the emerging picture shows a consolidation of the influential spheres of the different models for both the maximum and minimum thicknesses (Figure 9).

If we now turn towards those model simulations, in which the temperature-scaled precipitation forcing has been applied, both the mean, maximum, and minimum ice thickness distribution (Figure 10) are similar to the ones driven by the precipitation anomalies as discussed above (Figure 7). Also, the same models determine the ice-shelf thickness of the Filchner-Ronne and Ross Ice Shelves. The latter shows that primarily the ocean controls ice-shelf thickness changes in our simulations. However, we detect a stark contrast of the model determining the maximum and minimum ice thickness. For the maximum, we still have the same three models (CCSM4, CNRM-CM5, MIROC-ESM). However, the pattern has changed. CCSM4 controls a smaller area in the interior around the South Pole, and MIROC-ESM some coastal regions of the East Antarctic Continent. The remaining majority of the grounded ice is under the control of CNRM-CM5. The most striking changes occur for the minimum. Now, NorESM1-M determines the entire WAIS and also some parts of "EAIS Ind". MRI-CGCM3 dominates the remaining East Antarctic Ice Sheet.

In the latter case, temperature variations force the precipitation-driven ice thickness evolution exclusively (see Equation 1). These temperature changes do not necessarily reflect dynamical changes in the atmosphere that are accompanied by modified circulation patterns that ultimately transport and deliver the precipitation for Antarctica. Hence, the applied scaling or precipitation boundary condition impacts the temporal evolution of the Antarctic Ice Sheet geometry, which ultimately shapes Antarctica's contribution to the global sea level.

3.6 Ice losses

After the spin-up, the simulations have reached a quasi-equilibrium. For the discussion of the ice losses, we concentrate on the transient period 1850-2100. For all climate scenarios, the calving rate hardly changes (Figure A12), whereas the total ice-shelf area is nearly constant until 2000 and declines afterward (Figure A15). The ocean-driven basal melting is proportional to the squared temperature difference between the pressure-dependent melting temperature and the actual ocean temperature. Since the ocean temperature increases in general (Figure 2f, i, l and Figure 3c), also the mass loss by basal melting increases, while the total shelf ice area remains quasi-constant until 2000 and declines afterwards (Figure A15). For RCP8.5, the basal melting increases at the end of the 21st century quadratically. To conclude, the calving rate is nearly constant, while the basal melting increases by approximately $33\,\%$ between the years 2000 and 2100.

The mean calving rate is about $8000\,\mathrm{Gt\,year^{-1}}$ and $5000\,\mathrm{Gt\,year^{-1}}$ for the ensemble member utilizing the parameters and the initial state of PISM1Eq and PISM2Eq, respectively (Figure A12). The basal melting rates for PISM1Eq and PISM2Eq are similar, however, the loss rates for PISM1Eq are slightly larger than PISM2Eq (Figure A13). The ensemble mean starts at about $550\,\mathrm{Gt\,year^{-1}}$ in 1850 and reaches $900\,\mathrm{Gt\,year^{-1}}$ in 2100.

Since floating ice shelves nourish both ice losses, these ice losses do not directly impact the sea-level. Under the assumption that the inflow of former grounded ice compensates any shelf mass loss, the reported ice losses of $8500\,\mathrm{Gt\,year^{-1}}$–

$9000\,\mathrm{Gt\,year^{-1}}$ (5500–$6000\,\mathrm{Gt\,year^{-1}}$) would correspond to a sea-level rise of $2.58\,\mathrm{cm\,year^{1}}$–$2.74\,\mathrm{cm\,year^{1}}$ ($1.67\,\mathrm{cm\,year^{1}}$–$1.83\,\mathrm{cm\,year^{1}}$). The Integration over 250 years to match the period from 1850 to 2100 would generate a potential sea-level equivalent of $6.47\,\mathrm{m}$ – $6.85\,\mathrm{m}$ ($4.19\,\mathrm{m}$ – $4.57\,\mathrm{m}$). However, the actual ratio between total ice mass change and the corresponding potential sea level response is obviously not a 1:1 relation. Instead, on average less than $5\,\%$ of the total mass lost by both iceberg calving and floating ice-shelf melting is compensated by grounded ice that raises the sea level (Figure A8). Considering this ratio of $5\,\%$, the sea level impact reduces to $0.32\,\mathrm{m}$ – $0.34\,\mathrm{m}$ ($0,21\,\mathrm{m}$ – $0.23\,\mathrm{m}$) by 2100. It is less than integrated precipitation anomalies across the Antarctic continent (Figure 6a), which explains the total mass gains.

Anyhow, the integrated basal melting rates are too low (Figure A13 and the calving rates are too high (Figure A12) compared to observational estimates in our ensemble of ice-sheet model simulations. Besides the fact that the total loss exceeds recent observational estimates, our ice sheet is in a quasi-equilibrium after the spin-up. All this may indicate that the integrated precipitation driven accumulation resulting from the RACMO precipitation reference field might be too large. However, the surface mass balance of RACMO agrees well with observational estimates (Wang et al., 2016), while the uncertainty of the surface mass balance (sea-level equivalent of $\sim 0.25\,\mathrm{mm\,year^{-1}}$ (Van Wessem et al., 2014)) is of almost the same size as Antarctica's observational-based sea-level contribution ($\sim 0.2\,\mathrm{mm\,year^{-1}}$ between 1992 and 2011 (Shepherd et al., 2012; Wang et al., 2016)). Additionally, recent satellite-based estimates indicate clearly that the Antarctica Ice Sheet have lost mass (sea-level equivalent: $0.4\,\mathrm{mm\,year^{-1}}$) in the period 2011–2017 (Sasgen et al., 2019).

Beyond the year 2100 (Figure A14), the calving rates decrease and reach a minimum in the period 3000–4000. Afterward, calving increases again slightly. Basal melting rates are subject to a slight decreasing trend (RCP2.6), nearly constant values (RCP4.5), or a negligible upward trend after the year 4000 (RCP8.5).

3.7 Precipitation Boundary condition and Sea Level

In the following, we consider all ensemble members starting from both initial states PISM1Eq and PISM2Eq. They are driven by the climate scenarios RCP2.6, RPC4.5, or RCP8.5. For each CMIP5 model, the applied anomalies have been computed either relative to the first or last 50 years of the control run simulation (piControl). The simulated sea-level curves are shifted so that the simulated sea-level contribution is $0\,\mathrm{m}$ in the year 2000. Since the spread of individual ensemble members may not follow a normal distribution, we present beside the mean also the median sea-level contribution. For the RCP8.5 scenario, we highlight the spreading among models by depicting the standard deviation (1σ).

For the period 1850 until 2000, the simulated sea-level contribution of Antarctica fluctuates slightly. Hence, the accumulation balances nearly the ice loss at the margin while the basal melting rated of grounded ice is steady (Figure A9). Please note that there is no drift involved, as we have subtracted the trend from the continued ice-sheet simulations under the reference climate (Table 2). We also detect an amplified signal for the simulations driven by the precipitation anomalies compared to those forced by temperature-scaled precipitation anomalies, which corresponds to the above diagnosed sea-level impact of the precipitation (Figure 6).

After the year 2000, all our ensemble members, regardless of the forcing scenario, gain mass causing a falling simulated sea level (Figure 12). The basal melting of grounded ice does not impact the sea-level evolution, because this basal melting

rate is nearly constant so that the corresponding integrated sea-level equivalent grows linearly for all scenarios from 1850 until 2100, and only after the year 2500 these curves diverge. (Figure A9). Also, the combined loss of iceberg calving and basal melting of floating ice shelves does not vary considerably over the considered period. Consequently, the growth of simulated accumulation explains the net mass gains and, hence, the negative sea-level contributions from Antarctica after the year 2000 (Figure 12). Depending on the applied forcing and precipitation boundary condition, the global simulated sea-level drop ranges from $2\,\mathrm{cm}$ to $11\,\mathrm{cm}$ until 2100 (Figure 12). This result is in contrast to various publications, and we discuss it below.

If we continue our ensemble with the last 30 years of forcing until the year 5000, the simulated sea-level contribution of those ensemble members driven by the temperature-scaled precipitation starts to stabilize and reaches a minimum around the year 2500. Afterward, they begin to lose more ice at the margins than they gain in the interior. As a consequence, these simulations produce on average a positive contribution to the global simulated sea level after the year 3200 (RCP8.5) and 3900 (RCP2.6), which compensates for the negative contributions since 1850. In the year 5000 at the end of our simulations, these runs show a trend towards a continuously growing ice loss rate, because the curves have still an upward-directed tendency. Hence a quasi-equilibrium is not established. In contrast, the simulations driven by the precipitation anomalies continue to show a falling simulated sea level. They always contribute negatively to the global simulated sea until the year 5000, and their ensemble mean and median sea levels tend to converge at the end of the simulations.

3.7.1 Sea level contribution of corrected basal melting

Since the simulated sea level contribution of Antarctica disagrees with the currently observed state showing mass loss, we apply a corrected time series emulating the observational-based ocean-driven basal melting. This analysis shall reveal if a more vibrant basal melting rate in concert with the simulated ice sheet mass evolution leads to a less pronounced ice sheet growth or drives even ice loss. Ultimately, does a more vigorous melting of ice shelves raise the simulated sea level of all ensemble members?

By construction, the correct time series preserve the fluxes' amplification over time, which is essentially the ratio of the higher end value to the lower start value. Hence, the corrected basal melt flux replicates the original simulated amplification while the flux is identical to the observed reference value ($F_{\mathrm{ref}}(t_{\mathrm{ref}})$) at the reference time (t_{ref}). Under the assumption that only a fraction of the adjusted basal mass contributes to the global sea level, we apply the simulated ratio of the sea level change to the total ice mass change. For each ensemble member, this ratio is the median ratio over its entire time series (for details see Section A3 "Bias-corrected fluxes" on page 49 in the appendix). Since we examine enhanced mass loss, we do not adjust the iceberg calving rates that are already higher than observed.

By adjusting the basal melting flux, the determined temporal evolution of the sea level correction (Figure A5, Equation A8) does impact the global simulated sea level. Still, it does not change the sign of the contemporary sea-level evolution. Consequently, the impact on the simulated sea level is very small (Figure A6). If we assume instead that all of the additional mass loss of floating ice shelves rises the simulated ea level immediately, we would obtain too extensive corrections of $30\,\mathrm{cm}$ between 1850 and 2000. This corresponding sea-level rise would be larger than the observed integrated sea level rise of about $20\,\mathrm{cm}$ since 1850 (Church and White, 2011), which has been driven by world-wide land-water storage changes, shrinking glaciers

around the globe, enhanced melting from Greenland, and thermal expansion of the ocean (Cazenave and Remy, 2011; Leclercq et al., 2011; Church and White, 2011).

To conclude: The correction exceeds observational estimates significantly under the unrealistic assumption that all additional basal melting of ice shelves would raise the simulated sea level. It is unrealistic because disintegrating floating ice shelves do not impact the sea level directly. The correction hardly corrects the discrepancy if we apply the inferred ratio of about $5\,\%$ between the simulated total ice mass loss and the simulated sea level contribution.

4 Conclusions

It is crucial for numerical simulations of Antarctica's sea-level contribution, how the precipitation is specified in ice-sheet simulations. The commonly used method of scaling the precipitation changes with the simulated temperature changes from ice cores or global climate models leads to a positive Antarctic simulated sea-level contribution, i.e., a simulated sea-level rise. However, when considering the simulated precipitation changes from the global climate models, the situation changes. In this case, our numerical projections simulate a negative sea-level contribution. Major uncertainties affect these simulations, such as the partitioning of ice losses into calving and basal melt — which is quite different from observational estimates due to very crude representations in the ice-sheet model — or the omission of important processes, such as the interaction between ocean, ice shelves, and ice sheet. While we could improve some aspects of the involved process descriptions, our simulations are state-of-the-art and suffer, thence, the same limitations as others.

In all CMIP5 models, the 2m-air temperature warms across the entire Antarctic continent without any exception (Figure 2d, g, j, and 3a), because even the minimum 2m-air temperature anomaly is positive everywhere (Appendix Figure A2d, g, j). The warming enhances the hydrological cycle, which causes generally heavier precipitation (Figure 3b) in particular along the coast of Antarctica (Figure 2e, h, k). However, the changing precipitation does not increase at the same rate with increasing temperature because it is not only thermodynamically influenced but also dynamically controlled. Given that the ensemble mean temperature scaling is different for the West and East Antarctic Ice Sheet (Figure 5) and has a considerable spatial dependence, the dynamical component is not negligible. Instead, the region of reduced precipitation under rising air temperatures, which we have identified along the Siple Coast, highlights that the dynamics could compensate or even overcome the thermodynamics. The continent-wide scaling is per se problematic, even if we would adjust the scaling factor to reproduce the continental-wide average scaling. In this case, the integrated precipitation would be identical, but the spatial structure is still entirely different (Figure 4). Hence for a realistic projection of Antarctica's sea-level contribution, the spatial pattern of the future accumulation of precipitation shall also consider the dynamical effect.

Independent of the applied precipitation boundary condition, we detect regions where the ice thickness thins for all ensemble members. These regions are the Amundsen Sea Embayment with both Pine Island and Thwaites Glaciers, some outlet glaciers of the East Antarctic Ice Sheet (EAIS) between George V and Wilkens Land, Amery Ice Sheet, and the Northern Antarctica Peninsula. These regions correspond to those, which have been identified across sixteen models within a recent model intercomparison exercise, where ocean warming wanes marginal ice (Seroussi et al., 2019a).

The ocean (Etourneau et al., 2019) and atmosphere (Mulvaney et al., 2012; Thomas et al., 2009; Morris and Vaughan, 2003) is already warming along the Antarctic Peninsula. This results in a southward progressing of the annual 2m-air temperatures of -9°C or -5°C isotherm, which presents the range of thresholds for the stability of ice shelves suggested by Morris and Vaughan (2003, -9°C) and Doake (2001, -5°C), respectively. It may also enable the formation of meltwater ponds on ice shelves (Kingslake et al., 2017) that precedes (van den Broeke, 2005) or even triggers ice-shelf disintegration (Banwell et al., 2013, 2019). After an ice shelf has decayed, the feeding ice streams are losing more ice, as seen for Larsen-B (Rott et al., 2011), which lowers the thickness of grounded ice. Anyhow, ice shelves along the Antarctic Peninsula have collapsed or are retreating (Cook and Vaughan, 2010; Rott et al., 1996). In our simulations under the RCP8.5 scenario, this observed retreat and the related ice loss will continue.

For part of the EAIS, simulations show that grounded ice of the Wilkens Basin in the hinterland of George V Land may be prone to a massive ice loss if the ice front loses its buttressing effect (Mengel and Levermann, 2014). Our ensemble shows, on average, a stable situation here. Ice in deep troughs that are in contact with the warming ocean thins at some spots further to the west. It happens in front of the Astrolabe Trench (in Terre Adélie) and on the coast of the Wilkens Land, for example near the Totten Glacier. Ice also thins in the deep trench leading to the Amery Ice Shelf.

Both the Pine Island and Thwaites Glaciers in the Amundsen Sea as part of the marginal West Antarctic Ice Sheet lose ice (Jeong et al., 2016; Milillo et al., 2019; Rignot et al., 2014; Scambos et al., 2017). According to the ensemble projecting the future, for them, continuous ice loss is inevitable. It also shows that the Ferringo Ice Stream flowing into the Bellingshausen Sea will thin in the future.

Since our simulations presented here are in contrast to others that project a sea-level contribution from a shrinking Antarctic Ice Sheet, we highlight the differences before we discuss the limitations of our simulations. Some simulate Antarctica with a finer spatial resolution (Golledge et al., 2015; Pollard et al., 2015), which could improve the presentation of ice streams. These streams channelize the flow of grounded ice from the interior to the margins, where they feed the attached ice shelves and discharge directly into the ocean. However, the simulated surface velocity distribution reasonably reproduces satellite-based estimates (Appendix Figure A10 and Figure A11). Others used the cliff failure parameterization supporting ice loss together with a constant ocean temperature offset of +2°C (Pollard et al., 2015), twice as large as the amount found in our ensemble of nine CMIP5 models (Figure 3), or utilized continuously raising atmospheric and oceanographic temperature forcing (Golledge et al., 2015; Mengel et al., 2015; Winkelmann et al., 2012, 2015) beyond the year 2100. These stronger forcings alone explain a large part of the difference because we apply recurrently the forcing of the years 2071–2100 after 2100.

Since the precipitation boundary condition determines if Antarctica rises or lowers the global sea level, it may be appropriate to utilize a more sophisticated surface mass balance (SMB) model. The recent publication that indicates a Greenlandification of Antarctica's margin at the end of the century (Bell et al., 2018) supports this approach, but the required atmospheric inputs fields are not available at sufficient temporal resolution. Hence, this will be an option for simulations driven by the forthcoming CMIP6 model output.

As already discussed, the application of anomalies may trigger a small shock at the beginning of each simulation. This shock creates an artificial trend in the simulated sea-level time series initially. Nevertheless, the long-term positive and negative sea-

level contribution of Antarctica for simulations driven by temperature-scaled and directly-applied precipitation anomalies, respectively, are robust.

An issue could be the parameterization of the grounding line migration, where only extremely high resolution relaxes its need. However, PISM's grounding line parameterizations at medium to lower resolution is consistent with higher-order models (Feldmann et al., 2014). It explains that the present-day grounding line position resembles the current state reasonably, and the simulated grounding line retreat follows the bulk of simulations in the last model intercomparison (Seroussi et al., 2019a); hence, we consider our grounding line migration as reasonable. The apparent stability of ice shelves in the runs driven by the precipitation anomalies seems to comply with the safety band of ice shelves (Fürst et al., 2016), so the calving does stay outside of ice-shelf regions essential for providing buttressing for the inflowing grounded ice streams.

The ocean boundary condition, where ocean conditions are extrapolated into the ice-shelf cavities, drive basal ablation of ice shelves. Here, we could undoubtedly improve simulations if the ice shelves would be coupled to the driving ocean model, so that basal melting impacts the thermal structure of the ocean and, ultimately, the melt patterns. CMIP5 models neglect the ocean-ice-shelf interaction (Meijers, 2014), and their coarse resolution around Antarctica does not allow to represent the regional conditions (Heuzé et al., 2013; Sallée et al., 2013b). They are subject to unrealistic open-ocean convection (Heuzé et al., 2013; Meijers, 2014; Sallée et al., 2013a) instead of convection on or near the continental shelf (Årthun et al., 2013; Nicholls et al., 2009). All these taint the hydrographic structure along Antarctica's coasts. Hence, any improved parameterization can not rectify the existing biases in the ocean forcing. These biases are reduced if we apply ocean temperature anomalies on top of an observational-based climatological data set as performed in our study.

Since we extrapolate coastal ocean temperatures laterally into the ice-shelf cavities, the obtained ocean warming might be higher if we would include the rise of the strongly warming gyre centers. If this may have been incorporated in the forcing of other groups obtaining a higher ice loss, depends on the setup details. However, it may help to bridge the gap between other studies and our simulations.

Nevertheless, the simulated sea-level decrease for the used precipitation anomaly forcing is in agreement with a growing surface mass balance since 1800 AD, driven mainly by the Antarctic Peninsula region (Thomas et al., 2017). During intensive El Nino years, the accumulation-driven ice height increase between Dotson Ice Shelf and Ross Ice Shelf exceeds the height reduction by basal melting processes (Paolo et al., 2018), but the ice mass is still decreasing since the low-density snowfall replaces ice with a higher density. The stability arguments of Ritz et al. (2015) confirm the apparent stability of Antarctica in our simulations. Furthermore, various recent ice-sheet model simulations, driven by selected CMIP5 climate model fields in the framework of the ISMIP6 exercise, are subject to a negative sea-level contribution under a warming climate (Seroussi et al., 2019b).

To evaluate the impact of the precipitation boundary condition, fully coupled simulations between a dynamic ice-sheet/shelf model and a global climate model are inevitable. The system would include the ice-shelf-ocean interaction of coupled ocean-ice shelves at a sufficiently high spatial resolution around Antarctica. In addition, it would contain a sophisticated surface mass balance computation. We hope these coupled atmosphere-ocean/sea-ice–ice-sheet/shelf models will overcome the discussed limitations.

Code and data availability. The Code of the Parallel Ice Sheet Model is freely available from https://github.com/pism/pism. Modifications of the PISM's code are available from TK upon reasonable request. The data is available from the corresponding author or TS upon reasonable request.

Author contributions. CR performed the simulations and wrote the manuscript. All authors contributed to the interpretation of the results and proofreading of the manuscript.

Competing interests. The authors declare that they have no conflict of interest.

Acknowledgements. This work has been financed through the German Federal Ministry of Education and Research (Bundesministerium für Bildung und Forschung: BMBF) project ZUWEISS (grant agreement 01LS1612A). Parts of this work are supported by BMBF grant 01LP1503B (project PalMod1.2). The Deutsche Klima Rechenzentrum (DKRZ) supplied computer resources on the cluster "mistral". CR wants to thank the AWI's HPC administrators for their proactive and generous support enabling this work during the development phase. The development of PISM is supported by NASA grant NNX17AG65G and NSF grants PLR-1603799 and PLR-1644277. The data analyzes and the production of figures have been predominantly performed with the help of the following software products (alphabetic order): Climate Data Operators (CDO: https://code.mpimet.mpg.de/projects/cdo/), Generic Mapping Tools (GMT: https://www.generic-mapping-tools.org/), Ncview (http://meteora.ucsd.edu/~pierce/ncview_home_page.html), netCDF Operator (NCO, http://nco.sourceforge.net/), PyFerret (https://ferret.pmel.noaa.gov/Ferret/documentation/pyferret), python (python3, https://www.python.org/, including the following packages NumpPy: https://numpy.org, matplotlib: https://matplotlib.org, and xarray: https://xarray.pydata.org/). We thank the numerous authors and their financial supporters of these software products.

References

Adusumilli, S., Fricker, H. A., Siegfried, M. R., Padman, L., Paolo, F. S., and Ligtenberg, S. R. M.: Variable Basal Melt Rates of Antarctic Peninsula Ice Shelves, 1994-2016, Geophysical Research Letters, 45, 4086–4095, https://doi.org/10.1002/2017GL076652, 2018.

Agosta, C., Fettweis, X., and Datta, R.: Evaluation of the CMIP5 models in the aim of regional modelling of the Antarctic surface mass balance, The Cryosphere, 9, 2311–2321, https://doi.org/10.5194/tc-9-2311-2015, 2015.

Allen, M. R. and Ingram, W. J.: Constraints on future changes in climate and the hydrologic cycle, Nature, 419, https://doi.org/10.1038/nature01092, 2002.

Applegate, P., Kirchner, N., Stone, E., Keller, K., and Greve, R.: An assessment of key model parametric uncertainties in projections of Greenland Ice Sheet behavior, The Cryosphere, 6, 589–606, https://doi.org/10.5194/tc-6-589-2012, 2012.

Arneborg, L., Wåhlin, A., Björk, G., Liljebladh, B., and Orsi, A.: Persistent inflow of warm water onto the central Amundsen shelf, Nature Geoscience, 5, 876–880, https://doi.org/10.1038/ngeo1644, http://www.nature.com/doifinder/10.1038/ngeo1644, 2012.

Årthun, M., Holland, P. R., Nicholls, K. W., and Feltham, D. L.: Eddy-Driven Exchange between the Open Ocean and a Sub–Ice Shelf Cavity, Journal of Physical Oceanography, 43, 2372–2387, https://doi.org/10.1175/JPO-D-13-0137.1, 2013.

Bakker, P., Clark, P. U., Golledge, N. R., Schmittner, A., and Weber, M. E.: Centennial-scale Holocene climate variations amplified by Antarctic Ice Sheet discharge, Nature, pp. 1476–4687, https://doi.org/10.1038/nature20582, 2016.

Banwell, A. F., MacAyeal, D. R., and Sergienko, O. V.: Break-up of the Larsen B Ice Shelf Triggered by Chain-Reaction Drainage of Supraglacial Lakes, Geophysical Research Letters, 40, 5pp, https://doi.org/10.1002/2013GL057694, 2013.

Banwell, A. F., Willis, I. C., Macdonald, G. J., Goodsell, B., and MacAyeal, D. R.: Direct measurements of ice-shelf flexure caused by surface meltwater ponding and drainage, Nature Communications, 10, 730, 10p, https://doi.org/10.1038/s41467-019-08522-5, 2019.

Bell, R. E., Chu, W., Kingslake, J., Das, I., Tedesco, M., Tinto, K. J., Zappa, C. J., Frezzotti, M., Boghosian, A., and Lee, W. S.: Antarctic ice shelf potentially stabilized by export of meltwater in surface river, Nature, 544, 344–348, https://doi.org/10.1038/nature22048, 2017.

Bell, R. E., Banwell, A. F., Trusel, L. D., and Kingslake, J.: Antarctic surface hydrology and impacts on ice-sheet mass balance, Nature Climate Change, 8, 1044–1052, https://doi.org/10.1038/s41558-018-0326-3, 2018.

Bracegirdle, T. J., Stephenson, D. B., Turner, J., and Phillips, T.: The importance of sea ice area biases in 21st century multimodel projections of Antarctic temperature and precipitation, Geophysical Research Letters, 42, 10,832–10,839, https://doi.org/10.1002/2015GL067055, 2015.

Braithwaite, R. J.: Positive degree-day factors for ablation on the Greenland Ice-sheet studied by energy balance modeling, Journal of Glaciology, 41, 153–160, http://apps.isiknowledge.com.proxy.lib.umich.edu/full{_}record.do?product=WOS{&}search{_}mode=GeneralSearch{&}qid=48{&}SID=1FH@LoL1EM39J5IMpgJ{&}page=1{&}doc=1, 1995.

Bromwich, D. H., Nicolas, J. P., and Monaghan, A. J.: An Assessment of Precipitation Changes over Antarctica and the Southern Ocean since 1989 in Contemporary Global Reanalyses, Journal of Climate, 24, 4189–4209, https://doi.org/10.1175/2011JCLI4074.1, 2011.

Bromwich, D. H., Nicolas, J. P., Monaghan, A. J., Lazzara, M. A., Keller, L. M., Weidner, G. A., and Wilson, A. B.: Central West Antarctica among the most rapidly warming regions on Earth, Nature Geoscience, 6, 139–145, https://doi.org/10.1038/ngeo1671, 2012.

Bueler, E. and Brown, J.: Shallow shelf approximation as a "sliding law" in a thermomechanically coupled ice sheet model, Journal of Geophysical Research, 114, 21pp, https://doi.org/10.1029/2008JF001179, 2009.

Bueler, E., Lingle, C. S., and Brown, J.: Fast computation of a viscoelastic deformable Earth model for ice-sheet simulations, Annals of Glaciology, 46, 97–105, https://doi.org/10.3189/172756407782871567, 2007.

Cazenave, A. and Remy, F.: Sea level and climate: measurements and causes of changes, Wiley Interdisciplinary Reviews: Climate Change, 2, 647–662, https://doi.org/10.1002/wcc.139, 2011.

Church, J., Clark, P., Cazenave, A., Gregory, J., Jevrejeva, S., Levermann, A., Merrifield, M., Milne, G., Nerem, R., Nunn, P., Payne, A., Pfeffer, W., Stammer, D., and Unnikrishnan, A.: Sea Level Change, in: Climate Change 2013: The Physical Science Basis. Contribution of Working Group I to the Fifth Assessment Report of the Intergovernmental Panel on Climate Change, edited by Stocker, T., Qin, D., Plattner, G.-K., Tignor, M., Allen, S., Boschung, J., Nauels, A., Xia, Y., Bex, V., and Midgley, P., chap. 13, Cambridge University Press, Cambridge, UK and New York, NY, USA, http://www.ipcc.ch/report/ar5/wg1/, 2013a.

Church, J. A. and White, N. J.: Sea-Level Rise from the Late 19th to the Early 21st Century, Surveys in Geophysics, 32, 585–602, https://doi.org/10.1007/s10712-011-9119-1, 2011.

Church, J. A., White, N. J., Konikow, L. F., Domingues, C. M., Cogley, J. G., Rignot, E., Gregory, J. M., van den Broeke, M. R., Monaghan, A. J., and Velicogna, I.: Revisiting the Earth's sea-level and energy budgets from 1961 to 2008, Geophysical Research Letters, 38, 8p, https://doi.org/10.1029/2011GL048794, http://doi.wiley.com/10.1029/2011GL048794, 2011.

Church, J. A., White, N. J., Konikow, L. F., Domingues, C. M., Graham Cogley, J., Rignot, E., Gregory, J. M., van den Broeke, M. R., Monaghan, A. J., and Velicogna, I.: Correction to "Revisiting the Earth's sea-level and energy budgets from 1961 to 2008", Geophysical Research Letters, 40, 4066–4066, https://doi.org/10.1002/grl.50752, http://doi.wiley.com/10.1002/grl.50752, 2013b.

Cook, A. J. and Vaughan, D. G.: Overview of areal changes of the ice shelves on the Antarctic Peninsula over the past 50 years, The Cryosphere, 4, 77–98, https://doi.org/10.5194/tc-4-77-2010, 2010.

de Boer, B., van de Wal, R. S. W., Lourens, L. J., Bintanja, R., and Reerink, T. J.: A continuous simulation of global ice volume over the past 1 million years with 3-D ice-sheet models, Climate Dynamics, 41, 1365–1384, https://doi.org/10.1007/s00382-012-1562-2, 2013.

Depoorter, M., Bamber, J., Griggs, J., Lenaerts, J., Ligtenberg, S., van den Broeke, M., and Moholdt, G.: Calving fluxes and basal melt rates of Antarctic ice shelves., Nature, 502, 89–92, https://doi.org/10.1038/nature12567, 2013.

Doake, C.: Ice-shelf Stability, in: Encyclopedia of Ocean Sciences, edited by Steele, J. H., Thorpe, S. A., and Turekian, K. K., January 1995, pp. 1282–1290, Elsevier, Amsterdam, https://doi.org/10.1006/rwos.2001.0005, 2001.

Emori, S. and Brown, S. J.: Dynamic and thermodynamic changes in mean and extreme precipitation under changed climate, Geophysical Research Letters, 32, 1–5, https://doi.org/10.1029/2005GL023272, 2005.

Etourneau, J., Sgubin, G., Crosta, X., Swingedouw, D., Willmott, V., Barbara, L., Houssais, M.-n., Schouten, S., Damsté, J. S. S., Goosse, H., Escutia, C., Crespin, J., Massé, G., and Kim, J.-H.: Ocean temperature impact on ice shelf extent in the eastern Antarctic Peninsula, Nature Communications, 10, 304, https://doi.org/10.1038/s41467-018-08195-6, 2019.

Feldmann, J. and Levermann, A.: Collapse of the West Antarctic Ice Sheet after local destabilization of the Amundsen Basin, Proceedings of the National Academy of Sciences, 112, 14 191–14 196, https://doi.org/10.1073/pnas.1512482112, 2015.

Feldmann, J., Albrecht, T., Khroulev, C., Pattyn, F., and Levermann, A.: Resolution-dependent performance of grounding line motion in a shallow model compared with a full-Stokes model according to the MISMIP3d intercomparison, Journal of Glaciology, 60, 353–360, https://doi.org/10.3189/2014JoG13J093, 2014.

Foldvik, A. and Gammelsrød, T.: Notes on Southern Ocean hydrography, sea-ice and bottom water formation, Palaeogeography, Palaeoclimatology, Palaeoecology, 67, 3–17, https://doi.org/10.1016/0031-0182(88)90119-8, http://linkinghub.elsevier.com/retrieve/pii/0031018288901198, 1988.

Fortuin, J. and Oerlemans, J.: Parameterization of the Annual Surface Temperature and Mass Balance of Antarctica, Annals of Glaciology, 14, 78–84, https://doi.org/10.3189/S0260305500008302, 1990.

Fretwell, P., Pritchard, H. D., Vaughan, D. G., Bamber, J. L., Barrand, N. E., Bell, R., Bianchi, C., Bingham, R. G., Blankenship, D. D., Casassa, G., Catania, G., Callens, D., Conway, H., Cook, A. J., Corr, H. F. J., Damaske, D., Damm, V., Ferraccioli, F., Forsberg, R., Fujita, S., Gim, Y., Gogineni, P., Griggs, J. A., Hindmarsh, R. C. A., Holmlund, P., Holt, J. W., Jacobel, R. W., Jenkins, A., Jokat, W., Jordan, T., King, E. C., Kohler, J., Krabill, W., Riger-Kusk, M., Langley, K. A., Leitchenkov, G., Leuschen, C., Luyendyk, B. P., Matsuoka, K., Mouginot, J., Nitsche, F. O., Nogi, Y., Nost, O. A., Popov, S. V., Rignot, E., Rippin, D. M., Rivera, A., Roberts, J., Ross, N., Siegert, M. J., Smith, A. M., Steinhage, D., Studinger, M., Sun, B., Tinto, B. K., Welch, B. C., Wilson, D., Young, D. A., Xiangbin, C., and Zirizzotti, A.: Bedmap2: improved ice bed, surface and thickness datasets for Antarctica, The Cryosphere, 7, 375–393, https://doi.org/10.5194/tc-7-375-2013, 2013.

Frieler, K., Meinshausen, M., Mengel, M., Braun, N., and Hare, W.: A Scaling Approach to Probabilistic Assessment of Regional Climate Change, Journal of Climate, 25, 3117–3144, https://doi.org/10.1175/JCLI-D-11-00199.1, 2012.

Frieler, K., Clark, P. U., He, F., Buizert, C., Reese, R., Ligtenberg, S. R. M., van den Broeke, M. R., Winkelmann, R., and Levermann, A.: Consistent evidence of increasing Antarctic accumulation with warming, Nature Climate Change, 5, 348–352, https://doi.org/10.1038/nclimate2574, 2015.

Fürst, J. J., Durand, G., Gillet-Chaulet, F., Tavard, L., Rankl, M., Braun, M., and Gagliardini, O.: The safety band of Antarctic ice shelves, Nature Climate Change, 6, 479–482, https://doi.org/10.1038/nclimate2912, 2016.

Fyke, J., Lenaerts, J. T. M., and Wang, H.: Basin-scale heterogeneity in Antarctic precipitation and its impact on surface mass variability, The Cryosphere, 11, 2595–2609, https://doi.org/10.5194/tc-11-2595-2017, 2017.

Gill, A.: Atmosphere-ocean dynamics, vol. 30 of *International Geophysics Series*, Academic Press, San Diego, California 92101, 1982.

Golledge, N. R., Kowalewski, D. E., Naish, T. R., Levy, R. H., Fogwill, C. J., and Gasson, E. G. W.: The multi-millennial Antarctic commitment to future sea-level rise, Nature, 526, 421–425, https://doi.org/10.1038/nature15706, 2015.

Gomez, N., Mitrovica, J. X., Huybers, P., and Clark, P. U.: Sea level as a stabilizing factor for marine-ice-sheet grounding lines, Nature Geoscience, 3, 850–853, https://doi.org/10.1038/ngeo1012, http://www.nature.com/doifinder/10.1038/ngeo1012, 2010.

Gregory, J. and Huybrechts, P.: Ice-sheet contributions to future sea-level change., Philosophical transactions. Series A, Mathematical, physical, and engineering sciences, 364, 1709–31, https://doi.org/10.1098/rsta.2006.1796, 2006.

Hansen, J., Nazarenko, L., Ruedy, R., Sato, M., Willis, J., Del Genio, A., Koch, D., Lacis, A., Lo, K., Menon, S., Novakov, T., Perlwitz, J., Russell, G., Schmidt, G. A., and Tausnev, N.: Earth's energy imbalance: confirmation and implications., Science, 308, 1431–1435, https://doi.org/10.1126/science.1110252, http://www.ncbi.nlm.nih.gov/pubmed/15860591, 2005.

Hansen, J., Sato, M., Kharecha, P., and von Schuckmann, K.: Earth's energy imbalance and implications, Atmospheric Chemistry and Physics, 11, 13 421–13 449, https://doi.org/10.5194/acp-11-13421-2011, http://www.atmos-chem-phys.net/11/13421/2011/, 2011.

Haumann, F. A., Gruber, N., Münnich, M., Frenger, I., and Kern, S.: Sea-ice transport driving Southern Ocean salinity and its recent trends, Nature, 537, 89–92, https://doi.org/10.1038/nature19101, 2016.

Held, I. M. and Soden, B. J.: Robust Responses of the Hydrological Cycle to Global Warming, Journal of Climate, 19, 5686–5699, https://doi.org/10.1175/JCLI3990.1, 2006.

Hellmer, H. H., Kauker, F., Timmermann, R., Determann, J., and Rae, J.: Twenty-first-century warming of a large Antarctic ice-shelf cavity by a redirected coastal current, Nature, 485, 225–228, https://doi.org/10.1038/nature11064, 2012.

Heuzé, C., Heywood, K. J., Stevens, D. P., and Ridley, J. K.: Southern Ocean bottom water characteristics in CMIP5 models, Geophysical Research Letters, 40, 1409–1414, https://doi.org/10.1002/grl.50287, 2013.

Hock, R.: Glacier melt: a review of processes and their modelling, Progress in Physical Geography, 29, 362–391, https://doi.org/10.1191/0309133305pp453ra, 2005.

Hughes, T., Zhao, Z., Hintz, R., and Fastook, J.: Instability of the Antarctic Ross Sea Embayment as climate warms, Reviews of Geophysics, pp. 1–36, https://doi.org/10.1002/2016RG000545, 2017.

Jacobs, S.: Observations of change in the Southern Ocean., Philosophical transactions. Series A, Mathematical, physical, and engineering sciences, 364, 1657–81, https://doi.org/10.1098/rsta.2006.1794, 2006.

Jeong, S., Howat, I. M., and Bassis, J. N.: Accelerated ice shelf rifting and retreat at Pine Island Glacier, West Antarctica, Geophysical Research Letters, 43, 11 720–11 725, https://doi.org/10.1002/2016GL071360, 2016.

Kingslake, J., Ely, J. C., Das, I., and Bell, R. E.: Widespread movement of meltwater onto and across Antarctic ice shelves, Nature, 544, 349–352, https://doi.org/10.1038/nature22049, 2017.

Knutti, R., Masson, D., and Gettelman, A.: Climate model genealogy: Generation CMIP5 and how we got there, Geophysical Research Letters, 40, 1194–1199, https://doi.org/10.1002/grl.50256, 2013.

Krinner, G., Largeron, C., Ménégoz, M., Agosta, C., and Brutel-Vuilmet, C.: Oceanic Forcing of Antarctic Climate Change: A Study Using a Stretched-Grid Atmospheric General Circulation Model, Journal of Climate, 27, 5786–5800, https://doi.org/10.1175/JCLI-D-13-00367.1, 2014.

Leclercq, P., Oerlemans, J., and Cogley, J.: Estimating the Glacier Contribution to Sea-Level Rise for the Period 1800–2005, Surveys in Geophysics, 32, 519–535, https://doi.org/10.1007/s10712-011-9121-7, 2011.

Levermann, A., Albrecht, T., Winkelmann, R., Martin, M., Haseloff, M., and Joughin, I.: Kinematic first-order calving law implies potential for abrupt ice-shelf retreat, The Cryosphere, 6, 273–286, https://doi.org/10.5194/tc-6-273-2012, 2012.

Li, G., Harrison, S. P., Bartlein, P. J., Izumi, K., and Colin Prentice, I.: Precipitation scaling with temperature in warm and cold climates: An analysis of CMIP5 simulations, Geophysical Research Letters, 40, 4018–4024, https://doi.org/10.1002/grl.50730, 2013.

Lingle, C. S. and Clark, J. A.: A numerical model of interactions between a marine ice sheet and the solid earth: Application to a West Antarctic ice stream, Journal of Geophysical Research, 90, 1100–1114, https://doi.org/10.1029/JC090iC01p01100, 1985.

Liu, J.: Interpretation of recent Antarctic sea ice variability, Geophysical Research Letters, 31, 2000–2003, https://doi.org/10.1029/2003GL018732, 2004.

Liu, Y., Moore, J. C., Cheng, X., Gladstone, R. M., Bassis, J. N., Liu, H., Wen, J., and Hui, F.: Ocean-driven thinning enhances iceberg calving and retreat of Antarctic ice shelves, Proceedings of the National Academy of Sciences, 112, 3263–3268, https://doi.org/10.1073/pnas.1415137112, 2015.

Locarnini, R. A., Mishonov, A. V., Antonov, T. P., Boyer, T., and Garcia, H.: World Ocean Atlas 2009, Volume 1: Temperature, Tech. rep., NOAA Atlas NESDIS 68, U.S. Government Printing Office, Washington, D.C., https://www.nodc.noaa.gov/OC5/WOA09/pr{_}woa09.html, 2010.

Marshall, G. J., Thompson, D. W. J., and Broeke, M. R.: The Signature of Southern Hemisphere Atmospheric Circulation Patterns in Antarctic Precipitation, Geophysical Research Letters, 44, 11,580–11,589, https://doi.org/10.1002/2017GL075998, 2017.

Meijers, A. J. S.: The Southern Ocean in the Coupled Model Intercomparison Project phase 5, Philosophical Transactions of the Royal Society A: Mathematical, Physical and Engineering Sciences, 372, 20130 296–20130 296, https://doi.org/10.1098/rsta.2013.0296, 2014.

Mengel, M. and Levermann, A.: Ice plug prevents irreversible discharge from East Antarctica, Nature Climate Change, pp. 1–5, https://doi.org/10.1038/nclimate2226, 2014.

Mengel, M., Feldmann, J., and Levermann, A.: Linear sea-level response to abrupt ocean warming of major West Antarctic ice basin, Nature Climate Change, 6, 71–74, https://doi.org/10.1038/nclimate2808, 2015.

Milillo, P., Rignot, E., Rizzoli, P., Scheuchl, B., Mouginot, J., Bueso-Bello, J., and Prats-Iraola, P.: Heterogeneous retreat and ice melt of Thwaites Glacier, West Antarctica, Science Advances, 5, eaau3433, 8pp, https://doi.org/10.1126/sciadv.aau3433, 2019.

Mitrovica, J. X., Tamisiea, M. E., Davis, J. L., and Milne, G. A.: Recent mass balance of polar ice sheets inferred from patterns of global sea-level change, Nature, 409, 1026–1029, https://doi.org/10.1038/35059054, http://www.nature.com/articles/35059054, 2001.

Morris, E. M. and Vaughan, D. G.: Spatial and temporal variation of surface temperature on the Antarctic Peninsula and the limit of viability of ice shelves, in: Antarctic Peninsula Climate Variability: Historical and Paleoenvironmental Perspectives, edited by Domack, E., Levente, A., Burnet, A., Bindschadler, R. ., Convey, P., and Kirby, M., vol. 79 of *Antarctic Research Series*, pp. 61–68, American Geophysical Union, Washington, D.C., https://doi.org/10.1029/AR079p0061, 2003.

Moss, R. H., Edmonds, J. A., Hibbard, K. A., Manning, M. R., Rose, S. K., van Vuuren, D. P., Carter, T. R., Emori, S., Kainuma, M., Kram, T., Meehl, G. A., Mitchell, J. F., Nakicenovic, N., Riahi, K., Smith, S. J., Stouffer, R. J., Thomson, A. M., Weyant, J. P., and Wilbanks, T. J.: The next generation of scenarios for climate change research and assessment., Nature, 463, 747–56, https://doi.org/10.1038/nature08823, http://www.nature.com/nature/journal/v463/n7282/full/nature08823.html, 2010.

Mulvaney, R., Abram, N. J., Hindmarsh, R. C., Arrowsmith, C., Fleet, L., Triest, J., Sime, L. C., Alemany, O., and Foord, S.: Recent Antarctic Peninsula warming relative to Holocene climate and ice-shelf history., Nature, 489, 141–144, https://doi.org/10.1038/nature11391, http://www.ncbi.nlm.nih.gov/pubmed/22914090, 2012.

Nakayama, Y., Timmermann, R., Rodehacke, C. B., Schröder, M., and Hellmer, H. H.: Modeling the spreading of glacial melt water from the Amundsen and Bellingshausen Seas, Geophysical Research Letters, 41, 7942–7949, https://doi.org/10.1002/2014GL061600, http://doi.wiley.com/10.1002/2014GL061600, 2014.

Nakayama, Y., Menemenlis, D., Zhang, H., Schodlok, M., and Rignot, E.: Origin of Circumpolar Deep Water intruding onto the Amundsen and Bellingshausen Sea continental shelves, Nature Communications, 9, 3403, 9pp, https://doi.org/10.1038/s41467-018-05813-1, http://www.nature.com/articles/s41467-018-05813-1, 2018.

Naughten, K. A., Meissner, K. J., Galton-Fenzi, B. K., England, M. H., Timmermann, R., and Hellmer, H. H.: Future Projections of Antarctic Ice Shelf Melting Based on CMIP5 Scenarios, Journal of Climate, 31, 5243–5261, https://doi.org/10.1175/JCLI-D-17-0854.1, http://journals.ametsoc.org/doi/10.1175/JCLI-D-17-0854.1, 2018.

Nicholls, K. W., Østerhus, S., Makinson, K., Gammelsrød, T., and Fahrbach, E.: Ice-ocean processes over the continental shelf of the southern Weddell Sea, Antarctica: A review, Reviews of Geophysics, 47, 23pp, https://doi.org/10.1029/2007RG000250, http://www.agu.org/pubs/crossref/2009/2007RG000250.shtml, 2009.

Ohmura, A.: Physical Basis for the Temperature-Based Melt-Index Method, Journal of Applied Meteorology, 40, 753–761, https://doi.org/10.1175/1520-0450(2001)040<0753:PBFTTB>2.0.CO;2, http://journals.ametsoc.org/doi/abs/10.1175/1520-0450(2001)040{%}3C0753:PBFTTB{%}3E2.0.CO;2, 2001.

Orsi, A. H., Johnson, G., and Bullister, J. L.: Circulation, mixing, and production fo Antarctic Bottom Water, Progress In Oceanography, 43, 55–109, https://doi.org/10.1016/S0079-6611(99)00004-X, http://linkinghub.elsevier.com/retrieve/pii/S007966119900004X, 1999.

Palerme, C., Genthon, C., Claud, C., Kay, J. E., Wood, N. B., and L'Ecuyer, T.: Evaluation of current and projected Antarctic precipitation in CMIP5 models, Climate Dynamics, 48, 225–239, https://doi.org/10.1007/s00382-016-3071-1, 2017.

Paolo, F. S., Padman, L., Fricker, H. A., Adusumilli, S., Howard, S., and Siegfried, M. R.: Response of Pacific-sector Antarctic ice shelves to the El Niño/Southern Oscillation, Nature Geoscience, 11, 121–126, https://doi.org/10.1038/s41561-017-0033-0, http://www.nature.com/articles/s41561-017-0033-0, 2018.

Pollard, D. and DeConto, R. M.: Modelling West Antarctic ice sheet growth and collapse through the past five million years., Nature, 458, 329–32, https://doi.org/10.1038/nature07809, http://www.ncbi.nlm.nih.gov/pubmed/19295608, 2009.

Pollard, D., Deconto, R. M., and Alley, R. B.: Potential Antarctic Ice Sheet retreat driven by hydrofracturing and ice cliff failure, Earth and Planetary Science Letters, 412, 112–121, https://doi.org/10.1016/j.epsl.2014.12.035, http://dx.doi.org/10.1016/j.epsl.2014.12.035, 2015.

Rietbroek, R., Brunnabend, S.-E., Kusche, J., Schröter, J., and Dahle, C.: Revisiting the contemporary sea-level budget on global and regional scales, Proceedings of the National Academy of Sciences, 113, 1504–1509, https://doi.org/10.1073/pnas.1519132113, http://www.pnas.org/lookup/doi/10.1073/pnas.1519132113, 2016.

Rignot, E., Jacobs, S., Mouginot, J., and Scheuchl, B.: Ice-Shelf Melting Around Antarctica, Science, 341, 266–270, https://doi.org/10.1126/science.1235798, http://www.sciencemag.org/cgi/doi/10.1126/science.1235798, 2013.

Rignot, E., Mouginot, J., Morlighem, M., Seroussi, H., and Scheuchl, B.: Widespread, rapid grounding line retreat of Pine Island, Thwaites, Smith, and Kohler glaciers, West Antarctica, from 1992 to 2011, Geophysical Research Letters, 41, 3502–3509, https://doi.org/10.1002/2014GL060140, http://doi.wiley.com/10.1002/2014GL060140, 2014.

Rignot, E., Mouginot, J., and Scheuchl, B.: MEaSUREs Antarctic Grounding Line from Differential Satellite Radar Interferometry, Version 2., Boulder, Colorado USA. NASA National Snow and Ice Data Center Distributed Active Archive Center, https://doi.org/10.5067/IKBWW4RYHF1Q, last Accessed: 16. Aug. 2018, 2016.

Ritz, C., Edwards, T. L., Durand, G., Payne, A. J., Peyaud, V., and Hindmarsh, R. C. A.: Potential sea-level rise from Antarctic ice-sheet instability constrained by observations, Nature, 528, 115–118, https://doi.org/10.1038/nature16147, http://dx.doi.org/10.1038/nature16147, 2015.

Rott, H., Skvarca, P., and Nagler, T.: Rapid Collapse of Northern Larsen Ice Shelf, Antarctica, Science, 271, 788–792, https://doi.org/10.1126/science.271.5250.788, http://www.sciencemag.org/cgi/doi/10.1126/science.271.5250.788, 1996.

Rott, H., Müller, F., Nagler, T., and Floricioiu, D.: The imbalance of glaciers after disintegration of Larsen-B ice shelf, Antarctic Peninsula, The Cryosphere, 5, 125–134, https://doi.org/10.5194/tc-5-125-2011, http://www.the-cryosphere.net/5/125/2011/, 2011.

Sallée, J.-B., Shuckburgh, E., Bruneau, N., Meijers, A., Bracegirdle, T., and Wang, Z.: Assessment of Southern Ocean mixed-layer depths in CMIP5 models: Historical bias and forcing response, Journal of Geophysical Research: Oceans, 118, 18pp, https://doi.org/10.1002/jgrc.20157, http://doi.wiley.com/10.1002/jgrc.20157, 2013a.

Sallée, J.-B., Shuckburgh, E., Bruneau, N., Meijers, A., Bracegirdle, T., Wang, Z., and Roy, T.: Assessment of Southern Ocean water mass circulation and characteristics in CMIP5 models: Historical bias and forcing response, Journal of Geophysical Research: Oceans, 118, 1830–1844, https://doi.org/10.1002/jgrc.20135, http://doi.wiley.com/10.1002/jgrc.20135, 2013b.

Sasgen, I., Konrad, H., Helm, V., and Grosfeld, K.: High-Resolution Mass Trends of the Antarctic Ice Sheet through a Spectral Combination of Satellite Gravimetry and Radar Altimetry Observations, Remote Sensing, 11, 144, https://doi.org/10.3390/rs11020144, 2019.

Scambos, T. A., Bell, R. E., Alley, R. B., Anandakrishnan, S., Bromwich, D. H., Brunt, K., Christianson, K., Creyts, T., Das, S. B., DeConto, R., Dutrieux, P., Fricker, H. A., Holland, D., MacGregor, J., Medley, B., Nicolas, J. P., Pollard, D., Siegfried, M. R., Smith, A. M., Steig, E. J., Trusel, L. D., Vaughan, D. G., and Yager, P. L.: How much, how fast?: A science review and outlook for research on the instability of Antarctica's Thwaites Glacier in the 21st century, Global and Planetary Change, 153, 16–34, https://doi.org/10.1016/j.gloplacha.2017.04.008, http://dx.doi.org/10.1016/j.gloplacha.2017.04.008, 2017.

Schmidtko, S., Heywood, K. J., Thompson, A. F., and Aoki, S.: Multidecadal warming of Antarctic waters, Science, 346, 1227–1231, https://doi.org/10.1126/science.1256117, http://www.sciencemag.org/content/346/6214/1227.full.html, 2014.

Schoof, C.: A variational approach to ice stream flow, Journal of Fluid Mechanics, 556, 227–251, https://doi.org/10.1017/S0022112006009591, http://www.journals.cambridge.org/abstract{_}S0022112006009591, 2006.

Seroussi, H., Nowicki, S., Simon, E., Abe-Ouchi, A., Albrecht, T., Brondex, J., Cornford, S., Dumas, C., Gillet-Chaulet, F., Goelzer, H., Golledge, N. R., Gregory, J. M., Greve, R., Hoffman, M. J., Humbert, A., Huybrechts, P., Kleiner, T., Larour, E., Leguy, G., Lipscomb, W. H., Lowry, D., Mengel, M., Morlighem, M., Pattyn, F., Payne, A. J., Pollard, D., Price, S. F., Quiquet, A., Reerink, T. J., Reese, R., Rodehacke, C. B., Schlegel, N.-J., Shepherd, A., Sun, S., Sutter, J., Van Breedam, J., van de Wal, R. S. W., Winkelmann, R., and Zhang, T.: initMIP-Antarctica: an ice sheet model initialization experiment of ISMIP6, The Cryosphere, 13, 1441–1471, https://doi.org/10.5194/tc-13-1441-2019, https://www.the-cryosphere.net/13/1441/2019/, 2019a.

Seroussi, H., Nowicki, S., Simon, E., and ISMIP6: ISMIP6 Antarctic Projections: Parameterization of Climate Forcings and First Results, https://www.czech-in.org/cmPortalV15/CM_W3_Searchable/iugg19/normal#!abstractdetails/0000739190, 2019b.

Shepherd, A., Ivins, E., Geruo, A., Barletta, V., Bentley, M., Bettadpur, S., Briggs, K., Bromwich, D., Forsberg, R., Galin, N., Horwath, M., Jacobs, S., Joughin, I., King, M., Lenaerts, J., Li, J., Ligtenberg, S., Luckman, A., Luthcke, S., McMillan, M., Meister, R., Milne, G., Mouginot, J., Muir, A., Nicolas, J., Paden, J., Payne, A., Pritchard, H., Rignot, E., Rott, H., Sorensen, L., Scambos, T., Scheuchl, B., Schrama, E., Smith, B., Sundal, A., van Angelen, J., van de Berg, W., van den Broeke, M., Vaughan, D., Velicogna, I., Wahr, J., Whitehouse, P., Wingham, D., Yi, D., Young, D., and Zwally, H.: A Reconciled Estimate of Ice-Sheet Mass Balance, Science, 338, 1183–1189, https://doi.org/10.1126/science.1228102, http://www.sciencemag.org/cgi/doi/10.1126/science.1228102, 2012.

Sun, Y., Solomon, S., Dai, A., and Portmann, R. W.: How Often Will It Rain?, Journal of Climate, 20, 4801–4818, https://doi.org/10.1175/JCLI4263.1, http://journals.ametsoc.org/doi/abs/10.1175/JCLI4263.1, 2007.

Sutter, J., Fischer, H., Grosfeld, K., Karlsson, N. B., Kleiner, T., Liefferinge, B. V., and Eisen, O.: Modelling the Antarctic Ice Sheet across the mid-Pleistocene transition – implications for Oldest Ice, The Cryosphere, 13, 2023–2041, https://doi.org/10.5194/tc-13-2023-2019, 2019.

Taylor, K. E., Stouffer, R. J., and Meehl, G. A.: An Overview of CMIP5 and the Experiment Design, Bulletin of the American Meteorological Society, 93, 485–498, https://doi.org/10.1175/BAMS-D-11-00094.1, http://journals.ametsoc.org/doi/abs/10.1175/BAMS-D-11-00094.1, 2012.

The PISM Authors: PISM 's climate forcing components (v0.7), Tech. rep., http://www.pism-docs.org/, revision stable v0.7.1-2-g79b8840, Last Accessed: 22. Nov. 2017, 2015a.

The PISM Authors: PISM (Parallel Ice Sheet Model), User's manual (v0.7), Tech. rep., http://www.pism-docs.org/, revision stable v0.7.1-2-g79b8840, Last Accessed: 16. Jan. 2016, 2015b.

Thomas, E., Dennis, P., Bracegirdle, T., and Franzke, C.: Ice core evidence for significant 100-year regional warming on the Antarctic Peninsula, Geophysical Research Letters, 36, 5pp, https://doi.org/10.1029/2009GL040104, http://www.agu.org/pubs/crossref/2009/2009GL040104.shtml, 2009.

Thomas, E. R., van Wessem, J. M., Roberts, J., Isaksson, E., Schlosser, E., Fudge, T. J., Vallelonga, P., Medley, B., Lenaerts, J., Bertler, N., van den Broeke, M. R., Dixon, D. A., Frezzotti, M., Stenni, B., Curran, M., and Ekaykin, A. A.: Regional Antarctic snow accumulation over the past 1000 years, Climate of the Past, 13, 1491–1513, https://doi.org/10.5194/cp-13-1491-2017, https://www.clim-past.net/13/1491/2017/, 2017.

Thompson, A. F., Stewart, A. L., Spence, P., and Heywood, K. J.: The Antarctic Slope Current in a Changing Climate, Reviews of Geophysics, 56, 741–770, https://doi.org/10.1029/2018RG000624, http://doi.wiley.com/10.1029/2018RG000624, 2018.

Turner, J., Bracegirdle, T. J., Phillips, T., Marshall, G. J., and Hosking, J. S.: An Initial Assessment of Antarctic Sea Ice Extent in the CMIP5 Models, Journal of Climate, 26, 1473–1484, https://doi.org/10.1175/JCLI-D-12-00068.1, http://journals.ametsoc.org/doi/10.1175/JCLI-D-12-00068.1, 2013.

van den Broeke, M.: Strong surface melting preceded collapse of Antarctic Peninsula ice shelf, Geophysical Research Letters, 32, 4pp, https://doi.org/10.1029/2005GL023247, http://doi.wiley.com/10.1029/2005GL023247, 2005.

Van Wessem, J., Reijmer, C., Morlighem, M., Mouginot, J., Rignot, E., Medley, B., Joughin, I., Wouters, B., Depoorter, M., Bamber, J., Lenaerts, J., Van De Berg, W., Van Den Broeke, M., and Van Meijgaard, E.: Improved representation of East Antarctic surface mass balance in a regional atmospheric climate model, Journal of Glaciology, 60, 761–770, https://doi.org/10.3189/2014JoG14J051, https://www.cambridge.org/core/product/identifier/S0022143000203110/type/journal{_}article, 2014.

Vuuren, D. P., Edmonds, J., Kainuma, M., Riahi, K., Thomson, A., Hibbard, K., Hurtt, G. C., Kram, T., Krey, V., Lamarque, J.-F., Masui, T., Meinshausen, M., Nakicenovic, N., Smith, S. J., and Rose, S. K.: The representative concentration pathways: an overview, Climatic Change, 109, 5–31, https://doi.org/10.1007/s10584-011-0148-z, http://link.springer.com/10.1007/s10584-011-0148-z, 2011.

Wang, Y., Ding, M., van Wessem, J. M., Schlosser, E., Altnau, S., van den Broeke, M. R., Lenaerts, J. T. M., Thomas, E. R., Isaksson, E., Wang, J., and Sun, W.: A Comparison of Antarctic Ice Sheet Surface Mass Balance from Atmospheric Climate Models and In Situ Observations, Journal of Climate, 29, 5317–5337, https://doi.org/10.1175/JCLI-D-15-0642.1, 2016.

Wang, Y., Thomas, E. R., Hou, S., Huai, B., Wu, S., Sun, W., Qi, S., Ding, M., and Zhang, Y.: Snow Accumulation Variability Over the West Antarctic Ice Sheet Since 1900: A Comparison of Ice Core Records With ERA-20C Reanalysis, Geophysical Research Letters, pp. 1–9, https://doi.org/10.1002/2017GL075135, 2017.

Whitehouse, P. L.: Glacial isostatic adjustment modelling: Historical perspectives, recent advances, and future directions, Earth Surface Dynamics, 6, 401–429, https://doi.org/10.5194/esurf-6-401-2018, https://www.earth-surf-dynam.net/6/401/2018/esurf-6-401-2018.pdfhttps://www.earth-surf-dynam.net/6/401/2018/, 2018.

Whitworth III, T., Orsi, A. H., Kim, S. J., Nowlin Jr., W. D., Locarnini, R. A., Whitworth III, T., and Nowlin Jr., W.: Water masses and mixing near the Antarctic Slope Front, in: Ocean, Ice, and Atmosphere: Interactions at the Antarctic Continental Margin, edited by Jacobs, S. S. and Weiss, R. F., vol. 75, pp. 1–27, American Geophysical Union, Washington, DC, USA, https://doi.org/10.1029/AR075p0001, https://agupubs.onlinelibrary.wiley.com/doi/10.1029/AR075p0029, 2013.

Wingham, D. J., Shepherd, A., Muir, A., and Marshall, G. J.: Mass balance of the Antarctic Ice Sheet from 1992 to 2017, Nature, 558, 219–222, https://doi.org/10.1038/s41586-018-0179-y, 2018.

Winkelmann, R., Martin, M., Haseloff, M., Albrecht, T., Bueler, E., Khroulev, C., and Levermann, A.: The Potsdam Parallel Ice Sheet Model (PISM-PIK) – Part 1: Model description, The Cryosphere, 5, 715–726, https://doi.org/10.5194/tc-5-715-2011, 2011.

Winkelmann, R., Levermann, A., Martin, M., and Frieler, K.: Increased future ice discharge from Antarctica owing to higher snowfall, Nature, 492, 239–242, https://doi.org/10.1038/nature11616, 2012.

Winkelmann, R., Levermann, A., Ridgwell, A., and Caldeira, K.: Combustion of available fossil fuel resources sufficient to eliminate the Antarctic Ice Sheet, Science Advances, 1, e1500 589, 5pp, https://doi.org/10.1126/sciadv.1500589, 2015.

Yin, J., Gentine, P., Zhou, S., Sullivan, S. C., Wang, R., Zhang, Y., and Guo, S.: Large increase in global storm runoff extremes driven by climate and anthropogenic changes, Nature Communications, 9, 4389, 10pp, https://doi.org/10.1038/s41467-018-06765-2, 2018.

Zwally, H. J., Li, J., Robbins, J. W., Saba, J. L., Yi, D., and Brenner, A. C.: Mass gains of the Antarctic ice sheet exceed losses, Journal of Glaciology, 61, 1019–1036, https://doi.org/10.3189/2015JoG15J071, https://www.cambridge.org/core/journals/journal-of-glaciology/article/mass-gains-of-the-antarctic-ice-sheet-exceed-losses/983F196E23C3A6E7908E5FB32EB42268, 2015.

Tables

Table 1. List of CMIP5 models and the used RCP climate projections (Moss et al., 2010) beside historical (hist) piControl (piCtrl) scenarios. Since we do not use the RCP2.6 scenario of the CCSM4 model, the ensemble comprises 26 anomaly forcing scenarios. The climate anomalies are computed relative to the first or last 50 years of the corresponding piCtrl. Each scenario starts from the initial condition PISM1Eq (Figure A10) or PISM2Eq (Figure A11) and is driven by two precipitation conditions (see main text for details , e.g. section 3.2: "Precipitation scaling"). Hence, the ensemble of anomaly ice sheet simulations has 208 members.

Model Name	RCP Projections	Scenarios
CanESM2	RCP2.6, RCP4.5, RCP8.5	hist, piCtrl
CCSM4	RCP4.5, RCP8.5	hist, piCtrl
CNRM-CM5	RCP2.6, RCP4.5, RCP8.5	hist, piCtrl
CSIRO-Mk3.6.0	RCP2.6, RCP4.5, RCP8.5	hist, piCtrl
HadGEM2-ES	RCP2.6, RCP4.5, RCP8.5	hist, piCtrl
MIROC-ESM	RCP2.6, RCP4.5, RCP8.5	hist, piCtrl
MPI-ESM-LR	RCP2.6, RCP4.5, RCP8.5	hist, piCtrl
MRI-CGCM3	RCP2.6, RCP4.5, RCP8.5	hist, piCtrl
NorESM1-M	RCP2.6, RCP4.5, RCP8.5	hist, piCtrl

Table 2. Forcing used for ice-sheet model spin-up and as reference fields for the anomaly forcing.

Forcing	Period	Label	Reference Fields	Reference
Atmosphere	1979–2011	RACMO 2.3/ANT	2m-air temperature, Total precipitation	Van Wessem et al. (2014)
Ocean	Climatological mean	World Ocean Atlas 2009 (WOA09)	Potential ocean temperature	Locarnini et al. (2010)

Table 3. Temperature scaling of the precipitation for six ice core locations in Antarctica. The second column lists the ensemble mean scaling (RCP8.5, first 50 years, both initial states PISM1Eq and PISM2Eq) and standard deviation (2-sigma) across all ensemble members. The third column provides scaling factors deduced from ice cores (Frieler et al., 2015), including the provided error margins (2-sigma). Please inspect Figure 4 for the ice core locations.

Core Name Location	Scaling of Ensemble Mean	Scaling Ice Core
EDML	11.0±6.6	5.0±2.8
Vostok	14.0±5.6	6.1±2.5
Law Dome	5.8±6.3	5.2±2.3
EDC	11.0±5.0	5.9±2.2
Talos Dome	8.4±5.2	6.8±2.8
WAIS	6.8±5.4	5.5±1.2

Table 4. Defined areas as part of our diagnostic. The fraction is computed relative to "glaciered." Figure 4 and Figure 5 depict these areas.

Region Label	Area ($10^6\,\mathrm{km}^2$)	Fraction (%)	Longitude Range	Comment
glaciered	13.6	100.0	$[-180°\mathrm{E}, +180°\mathrm{E}[$	Antarctica incl. ice shelves
grounded	11.9	87.5	$[-180°\mathrm{E}, +180°\mathrm{E}[$	Without ice shelves
EAIS Atl	3.77	27.6	$[-45°\mathrm{E}, +55°\mathrm{E}]$	Including floating ice shelves
EAIS Ind	5.66	41.1	$[+55°\mathrm{E}, +155°\mathrm{E}]$	
WAIS	4.26	31.3	$[+155°\mathrm{E}, -45°\mathrm{E}]$	
Siple Coast	0.69	5.12	$[+155°\mathrm{E}, -140°\mathrm{E}]$	Latitude$> 85°\mathrm{S}$

Figures

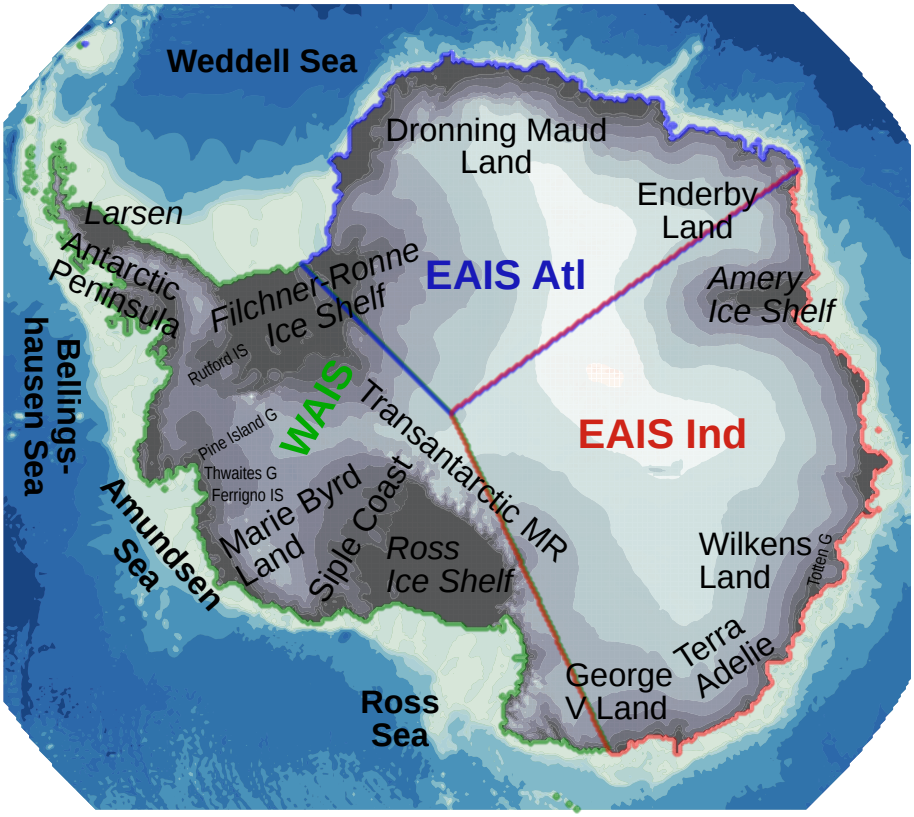

Figure 1. Map of Antarctica. The seafloor depth is shown with a blue color scale, while the elevation of Antarctica above sea level is depicted by a colorbar of dark-gray (low elevation) to white colors (high elevation). The font style of ocean labels is in bold and of ice shelves is in italic. The smaller font size tags individual glacier (G) and ice streams (IS). The abbreviation "MR" stands for "Mountain Range". Colored labels define three regions: WAIS: West Antarctic Ice Sheet (green), EAIS Atl: East Antarctic Ice - Sheet Atlantic Sector (blue), EAIS Ind: East Antarctic Ice Sheet - Indian Ocean Sector (red). These regions bound by the coastal areas by their shared boundaries in the interior. Also the Figures 4 and 5 show the boundaries of these regions. The here depicted bedrock topography and surface orography are taken from Fretwell et al. (2013).

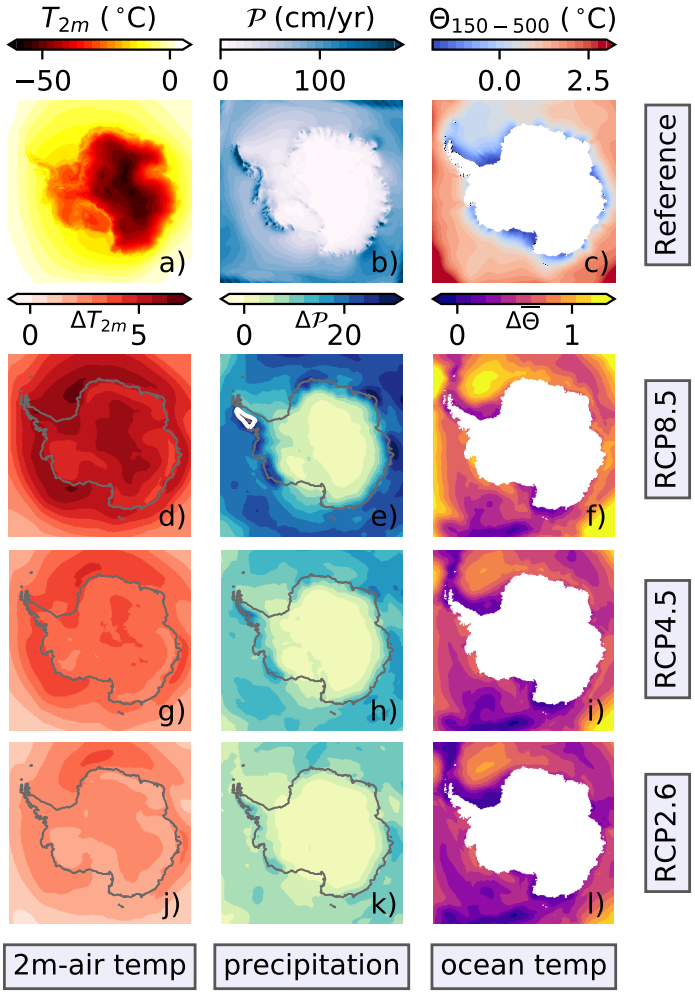

Figure 2. Atmospheric (a, b) and oceanographic (c) reference forcing; ensemble mean anomalies (d–l). The top row represents the reference fields to spin-up the ice-sheet model (Table 2). The 2m-air temperature (a) and the total precipitation (b) are mean fields from the regional RACMO model, while the ocean temperatures come from the World Ocean Atlas 2009 (c); see Table 2 for more details. Each reference field has its colorbar above its plot. Below each reference field, the related anomalies, including their colorbar, are compiled for the period 2071–2100. Here, the second (third and fourth) row shows the anomalies for RCP8.5 (RCP4.5, RCP2.6). In these atmospheric anomaly plots, the dark-gray line follows the current coastline. All potential ocean temperatures (c, f, i, l) are a vertical mean of the depth interval from 150 m to 500 m. The white contour lines in the anomaly plots highlight the following precipitation threshold (e, h, k): 30 cm/yr. All these anomalies are the ensemble mean of the models listed in Table 1; please note that CCSM4 is not part of RCP2.6. Appendix Figure A1 and Figure A2 show the corresponding ensemble maximum and minimum fields, respectively. Antarctica's contours are deduced from Fretwell et al. (2013).

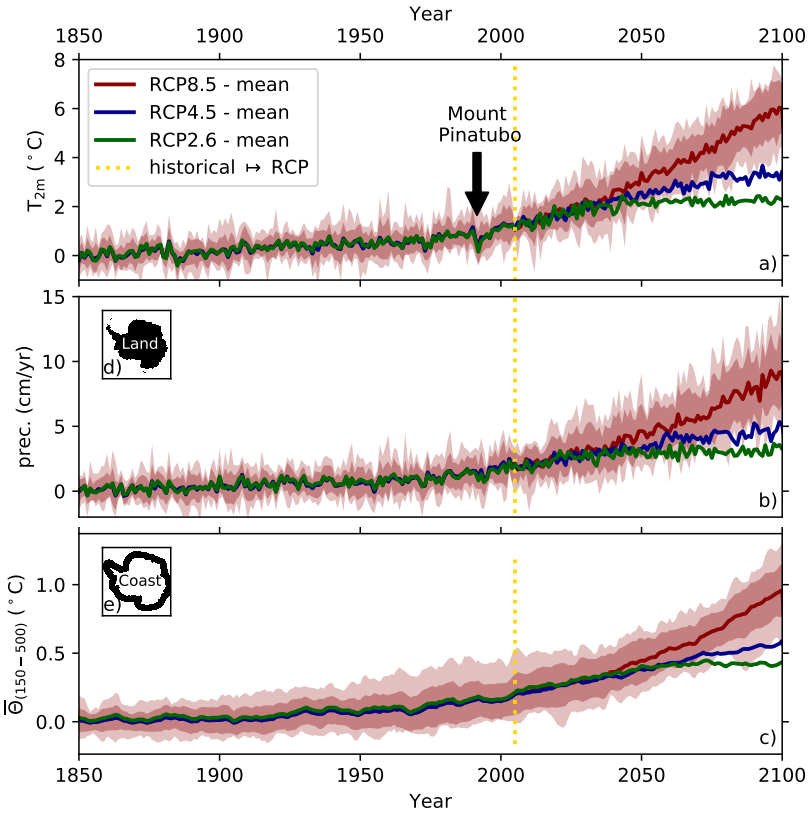

Figure 3. Spatial mean of the a) 2m-air temperature and b) total precipitation anomalies on Antarctica (d). Spatial c) potential ocean temperature mean averaged over the depth interval from $150\,\mathrm{m}$ to $500\,\mathrm{m}$ in the coastal zone (e) surrounding Antarctica. The ensemble mean values are shown for the scenarios according to the legend in a). The dark red band highlights the 1-sigma standard deviation ($66\,\%$), while the light red band shows the full range covered by all ensemble members for RCP8.5 only. The vertical golden line marks the transition from the historical forcing to the RCP. The distinct temperature jump during the historical period in 1991 marks the Mount Pinatubo volcano eruption. The contours of the Antarctic continent (d) follow the outer edges defined by the data set of Fretwell et al. (2013), while the coastal strip (e) is an extension into the sea with smoothed northern edges (typical width of about $500\,\mathrm{km}$).

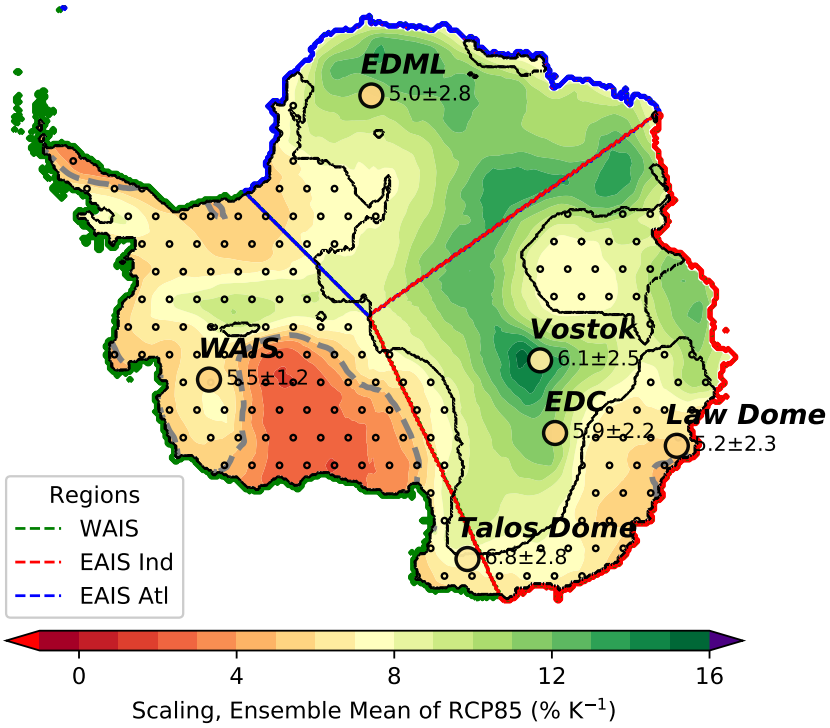

Figure 4. Ensemble mean of the temperature-scaled precipitation for the period 2051–2100. This scaling under the RCP8.5 scenario comes from nine CMIP5 models (Table 1), which are driven by anomalies relative to the first 50 years of piControl. In the dotted regions enclosed by black contours, the combined simulated scaling and the standard deviation contains the value of $5\,\%\mathrm{K}^{-1}$. Gray dashed lines follow this $5\,\%\mathrm{K}^{-1}$ contour. The scaling values deduced from ice cores are shown at their location (Frieler et al., 2015) by using the same colorbar as the spatial distribution within the circle. The neighboring printed values are the mean and the 2-sigma uncertainty. Three defined regions (Table 4) named "WAIS", "EAIS Atl", and "EAIS Ind" are outlined by their green, blue, and red, respectively, boundaries (lower left legend). For further details, inspect the text, please. Appendix Figure A3 provides corresponding distributions for each climate model ensemble member. Antarctica's contour is deduced from Fretwell et al. (2013).

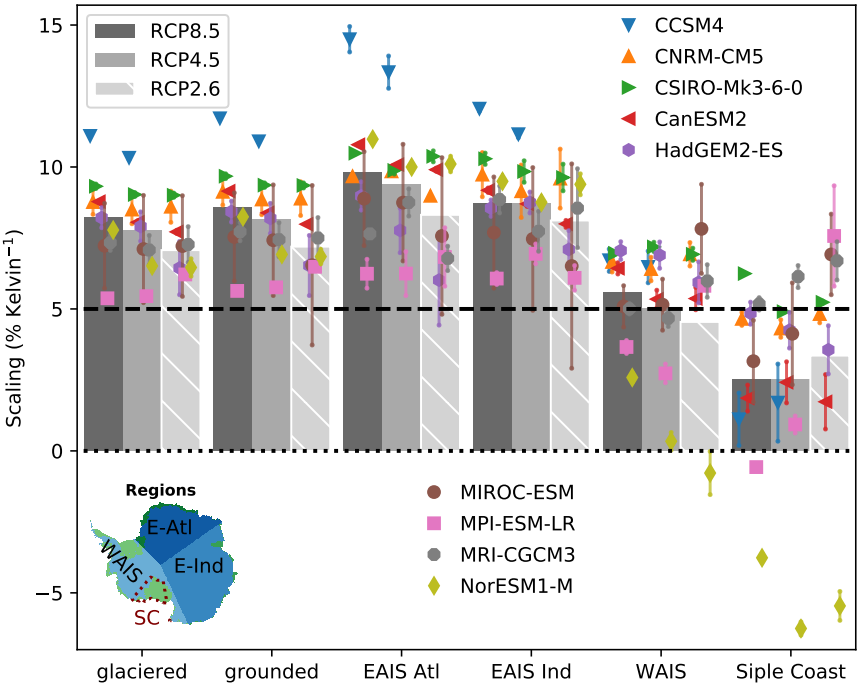

Figure 5. Temperature-precipitation scaling deduced for the nine CMIP5 models (Table 1) and three future scenarios (legend) in six defined regions in Antarctica (see map in the lower-left corner and Table 4. The coastlines and the grounding line positions are deduced from Fretwell et al. (2013)). The gray bars represent the ensemble mean, whereas the individual symbols stand for CMIP5 models. Here the results apply for both reference periods, where the anomalies are computed relative to the first or last 50 years of piControl. Each symbol is the model average of both reference periods, while the attached line indicates the scatter range between the first and last 50 years reference period. Please note, that the RCP2.6 scenario does not include the CCSM4 model; hence, the corresponding bar is hatched.

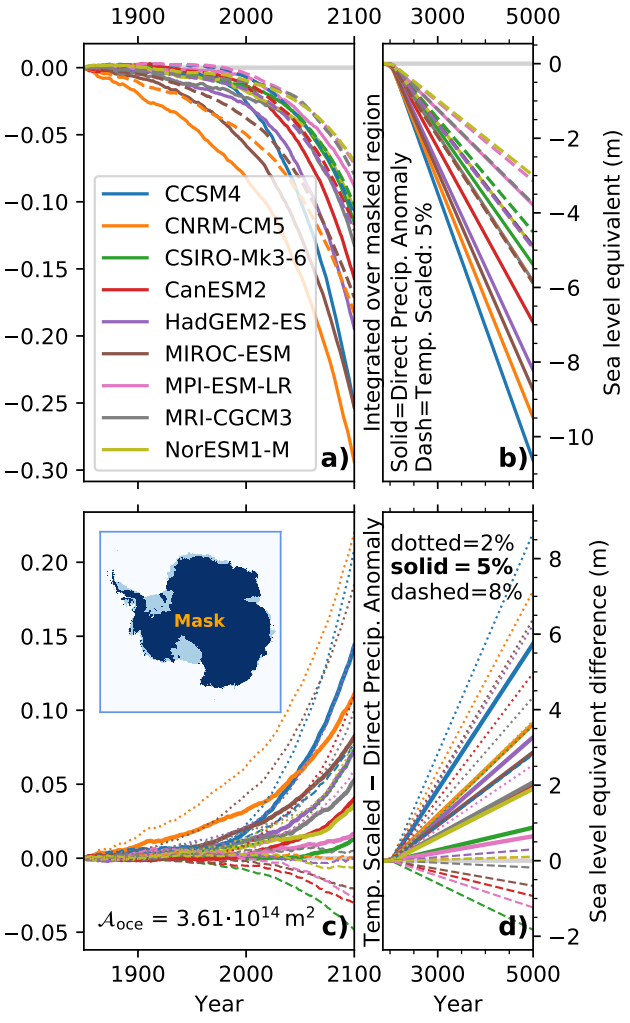

Figure 6. The top row (a, b) shows the integrated potential sea-level equivalent of the precipitation falling on grounded ice in Antarctica (see dark-blue mask in the lower left, the light-blue parts highlight ice shelves; The grounded and floating ice areas are derived from Fretwell et al. (2013)) for the anomaly forcing (solid lines) and temperature-scaled precipitation (dashed lines) considering a scaling of $5\,\%\mathrm{K}^{-1}$. The difference in the potential sea-level impact between the anomalies and the temperature-scaled precipitation is depicted in the lower row (c, d). Here, the solid lines consider scaling of $5\,\%\mathrm{K}^{-1}$, while the dotted and dashed lines consider a scaling of $2\,\%\mathrm{K}^{-1}$ and $8\,\%\mathrm{K}^{-1}$, respectively. The left subfigures a) and c) are restricted to the period 1850-2100, while b) and d) cover the full period from 1850 until 5000. Every single colored line (see legend in the upper left) represents one CMIP5 model (Table 1). The corresponding curves for the scenario RCP4.5 as well as for a different mask that covers the entire continent are available in the Appendix Figure A4.

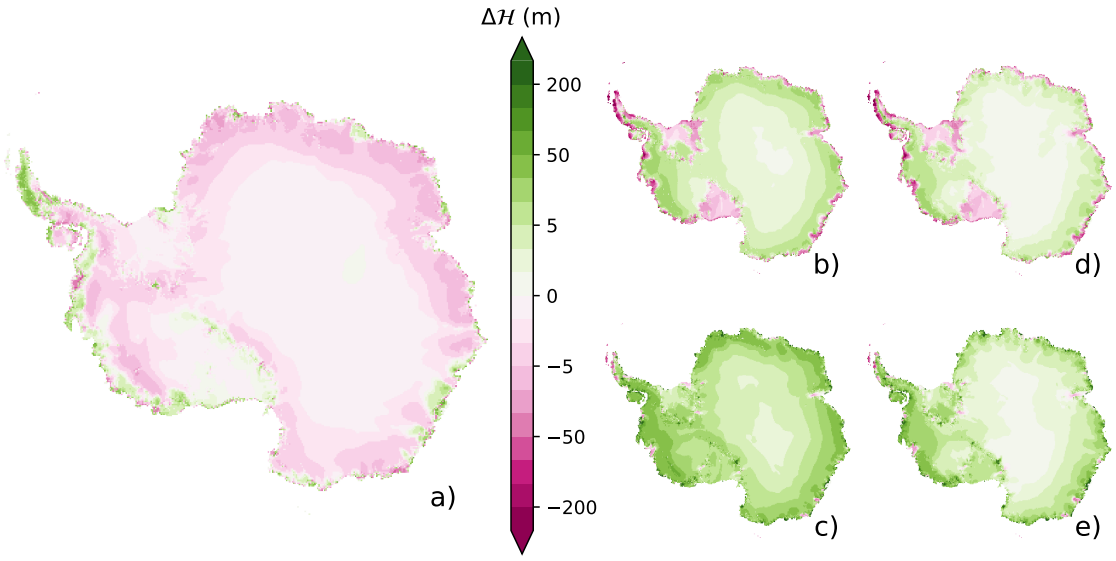

Figure 7. Ice thickness changes under the RCP8.5 scenario in the year 2100 since the year 1850. The ensemble mean difference between the runs forced by the scaled precipitation and the precipitation anomalies (a). For each climate model scenario, the anomalies are computed relative to the 50 years of the related piControl scenario. The simulations driven with the precipitation anomaly (b, c) have the mean ice thickness (b), and the maximum ice thickness (c) changes. The temperature-scaled precipitation of $5\,\%\mathrm{K}^{-1}$ gives the corresponding ensemble mean (d) and maximum (e). Please note that all subplots share the same colorbar.

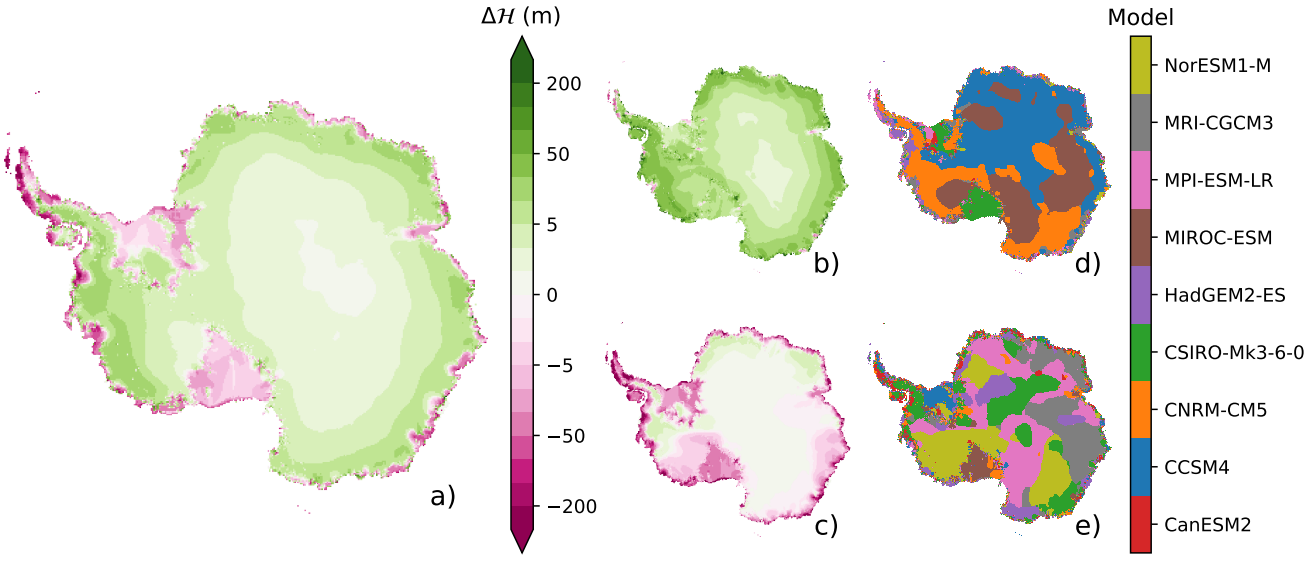

Figure 8. Ice thickness changes since 1850 under the RCP8.5 scenario for the actually applied precipitation anomaly in the year 2100. Highlighted are the (a) ensemble mean, maximum (b), and minimum (c). The climate model that is used to drive the ice-sheet model simulation causing the maximum and minimum thickness are shown in (d) and (e), respectively, next to the ensemble maximum (b) and minimum (c).

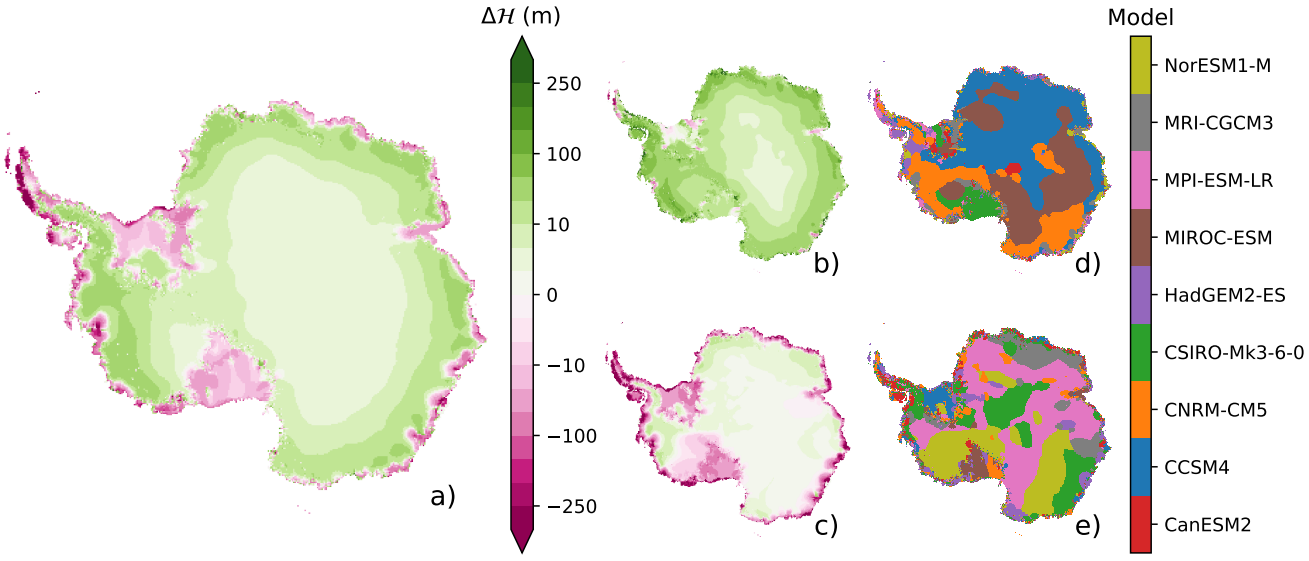

Figure 9. Ice thickness changes since 1850 under the RCP8.5 scenario for applied precipitation anomalies in the year 2200. Highlighted are the (a) ensemble mean, maximum (b), and minimum (c). The climate model that is used to drive the ice-sheet model simulation causing the maximum and minimum thickness are shown in (d) and (e), respectively, next to the ensemble maximum (b) and minimum (c).

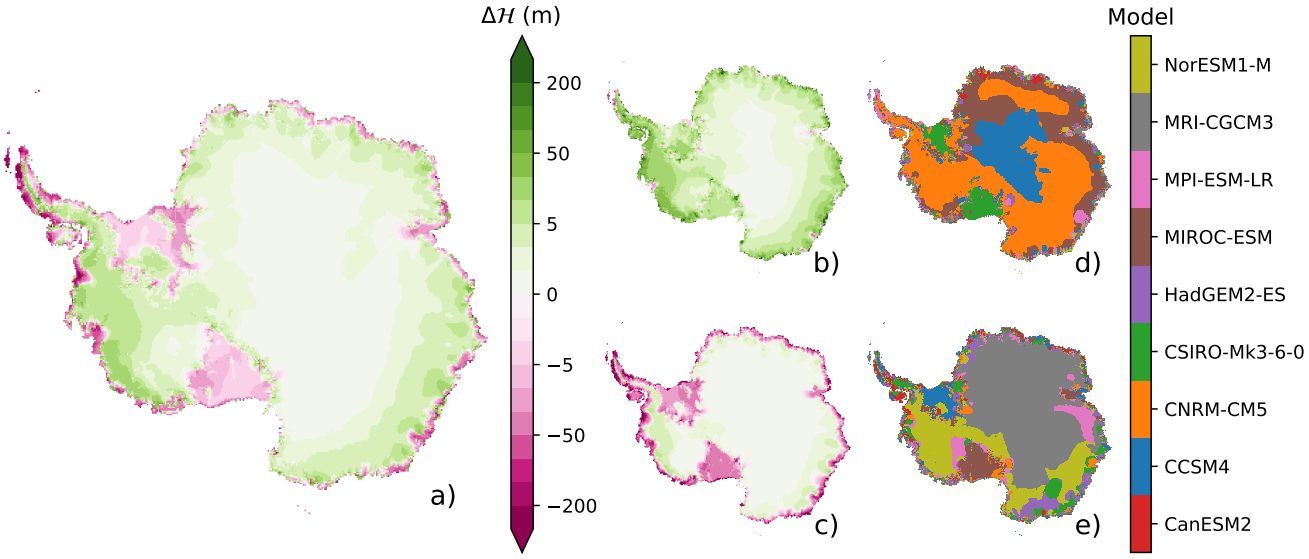

Figure 10. Ice thickness changes since the year 1850 under the RCP8.5 scenario in the model year 2100. Here the precipitation is scaled by the temperature anomaly with a value of $5\,\%\mathrm{K}^{-1}$. Depicted are the (a) ensemble mean, maximum (b), and minimum (c). The climate model that is used to drive the ice-sheet model simulation causing the maximum and minimum thickness is shown in (d) and (e), respectively, next to the ensemble maximum (b) and minimum (c). This figure is similar to Figure 8, but there the results under precipitation anomalies are shown.

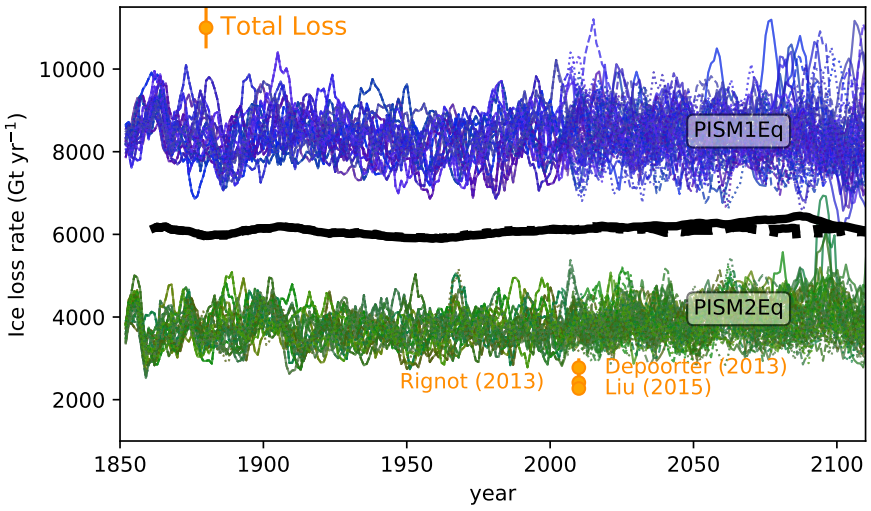

Figure 11. Temporal evolution of the ocean-driven ice loss rates of the fringing ice shelves around Antarctica for the period from 1850 to 2100. The ice loss comprises iceberg discharge and basal melting of ice shelves. The thin blue lines are all ensemble members starting from the initial state PISM1Eq, where the Eigen-calving parameter amounts 10^{18}, while the green lines are the corresponding simulations starting from PISM2Eq (Eigen-calving parameter 10^{17}). A running mean with a window of 5 years has been applied for the thin lines. All simulations start under historical conditions and continue after 2005 under the RCP8.5 (solid lines), RCP4.5 (dashed lines) or RCP2.6 (dotted lines) scenario. The thick black lines represent the ensemble mean of the three future scenarios with a moving window length of 25 years. Recent estimates of the total loss rates (Top-left legend with the golden circles). Estimated uncertainties are given as vertical lines if the uncertainties are larger than the symbol size.

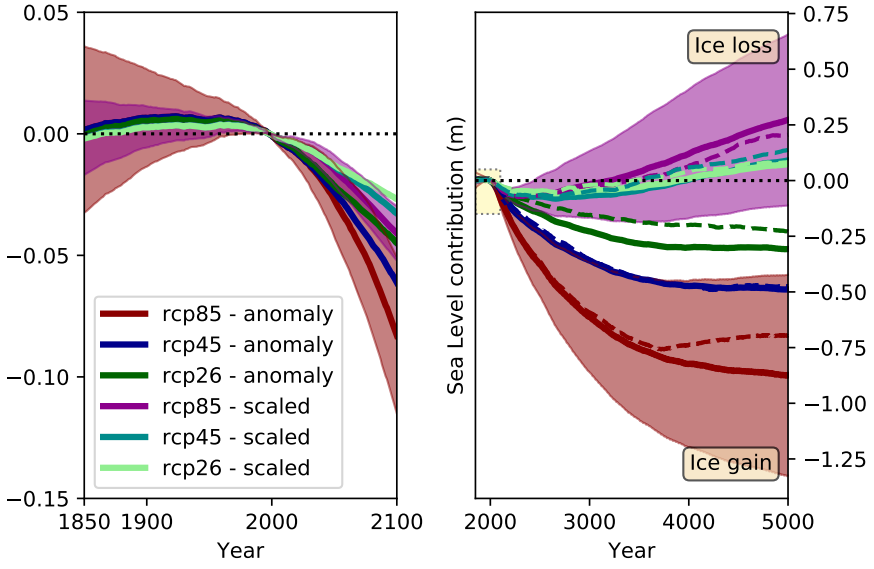

Figure 12. Sea level contribution of Antarctica computed by the ensemble of ice-sheet simulations (please see text for details). The solid lines represent the ensemble averages for the applied precipitation anomalies and the temperature-scaled precipitation boundary conditions according to the legend (lower left), while the dashed lines are the corresponding medians. For the RCP8.5 scenario, the shading highlights the standard deviation (1-sigma) as a measure of the variability among the ice-sheet ensemble members driven by various climate models (Table 1).

Appendix A: Additional Discussion

Regarding oceanic influence, we focus on the changes of the ensemble mean ocean temperature under the RCP8.5 scenario in a depth range between $150\,\mathrm{m}$ and $500\,\mathrm{m}$ (Figure 3), because these water masses flow into the ice-sheet cavities and are in contact with the ice shelve bases. Highest temperature increases occur in the Bellingshausen and the Amundsen Seas as part of the West Antarctic Ice Sheet (WAIS) and some spots along the East Antarctic Ice Sheet (EAIS) according to observations (Schmidtko et al., 2014; Jacobs, 2006). In the Bellingshausen and the Amundsen Sea, warm water masses flow into ice-shelf cavities as indicated by observations (Arneborg et al., 2012; Thompson et al., 2018) and model simulations (Nakayama et al., 2018). These water masses drive the highest basal melting rates (Nakayama et al., 2014) that trigger potential the Marine Ice Sheet Instability (MISI) because WAIS has a retrograde bedrock topography. The tremendous ice shelves, Filchner-Ronne, Ross, and Amery, are influenced by moderate temperature increases. However, our setup misses the interaction between the ice-shelf topography and the underlying dynamically evolving ocean. Hence, the setup does not describe related circulation changes that may bring warmer water masses into the ice cavities. For instance, it has been found that warmer water masses could find their way into these ice-shelf cavities and cause a strongly amplified basal mass loss under a changing climate (Hellmer et al., 2012). They have simulated an ocean warming by more then $2\,^{\circ}\mathrm{C}$ in the Filchner Trough (eastern Filchner-Ronne Ice Shelf). At the ice shelves edge of the Filchner-Ronne Ice Shelf, our ensemble maximum ocean temperature anomaly (Figure A1) of about $1.5\,^{\circ}\mathrm{C}$ generates a much weaker forcing.

A1 Temperature Scaling of Precipitation derived from Climate Models

If one calculates temperature scaling factors out of the CMIP5 model simulated temperature and precipitation changes, it turns out that the temperature scaling factor of the precipitation is different for each model and therefore shows an inhomogeneous spatial pattern (Appendix Figure A3). Furthermore, the details of the scaling factors depend on the time period we chose as a reference, which drive our ice-sheet simulations, relative to the first or last 50 years of the corresponding piControl runs. If we alternatively compute the anomalies relative to the first 30 years of the transient historical period (1850–2005), we obtain also slightly different results. However, these differences do not significantly change the spatial structure. Their impact is negligible compared to the choice of the driving model.

The scaling across all model tends to be highest for the EAIS, where the part facing the Atlantic Ocean exhibits highest scalings (Figure 5). The WAIS has a lower scaling and the embedded region “Siple Coast” has on average the lowest scaling. There is a tendency for a higher scaling under a more vigorously changing climate across all regions, except for the smallest region “Ross.” This tendency exists for the ensemble mean and across models characterized by a larger than average scaling. Most models represent the detected precipitation deficit (shrinking precipitation rates), captured by reanalysis data and shallow ice cores in the “Siple Coast” region (Wang et al., 2017). Only NorESM1-M reproduces less precipitation (precipitation deficit) under rising air temperatures across all future climate scenarios. When considering the whole Antarctica, the difference between the grounded ice sheet only and all glaciated regions (including ice shelves) is small.

The highest scaling spread between the first and last 50 years piControl reference period has MIROC-ESM across all inspected regions and scenarios, which is probably related to the pronounced trend of the global 2m-air temperature (0.67°C) between these two reference periods in our ensemble. Otherwise, the spread is related to enhanced/amplified long-term regional climate variability expressed by differing values in the reference period. For example, CCSM4 or MPI-ESM-LR are subject to a larger spread in the Atlantic sector of the EAIS, while in the neighboring Indian sector the variability is negligible. The higher spread of the smaller subregion Ross within the WAIS sector supports this interpretation (at least for the models CCSM4, CanESM2, HadGEM2-ESM).

There exists a tendency towards a higher scaling of coastal areas that are subject to incoming storm tracks, which potentially deliver heavier precipitation events that are also controlled by the rising topography height towards the interior of Antarctica. In the majority of the simulations, we identify a lower scaling in WAIS and also a low to negative scaling in the area of the Ross Ice Shelf and the adjacent parts of the WAIS.

A2 Marginal Ice Loss by ocean-driven Basal Melting and Iceberg Calving

We turn our analysis to the individual mass balance terms: Iceberg calving, basal melting in the ice-shelf cavities, and surface mass balance. To recap: the surface mass balance is obtained by applying the individual spatial atmospheric model forcing on top of the reference fields obtained from RACMO, while the basal melting is calculated by adding ocean anomalies on top of the World Ocean Atlas climatology (Table 2). The calving is composed of three processes (thickness calving, Eigen-calving, kill mask calving) as part of the Parallel Ice Sheet Model (PISM) simulations. Here, the analysis focuses predominantly on the period from 1850 to 2100, because after 2100, we reapply the forcing from 2071–2100 recurrently.

Until 2100, the temporal evolution of the iceberg calving rates of individual ensemble members is subject to some variability, which is typical for such event-based mass losses. For some models, we could identify some reduced calving of $20\,\%$ around 1850 and 1970, and some enhanced calving of $25\,\%$ around 1920 and 2050. These trends are noisy and are independent of the applied forcing scenario RCP2.6, RCP4.5, and RCP8.5 (Figure A12). Overall, the temporal evolution of the calving does not show a clear trend, and the average calving loss rate of the entire ensemble is about $5500\,\mathrm{Gt\,year^{-1}}$ (Figure A12). Clearly separated are the calving rates of ensemble members starting from either the initial state PISM1Eq or PISM2Eq. The members of the group starting from PISM1Eq have on average a calving rate of approximately $7500\,\mathrm{Gt\,year^{-1}}$, while it amounts to about $3500\,\mathrm{Gt\,year^{-1}}$ in the PISM2Eq. So a reduction of the Eigen-calving constant by an order of magnitude from 10^{18} (PISM1Eq) to 10^{17} (PISM2Eq) halves approximately the total calving rate, while in both cases the thickness calving is active for marginal ice-shelf point with a thickness of less than $150\,\mathrm{m}$.

According to observational estimates control iceberg calving and basal ice-shelf melting the overall mass loss of Antarctica, while the relative contribution is the subject of current research. Depoorter et al. (2013) report a nearly equal share between calving ($1321 \pm 144\,\mathrm{Gt\,year^{-1}}$) and basal melting ($1454 \pm 174\,\mathrm{Gt\,year^{-1}}$), Rignot et al. (2013) detect a slightly higher contribution from basal melting ($1325 \pm 235\,\mathrm{Gt\,year^{-1}}$ compared to calving with $1089 \pm 139\,\mathrm{Gt\,year^{-1}}$), while Liu et al. (2015) find that the basal melting ($1516 \pm 106\,\mathrm{Gt\,year^{-1}}$) contribution is twice as much as the calving ($755 \pm 24\,\mathrm{Gt\,year^{-1}}$) contribution.

Both ensemble branches starting from PISM1Eq and PISM2Eq overestimate the currently observed calving rates of less than $1500\,\mathrm{Gt\,year^{-1}}$ (Depoorter et al., 2013; Liu et al., 2015; Rignot et al., 2013). Also the combined observed mass loss by calving and basal melting of ice shelves, which is about $2500\,\mathrm{Gt\,year^{-1}}$ (Depoorter et al., 2013; Liu et al., 2015; Rignot et al., 2013), is on average smaller than the lower simulated calving rate from our ensemble members starting from PISM2Eq. Therefore, our ensemble mean ice loss rate exceeds current estimates, which could lead to an overestimation of the total sea-level rise in our simulations.

The basal melting rate of floating ice shelves (hereinafter basal melting rates) is the second ocean-driven ice mass loss process beside iceberg calving. In broad terms, the basal melt rate increases generally by $10\,\%$–$100\,\%$ over the period 1850–2100 (Figure A13). In the beginning, the melting rises slowly because the additional ocean-temperature forcing remains weak (Figure3). Starting around the year 1970, the raise becomes nonlinear, and basal melting accelerates. The simulated historical trend is nearly independent of the initial state (PISM1Eq and PISM2Eq) as well as to the reference period selected for the computation of the ocean temperature anomaly. For each climate model scenario, the anomalies are computed relative to the first or last 50 years of the pre-industrial climate (piControl) simulations. However, only for MIROC-ESM the reference state (first vs. last 50 years piControl) matters, because this model is subject to not negligible trend ($0.08\,\mathrm{m}$) during the piControl phase. For instance, the average of the global absolute 2m-air temperature difference between the first and last 50 years of piControl amounts $0.17\,\mathrm{K}$ (median $0.12\,\mathrm{K}$) for all CMIP5 models considered in our study. In contrast, MIROC-ESM's value is $0.67\,\mathrm{K}$.

In future projections, the basal melting rate increases between $10\,\%$ and more than $100\,\%$ until the year 2100 relative to the 50 years reference period 1951–2000. The latter increase is consistent with results from dedicated ocean simulations. These simulations resolve ice shelves, include the ocean-ice-sheet interaction explicity, are driven by future projection from various climate models (Naughten et al., 2018; Hellmer et al., 2012).

The temporal evolution of the actual basal melting rate (Figure A13) increases until 2100 and falls back afterward onto the value of the year 2071 because we apply the last 30-years-forcing recurrently after 2100. Also, for the basal melting the separation of ensemble members starting from PISM1Eq and PISM2Eq is self-evident. However, both groups are close to the ensemble mean, which is in contrast to the calving rate. The basal melting rates of all ensemble members underestimate the observational basal melting rates.

Since, in general, the observed calving rate is lower than the basal melting rate, our model ensemble swaps the importance of basal melting and iceberg calving. Also the sum of the calving rate and basal melting rate exceeds the observed estimates. Hence, our simulations could tend to overestimate ice loss and, ultimately, sea-level rise.

The ensemble mean calving and basal melting rates stay nearly constant or reach a maximum of around 2100 and scenarios with a higher forcing (RCP8.5 vs. RCP4.5, for instance) cause more ice loss by both calving and basal melting. Beyond 2100, ice loss rates decrease in general (Figure A14). Since the temporal variability remains high also after 2100, our approach works to construct the forcing beyond the year 2100 (see section 2: "Material and Methods"). To highlight the primary trend in the temporal evolution after 2100, a 250-year running mean is applied after 2100.

The basal melting rates of the stronger forcing scenario RCP8.5 show a minimum of around the year 3500 and increase afterward slightly, while the other scenarios (RCP4.5 and RCP2.6) indicate a tendency for stabilization at the end of our simulation in the year 5000 (Figure A14). Over the entire period, the basal melting rate is higher for the stronger forcing scenarios. This result reflects the dependence of the basal melting on the ocean temperature because a warmer climate scenario induces higher ocean temperature anomalies.

The calving rates before 2100 tend to be slightly higher for the RCP8.5 scenario. However, after 2100, we detect the sharpest fall of the ice loss rates for the scenario RCP8.5 and an intermediate decrement for RCP4.5 and a moderate reduction for RCP2.6 (Figure A14). Around 3000, RCP8.5 calving reaches its minimum, followed by an enhanced increase for 500 years and a moderate increase afterward. Forcing scenarios with a lower strength reach the minimum later, so that RCP4.5 has its minimum around 3200, while RCP2.6 shows the minimum around 3700. At this time, the ensemble mean calving rates of the RCP4.5 and RCP2.6 are similar (please note that RCP2.6 does not include simulations driven by CCSM4). The trends of all scenarios converge around 4000.

In the long term, the most active basal melting occurs for the stronger forcing scenarios, while the highest calving occurs under scenarios with a lower forcing. The calving rate controls the evolution of the total ice mass loss in our simulations. Before the year 2100, RCP8.5 has the highest calving rates, while these are lowest shortly afterward. The ordering of the scenarios with the highest calving rates (RCP2.6) is those with the lowest forcing (RCP2.6) and vise versa (RCP8.5). The ensemble mean of the basal melting increases by $60\,\%$–$70\,\%$, $70\,\%$–$85\,\%$, and $90\,\%$–$115\,\%$, for RCP2.6, RCP4.5, and RCP8.5, respectively. The fractional calving change of the ensemble mean is between $+2\,\%$– $-4\,\%$, $+2\,\%$– $-10\,\%$, and $+2\,\%$– $-19\,\%$ for RCP2.6, RCP4.5, and RCP8.5, respectively. Across these, we detect that the most substantial ice-shelf area reduction occurs for RCP8.5 and the lowest for RCP2.6. Our simulations suggest that the warmer climate causes a stronger ice-shelf retreat and a stronger drop in the calving rate in the period, where the ice shelf could adjust to the quasi-equilibrium forcing. Based on these results we conclude: warmer climate drives more basal melting and enhances calving so that we obtain smaller ice shelves. The total area of ice shelves is, in general, smaller when a warmer climate scenario impacts these ice shelves (Figure A15) and the degraded total ice shelf area downgrades the calving probability. Ultimately, the integrated calving rate is lower under a warmer climate.

A3 Bias-corrected Fluxes

Since the simulated ocean-driven basal melting rates are lower than observational-based estimates (Figure A13), the impact of flux corrected basal melting rates on the model results are discussed in the main text (Section 3.7.1 "Sea level contribution of corrected basal melting" on page 16). This section describes the method.

Starting from original simulated ablation flux F_{org}, which could be the basal melting flux $F^{B}_{\mathrm{org}}(t)$ or the iceberg discharge flux $F^{D}_{\mathrm{org}}(t)$, and the corresponding reference flux $F_{\mathrm{ref}}(t_{\mathrm{ref}})$ at time t_{ref}, we define the following ratios. The fraction of the temporal evolving flux ($F_{\mathrm{org}}(t)$) to the original flux at the reference time (t_{ref}):

$$r(t) = \frac{F_{\mathrm{org}}(t)}{F_{\mathrm{org}}(t_{\mathrm{ref}})} \Longrightarrow r(t_{\mathrm{ref}}) = 1, \tag{A1}$$

and the fraction of the original simulated flux to the reference flux (F_{ref})

$$q = q(t_{\mathrm{ref}}) = \frac{F_{\mathrm{ref}}(t_{\mathrm{ref}})}{F_{\mathrm{org}}(t_{\mathrm{ref}})}. \tag{A2}$$

The corrected flux F_{cor} using Equation A1 is defined as

$$F_{\mathrm{cor}}(t) = r(t) \cdot F_{\mathrm{ref}}(t_{\mathrm{ref}}), \tag{A3}$$

so that the flux difference $\Delta F(t)$ is

$$\begin{aligned}\Delta F(t) &= F_{\mathrm{cor}}(t) - F_{\mathrm{org}}(t) \\ &= F_{\mathrm{org}}(t) \left[\frac{F_{\mathrm{ref}}(t_{\mathrm{ref}})}{F_{\mathrm{org}}(t_{\mathrm{ref}})} - 1 \right].\end{aligned}$$

With Equation A2 we obtain

$$\Delta F(t) = F_{\mathrm{org}}(t) \left[q - 1 \right]. \tag{A4}$$

To relate the sea-level change to the ice mass evolution, we define the ratio $p(t)$ of the sea level temporal deviation to the ice mass temporal deviation as

$$p(t) = \frac{\dfrac{dz_l(t)}{dt}}{\dfrac{dm_{\mathrm{ice}}(t)}{dt}}, \tag{A5}$$

where z_l is the sea level and m_{ice} the total ice mass, which includes grounded and floating ice. We use here $p = \mathrm{median}(p(t))$ so that each ensemble member is characterized by one value for its entire time series. If $p = \frac{1}{\rho A_{\mathrm{oce}}}$, $100\,\%$ of flux difference (Equation A4) contributes immediately to the sea level of the global ocean with an area of A_{oce}.

The total ice mass (m_{ice}) changes are driven by four terms

$$\frac{m_{\mathrm{ice}}}{dt} = \underbrace{\left[F^{SMB}(t) + F^{G}(t)\right]}_{\text{unchanged under correction}} + F^{B}(t) + F^{D}(t),$$

where $F^{SMB}(t)$ is the surface mass balance flux and $F^{G}(t)$ the basal mass flux of grounded ice (Figure A9). We assume that these two terms in the brackets do not change regardless of the applied corrections to the last two terms F^{B} and F^{D}. Hence the difference in the ice mass change is

$$\Delta \frac{dm_{\mathrm{ice}}}{dt} = \Delta F^{B}(t) + \Delta F^{D}(t) \tag{A6}$$

Now we relate the temporal evolution of the sea level to the total ice mass changes by utilizing the Equation A5

$$\frac{z_{l\,\mathrm{cor}}}{dt} = \frac{z_{l\,\mathrm{org}}}{dt} + p(t) \cdot \left[\Delta F^{B}_{\mathrm{cor}}(t) + \Delta F^{D}_{\mathrm{cor}}(t)\right],$$

so that we obtain:

$$z_{l_{\mathrm{cor}}} = z_{l_{\mathrm{org}}} + \Delta z_l(t), \tag{A7}$$

where the sea-level difference $\Delta z_l(t)$ is

$$\Delta z_l(t) = \int_{t_0}^{t} p(\hat{t}) \left[\Delta F^B_{\mathrm{cor}}(\hat{t}) + \Delta F^D_{\mathrm{cor}}(\hat{t})\right] d\hat{t}. \tag{A8}$$

The Figures A5 and A7 depict the sea-level difference for two cases. If the additional mass loss contributes immediately to a rising sea level (Figure A7), the corresponding sea level rise of $30\,\mathrm{cm}$ would be larger than the actual sea level rise since 1850 of about $20\,\mathrm{cm}$ (Church and White, 2011).This case is not realistic because a melting floating ice shelf does not impact the sea level. Only the flow of grounded ice across the grounding line, to feed an ice shelf, or the direct loss of grounded ice contributes to the sea level.

In contrast, the sea level changes hardly (Figure A5) if the deduced ratio $\overline{p(t)}$, which corresponds to the ratio defined in Equation A5. It is computed for each ensemble mean as median of its time series. Whether the ratio between ice loss and sea-level rise is constant under amplified basal melting of ice shelves is an open question. Strongly intensified ocean-driven ice loss will probably cause a retreating grounding line on a longer time scale, which ultimately releases grounded ice into the sea and increases the sea level.

Figure A8 shows the proportion of the deduced ratio to the $100\,\%$ ratio. Only very few ensemble member lose about 15% of the maximum value of $p = 1/(\rho \cdot A_{\mathrm{oce}})$. In contrast, the mean and median value of this proportion is generally less then $5\,\%$. For all ensemble members driven by the precipitation anomaly, this proportion is on average $4.7\,\%$ with a median of $3.9\,\%$. It is even lower for ensemble members driven by the temperature-scaled precipitation. The median amounts $0.7\,\%$ and the corresponding mean is $0.9\,\%$. Please note that some ensemble members under the temperature-scaled precipitation are subject to a negative scaling. This result confirms the above presented low positive and negative scaling seen for restricted regions (Figure 5). It highlights also that simulations driven by temperature-scaled precipitation could show unexpected results.

A4 Appendix Figures

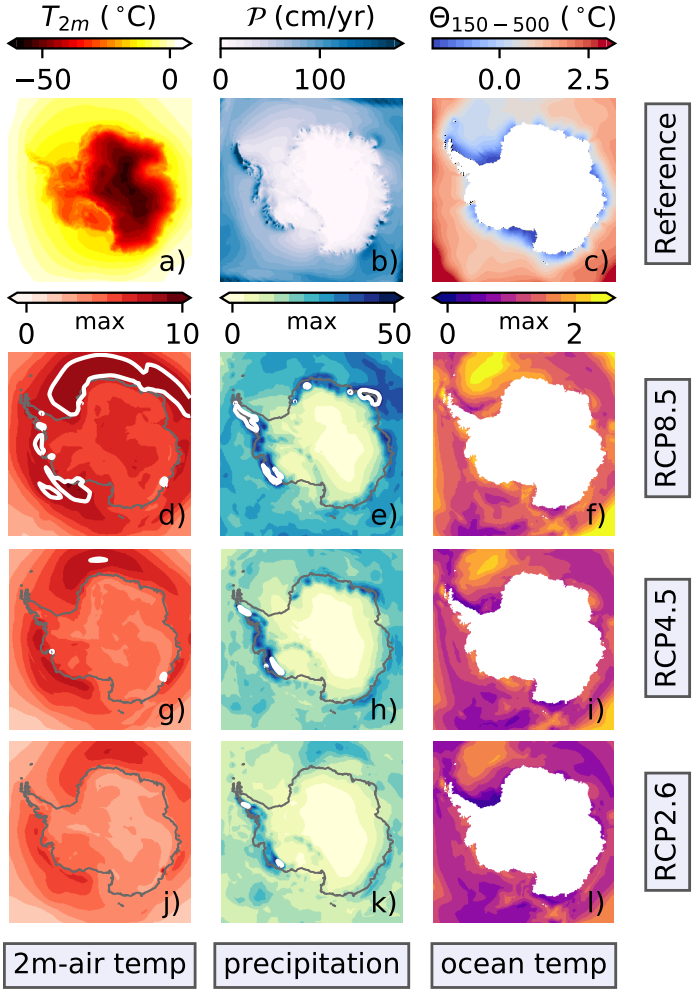

Figure A1. Atmospheric (a, b) and oceanographic (c) reference forcing; ensemble maximum anomalies (d–l). The top row represents the reference fields to spin-up the ice-sheet model (Table 2). The 2m-air temperature (a) and the total precipitation (b) are mean fields from the regional RACMO model, while the ocean temperatures come from the World Ocean Atlas 2009 (c). Below each reference field, the related maximum anomalies are compiled for the period 2071–2100. Here, the second (third and fourth) row shows the anomalies for RCP8.5 (RCP4.5, RCP2.6). The dark-gray line follows the current coastline. All potential ocean temperatures (c, f, i, l) are a vertical mean of the depth interval from 150 m to 500 m. The white contour lines in the anomaly plots highlight the following thresholds. 2m-air temperature (d, g, j): 8°C; total precipitation (e, h, k) $50\,\mathrm{cm\,year^{-1}}$. All these anomalies are the ensemble maximum of the models listed in Table 1; CCSM4 is not part of RCP2.6. Figure 2 shows the corresponding ensemble mean fields, where the white contour line in the precipitation field corresponds to $30\,\mathrm{cm\,year^{-1}}$.

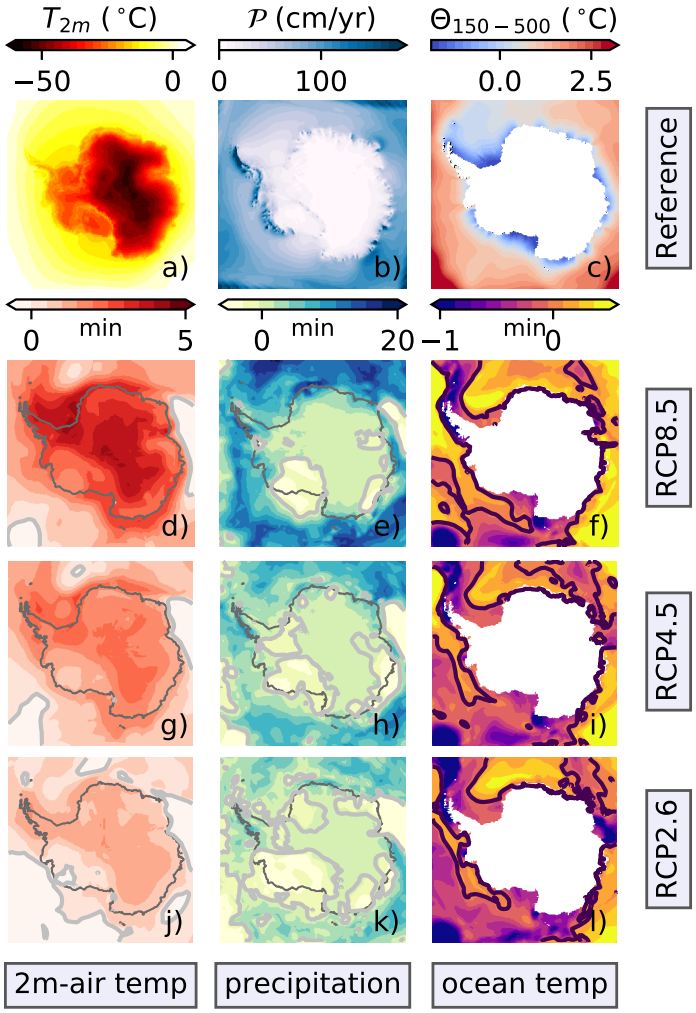

Figure A2. Atmospheric (a, b) and oceanographic (c) reference forcing; ensemble minimum anomalies (d–l). The top row represents the reference fields to spin-up the ice-sheet model (Table 2). The 2m-air temperature (a) and the total precipitation (b) are mean fields from the regional RACMO model, while the ocean temperatures come from the World Ocean Atlas 2009 (c). Below each reference field, the related minimum anomalies are compiled for the period 2071-2100. Here, the second (third and fourth) row shows the anomalies for RCP8.5 (RCP4.5, RCP2.6). The dark-gray line follows the current coastline. All potential ocean temperatures (c, f, i, l) are a vertical mean of the depth interval from $150\,\mathrm{m}$ to $500\,\mathrm{m}$. The light-gray lines in the anomaly plots highlight the following thresholds. 2m-air temperature (d, g, j): 0°C; total precipitation (e, h, k) $0\,\mathrm{cm\,year}^{-1}$; potential ocean temperature 0°C. All these anomalies are the ensemble minimum of the models listed in Table 1; please note that CCSM4 is not part of RCP2.6. Figure 2 shows the corresponding ensemble mean fields.

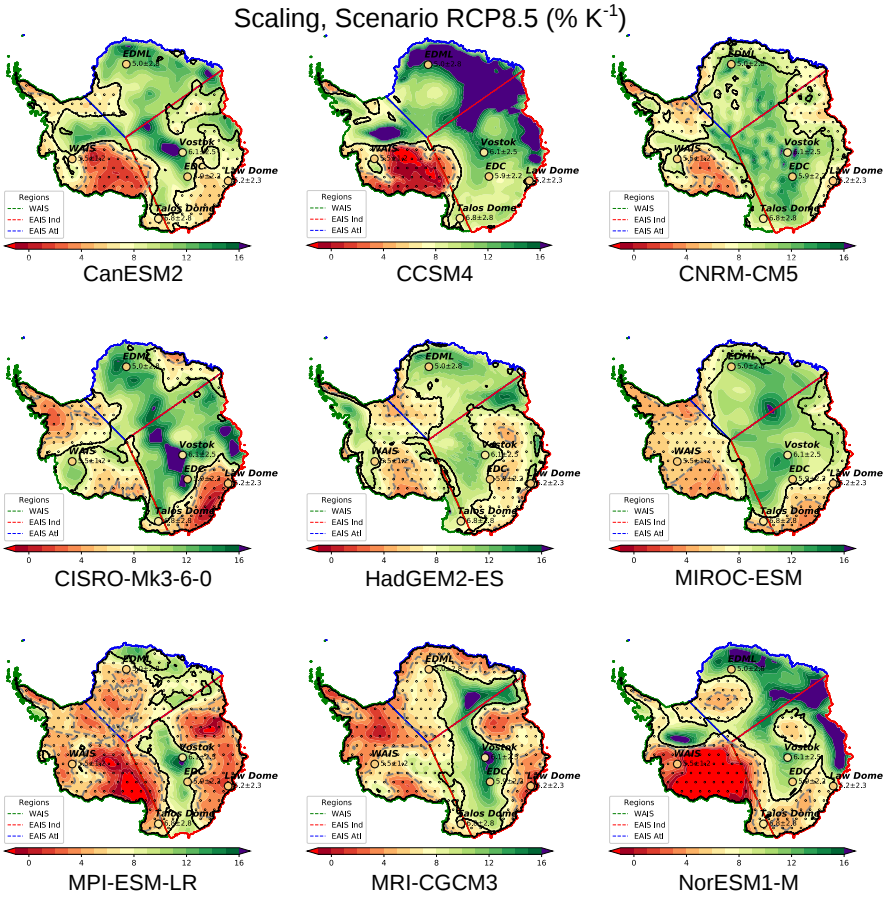

Figure A3. temperature-scaled precipitation under the RCP8.5 scenario for nine CMIP5 models (Table 1): Period 2051–2100. The ice-sheet simulations are driven by anomalies relative to the first 50 years of the related piControl climate scenario. In the dotted regions enclosed by black contours, the combined simulated scaling and the standard deviation contains the value of $5\,\%\mathrm{K}^{-1}$. Gray dashed lines follow this $5\,\%\mathrm{K}^{-1}$ contour. The scaling values deduced from ice cores are shown at their location (mean and the 2-sigma uncertainty). The regions named "WAIS," "EAIS Atl," and "EAIS Ind" are outlined by their green, blue, and red, respectively, boundaries (lower left legend). For further details, inspect the text, please. Figure 4 shows the corresponding ensemble mean. The contours of the Antarctic continent are deduced from Fretwell et al. (2013).

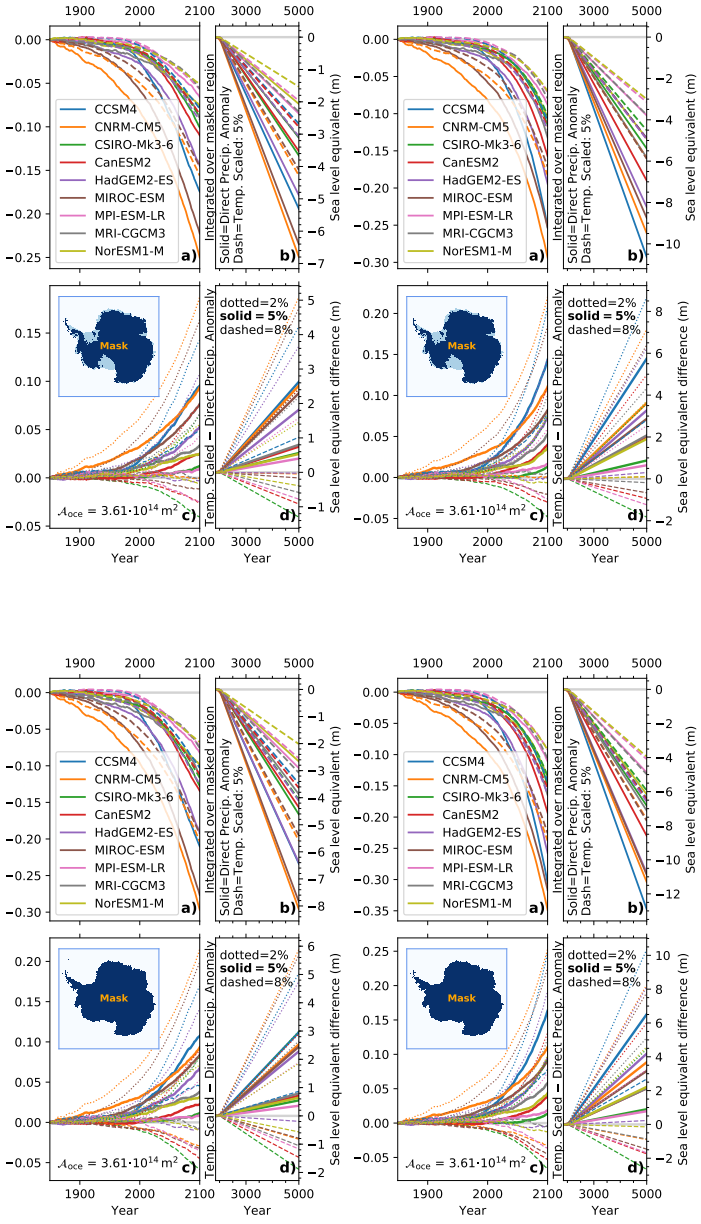

Figure A4. Integrated potential sea-level equivalent of the precipitation falling on Antarctica (see the mask in each subpanel) from the anomaly forcing (a, b: solid lines) and temperature-scaled precipitation (a, b: dashed lines). The potential sea-level impact between the anomalies and the temperature-scaled precipitation (c, d) is depicted for each CMIP5 model (legend on the lower left). The subpanels in the left and right columns show the results under the RCP4.5 and RCP8.5 scenarios, respectively. The upper row depicts the scaling for the entire Antarctic continent ("glaciered"), while the lower row is restricted to grounded ice. The lower left subpanel is identical to Figure 6. Please inspect this figure for further details. The grounded and floating ice areas are derived from Fretwell et al. (2013)

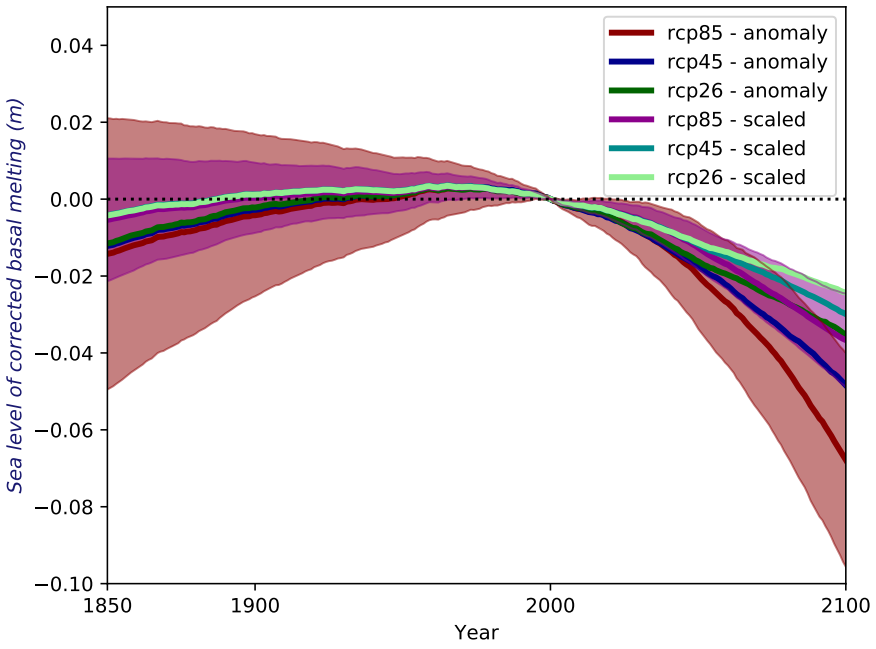

Figure A5. The sea level correction as defined by Equation A8 covers the period from 1850 until 2100. Here, the ratio $p(t)$ (Equation A5) is the temporal median for each ensemble member (please see Figure A7 for the corresponding figure assuming that all additional mass loss rises the global simulated sea level). The correction is computed relative to the year 2000 as in Figure 12. The resulting simulated sea level for the entire period from 1850 until 5000 depicts the Figure A6. As reference value for the basal melting rate $F^B_{\mathrm{ref}}(t_{\mathrm{ref}})$, we use $1431\,\mathrm{Gt\,year}^{-1}$, which corresponds to the estimate of Depoorter et al. (2013) with $1454 \pm 174\,\mathrm{Gt\,year}^{-1}$, while it falls below the values of Liu et al. (2015) ($1516 \pm 106\,\mathrm{Gt\,year}^{-1}$), but is also exceed the rate of $1325 \pm 235\,\mathrm{Gt\,year}^{-1}$ reported by Rignot et al. (2013); our reference $F^B_{\mathrm{ref}}(t_{\mathrm{ref}})$ corresponds to the mean of all these basal melting estimates: $1431\,\mathrm{Gt\,year}^{-1}$.

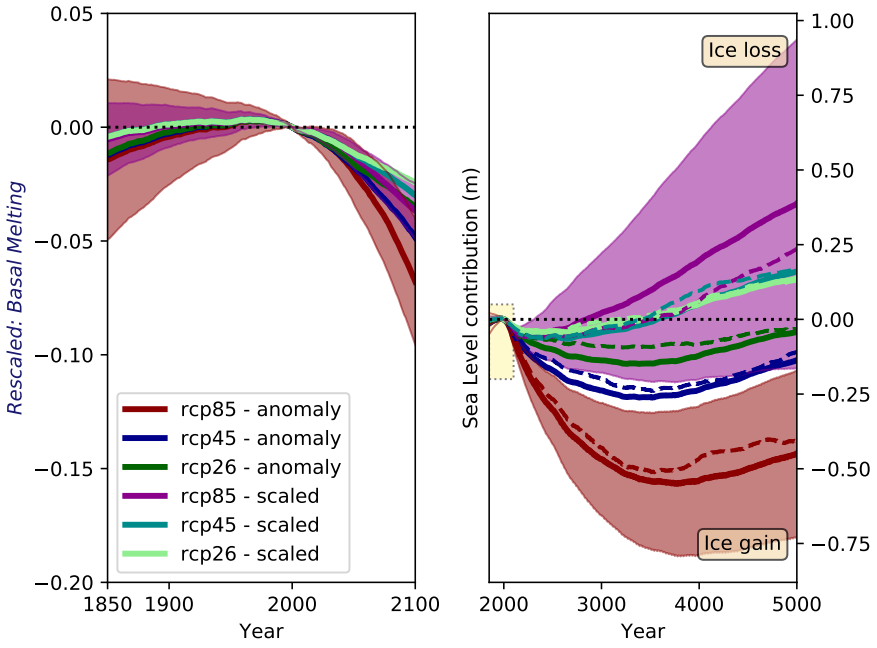

Figure A6. The simulated sea level considering the correction as defined by Equation A8 and Figure A5. The sea level (in meter) is computed relative to the year 2000 as in Figure 12. Please inspect the Figure 12 for further details.

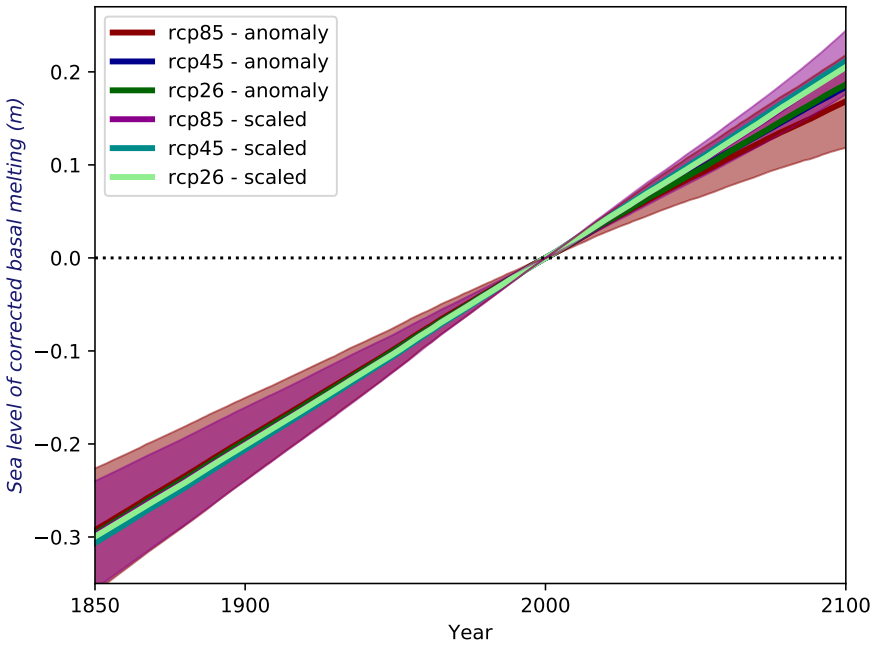

Figure A7. The sea level correction as defined by equation A8 covers the period from 1850 until 2100, where $100\,\%$ of the additional mass loss contributes immediately to a rising sea level, hence the ratio p (Equation A5) equals $p = 1/(\rho A_{\mathrm{oce}})$. The correction is computed relative to the year 2000 as in Figure 12. The corresponding Figure A5 depicts the case where the correction considers the actual deduced ratio $p(t)$.

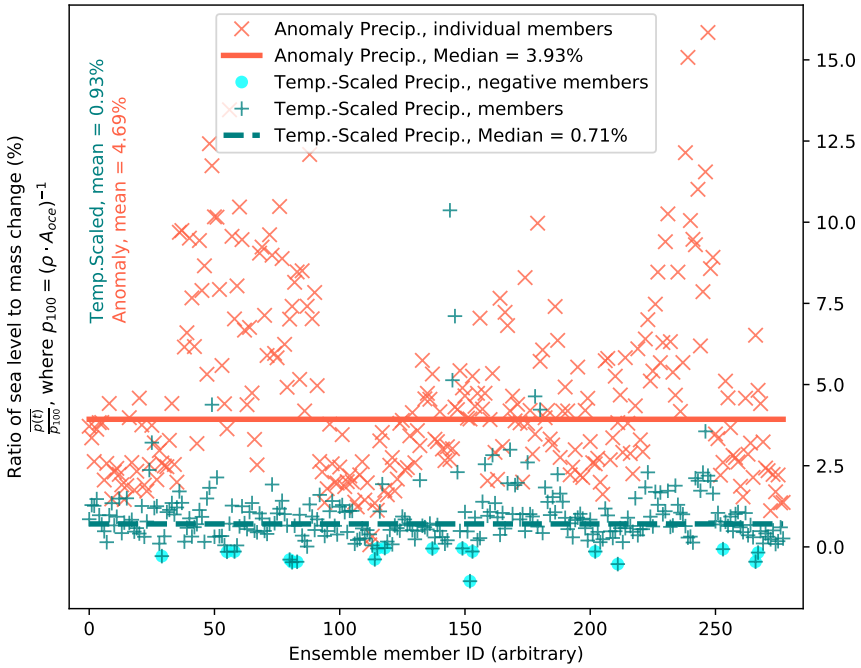

Figure A8. The ratio between the actual sea level contribution due to mass loss and the sea level equivalent of corresponding mass. Individual ensemble members are shown as crosses. A red "x" represents a member that is driven by the precipitation anomaly, while a blue-green "+" indicates those driven by the temperature-scaled precipitation. In the latter case, light blue circles highlight members with negative ratios. Vertical lines mark median values for these two groups; see also legend. The corresponding mean values are listed on the left side. The term $\overline{p(t)}$ is defined by the Equation A5 and $p_{100} = \frac{1}{\rho \cdot A_{\mathrm{oce}}}$, where ρ is the density and A_{oce} represents the global ocean area.

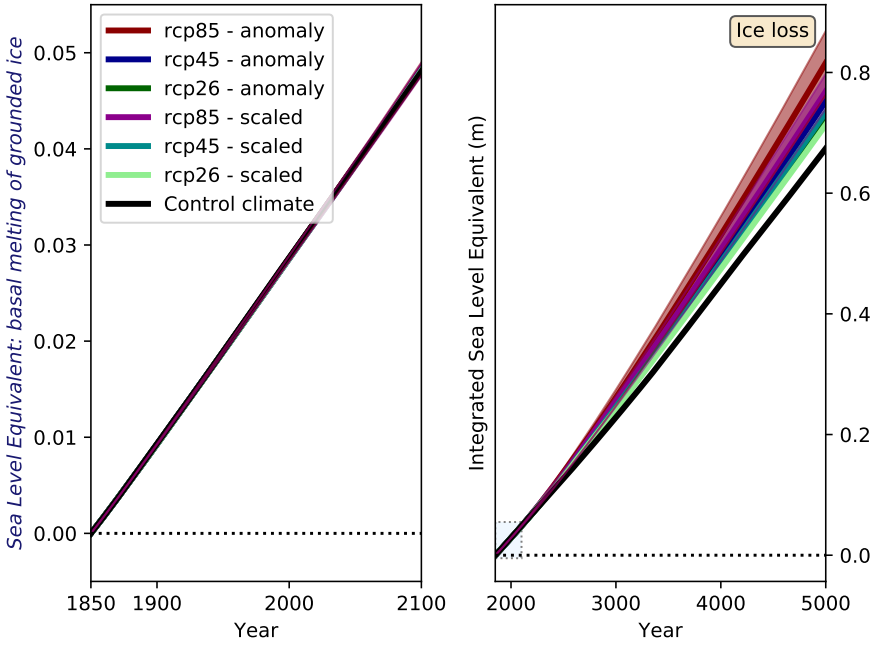

Figure A9. Cumulated basal melting of grounded ice as sea level equivalent. Shown are the results of the entire ensemble of ice-sheet simulations. The solid lines represent the ensemble averages for the applied precipitation anomalies and the temperature-scaled precipitation boundary conditions according to the legend (lower left). For the RCP8.5 scenario, the shading highlights the standard deviation (1-sigma) as a measure of the variability among the ice-sheet ensemble members driven by various climate models (Table 1).

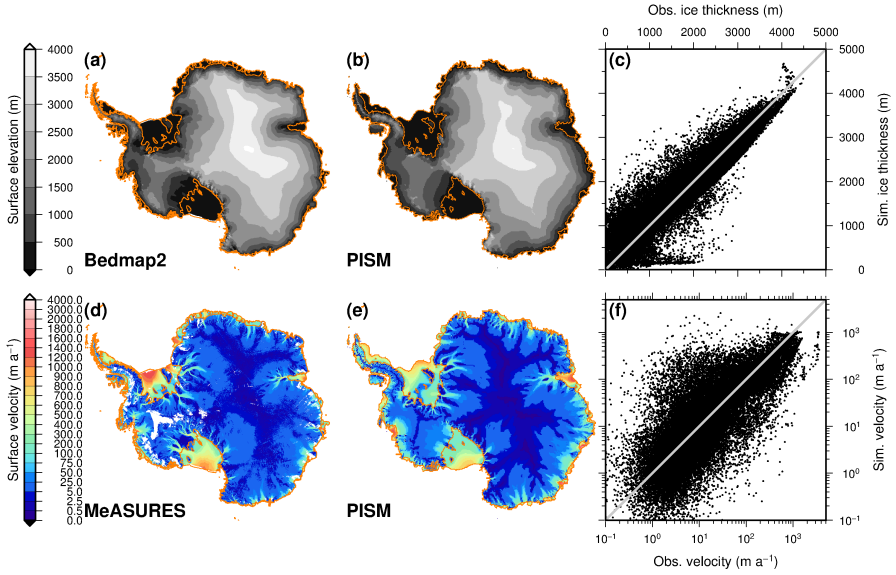

Figure A10. Comparison between the initial state PISM1Eq and observational estimates. The top row depicts the surface elevation: a) Bedmap2 data set (Fretwell et al., 2013), b) simulated ice elevation in PISM and c) point-wise comparison. The lower row shows the surface velocity distribution: d) Observations (Rignot et al., 2016), e) simulation and f) point-wise comparison; please note that both axes are logarithmic. For the point-wise comparison, the observations follow the x-axis (abscissa) while simulated values follow the y-axis (ordinate). Essential information about the initial ice-covered area and volume and its comparison with the other initial state PISM1Eq (Figure A11) lists the table A1.

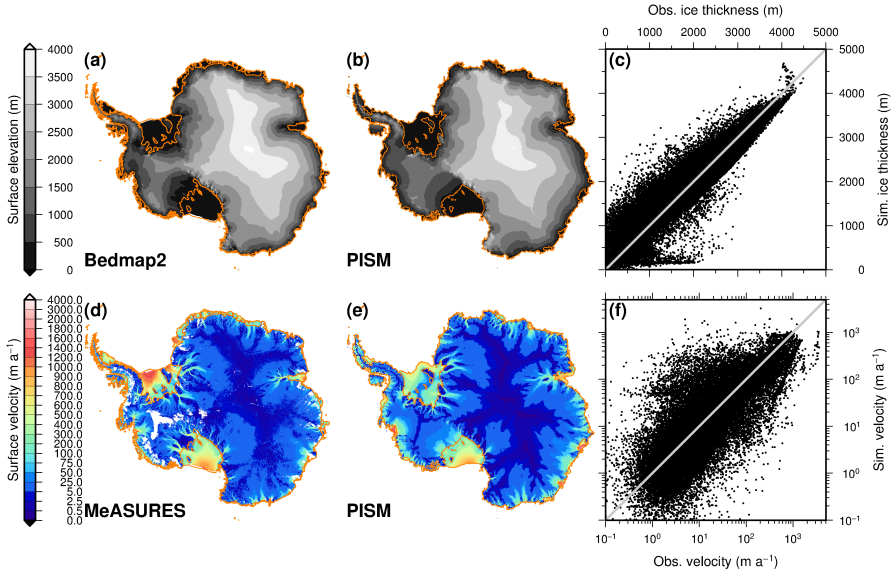

Figure A11. Comparison between the initial state PISM2Eq and observational estimates. The top row depicts the surface elevation: a) Bedmap2 data set (Fretwell et al., 2013), b) elevation in PISM and c) point-wise comparison, while the lower row shows the surface velocity: d) Observations (Rignot et al., 2016), e) simulation and f) point-wise comparison. Please see also Figure A10 (PISM1Eq) for further details, and inspect the table A1 for essential information and a comparision between both states.

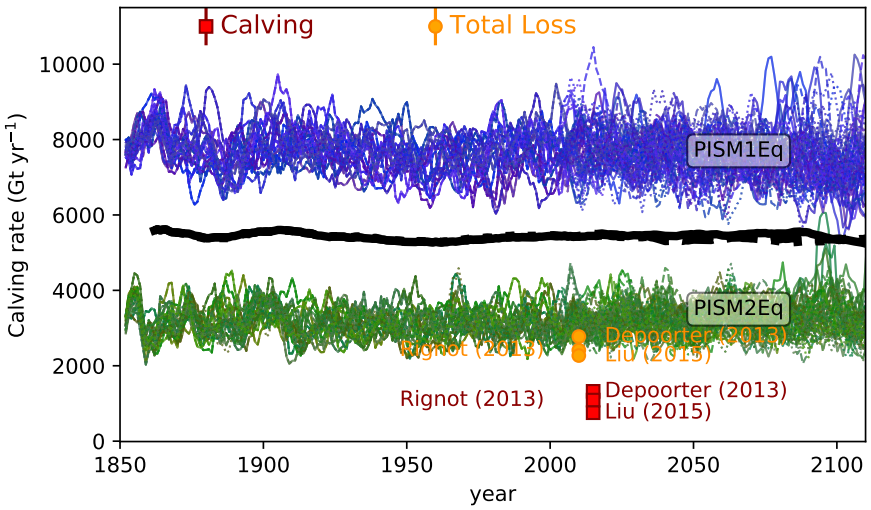

Figure A12. Temporal evolution of Antarctic-wide calving rates for the period from 1850 to 2100. All simulations start under historical conditions and continue after 2005 under the RCP8.5 (solid lines), RCP4.5 (dashed lines) or RCP2.6 (dotted lines) scenario. After the year 2100, the forcing of the last thirty years until 2100 drives the model recurrently. The thin blue lines are all ensemble members starting from the initial state PISM1Eq, where the Eigen-calving parameter amounts 10^{18}, while the green lines are the corresponding simulations starting from PISM2Eq (Eigen-calving parameter 10^{17}). A running mean with a window of 5 years has been applied for the thin lines. The thick black lines represent the ensemble mean of the three future scenarios with a moving window of 25 years. The applied running means shift the apparent maximum backward in time so that it occurs visually before the year 2100. Recent estimates of the total (orange circles) and the calving (red squares) ice mass loss are given for three studies (legend at the top). Vertical bars depict the reported uncertainties of the shown estimates by Liu et al. (2015); Depoorter et al. (2013); Rignot et al. (2013).

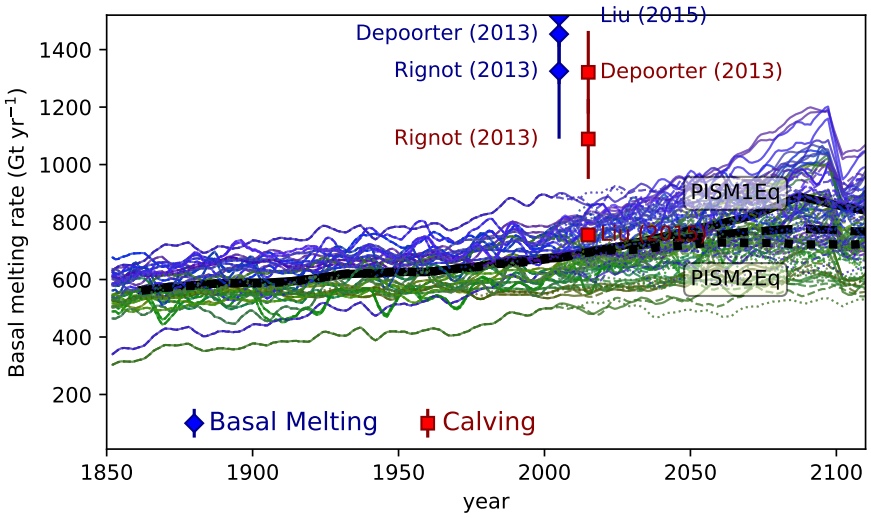

Figure A13. Temporal evolution of the basal melting rates in fringing ice shelves around Antarctica for the period from 1850 to 2100. All simulations start under historical conditions and continue after 2005 under the RCP8.5 (solid lines), RCP4.5 (dashed lines) or RCP2.6 (dotted lines) scenario. After the year 2100, the forcing of the last thirty years until 2100 drives the model recurrently. The thin blue lines are all ensemble members starting from the initial state PISM1Eq, where the Eigen-calving parameter amounts 10^{18}, while the green lines are the corresponding simulations starting from PISM2Eq (Eigen-calving parameter 10^{17}). A running mean with a window of 5 years has been applied for the thin lines. The thick black lines represent the ensemble mean of the three future scenarios with a moving window length of 25 years. The applied running means shift the apparent maximum backward in time so that it occurs visually before the year 2100. Recent estimates of the basal melting (blue diamonds) and the calving (red squares) ice mass loss are given for three studies (legend at the bottom, Liu et al. (2015); Depoorter et al. (2013); Rignot et al. (2013)). Related uncertainties are given as vertical lines if the uncertainties are larger than the symbol size.

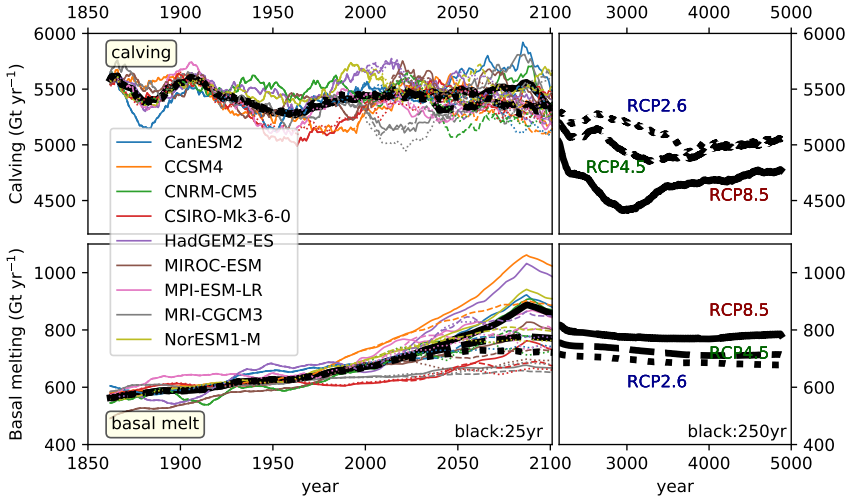

Figure A14. Long-term temporal evolution of the ensemble mean basal melting and calving ice loss rates from 1850 to 2100 and beyond until the year 5000. The upper panels show the calving rates, while the lower panels depict the basal melting rates. In the left columns, individual model simulations (colored lines according to the legend) are grouped together, while the thick black lines are the overall means as shown in the corresponding figures Figure A12 and A13. For the ensemble means of the period 1850–2100, a smoothing with a moving window of 25 years is applied (left column), while the smoothing window length is 250 years for the right column covering the period from 2100 until 5000. The applied running means shift the apparent maximum backward in time so that it occurs visually before the year 2100. Solid (dashed, dotted) lines represent the RCP8.5 (RCP4.5, RCP2.6) scenario.

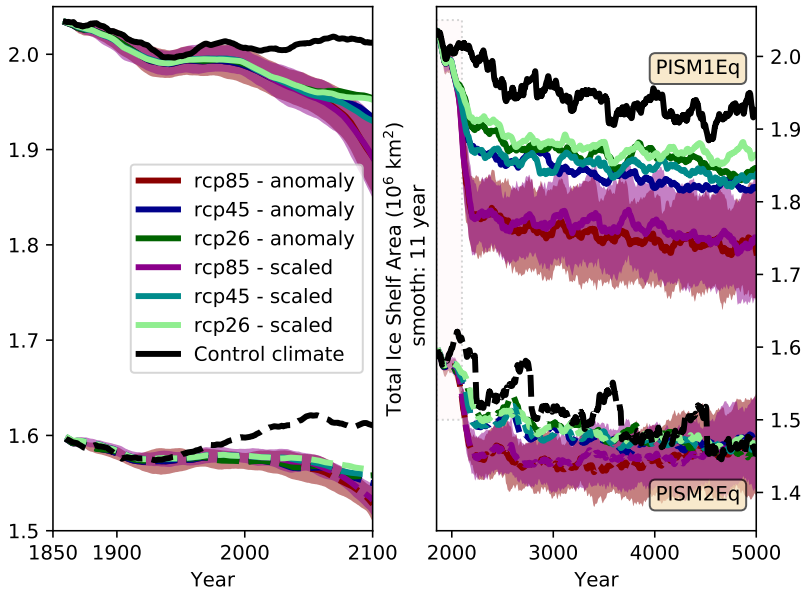

Figure A15. Area of floating ice shelves. A running mean window of 11 years is used for the entire ensemble of ice-sheet simulations. The solid lines represent the ensemble averages for the PISM1Eq starting conditions, while the dashed lines are the corresponding PISM2Eq condition. For the RCP8.5 scenario, the shading highlights the standard deviation (1-sigma) as a measure of the variability among the ice-sheet ensemble members driven by various climate models (Table 1). Please note the different axes for both subfigures. The dashed frame in the right subfigure depicts the value range of the left subfigure.

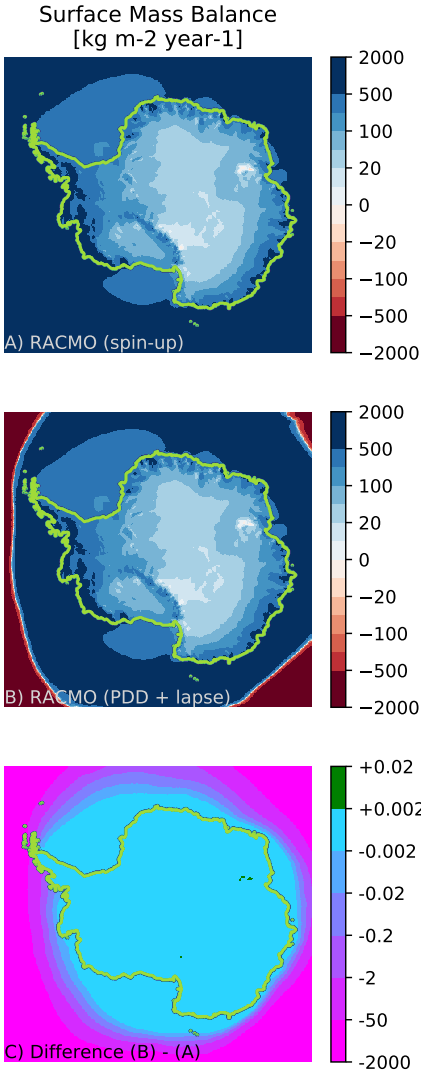

Figure A16. Surface mass balance (SMB) used during the spin-up (upper subplot, a), the surface mass balance computed via the here applied positive degree day (PDD) approach (middle subplot, b) under pre-industrial conditions and the difference between these (lower subplot, c). For the subplot under pre-industrial conditions (middle subplot, b), also the lapse correction is active, which does not impact the results because the height difference is neglectable initially. The unit of the surface mass balance and its difference are $\mathrm{kg\ m^{-2}\ year^{-1}}$. In each subplot, the light-green contour lines represent the outer edge of the ice sheet or ice shelves, respectively. Approximately south of the annual sea ice edge, the difference between both SMB fields is essentially zero except for two restricted areas. One near the Amery Ice Shelf and the other at the Transantarctic Mountain Range east of the Ross Ice Shelf. These two regions are characterized by a negative SMB in the spin-up data distribution (upper subplot, a), which is absent in the PDD-deduced SMB (middle subplot, b). Besides, only the northern tip of the Antarctic Peninsula experiences a different forcing. Further north, the difference is significant; however, this difference does not impact the Antarctic ice sheet.

A1 Appendix Table

Table A1. Characteristics of the both initial states PISM1Eq (Figure A10) and PISM2Eq (Figure A11). These are the total areas covered of grounded (A_g) and floating ice (A_f). It shows the volumes of all grounded ice (V_g), grounded ice above the sea level of $z = 0$ (V_{g0}), and all floating ice (V_f). The last row presents the ratio, expressed as a percentage value, between grounded ice above the sea level and all grounded ice. The right column represents the ratio of the quantities between both initial states.

Quantity	PISM1Eq	PISM2Eq	Ratio (PISM1Eq/PISM2Eq)
Area (A_f): grounded ice (km^2)	$1.255 \cdot 10^7$	$1.257 \cdot 10^7$	0.9985
Area (A_g): floating ice (km^2)	$2.005 \cdot 10^6$	$1.569 \cdot 10^6$	1.278
Volume (V_g): grounded ice (km^3)	$2.588 \cdot 10^7$	$2.605 \cdot 10^7$	0.9936
Volume (V_{g0}): grounded ice above $z = 0$ (km^3)	$2.313 \cdot 10^7$	$2.325 \cdot 10^7$	0.9947
Volume (V_f): floating ice (km^3)	$6.681 \cdot 10^5$	$5.421 \cdot 10^5$	1.232
Ratio of grounded ice: V_{g0}/V_g (%)	89.35	89.25	1.001